63-4-5

ARL 63-125

RESEARCH ON EXPERIMENTAL EVALUATION OF SPUTTERING YIELD RATES

K. B. CHENEY
E. E. ROGERS
E. T. PITKIN

THE MARQUARDT CORPORATION
VAN NUYS, CALIFORNIA

JULY 1963

AEROSPACE RESEARCH LABORATORIES
OFFICE OF AEROSPACE RESEARCH
UNITED STATES AIR FORCE

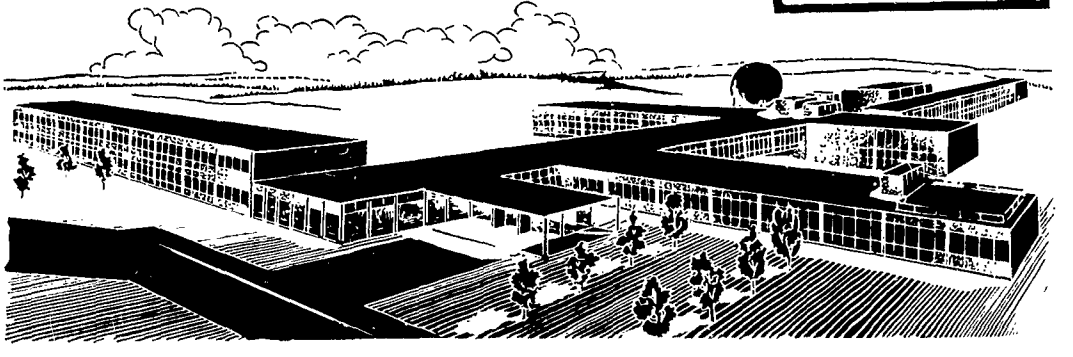

NOTICES

When Government drawings, specifications, or other data are used for any purpose other than in connection with a definitely related Government procurement operation, the United States Government thereby incurs no responsibility nor any obligation whatsoever; and the fact that the Government may have formulated, furnished, or in any way supplied the said drawings, specifications, or other data, is not to be regarded by implication or otherwise as in any manner licensing the holder or any other person or corporation, or conveying any rights or permission to manufacture, use, or sell any patented invention that may in any way be related thereto.

- - - - - - - - -

Qualified requesters may obtain copies of this report from the Armed Services Technical Information Agency, (ASTIA), Arlington Hall Station, Arlington 12, Virginia.

- - - - - - - - -

This report has been released to the Office of Technical Services, U. S. Department of Commerce, Washington 25, D. C. for sale to the general public.

Stock available at OTS $2.25.....

- - - - - - - - -

Copies of ARL Technical Documentary Reports should not be returned to Aeronautical Research Laboratory unless return is required by security considerations, contractual obligations, or notices on a specific document.

400 - September 1963 - 162 - 3-18

ARL 63-125

RESEARCH ON EXPERIMENTAL EVALUATION OF SPUTTERING YIELD RATES

K. B. CHENEY
E. E. ROGERS
E. T. PITKIN

ASTRO
A DIVISION OF THE MARQUARDT CORPORATION
VAN NUYS, CALIFORNIA

JULY 1963

Contract AF 33(616)-8120
Project 7116
Task 7116-03

AEROSPACE RESEARCH LABORATORIES
OFFICE OF AEROSPACE RESEARCH
UNITED STATES AIR FORCE
WRIGHT-PATTERSON AIR FORCE BASE, OHIO

FOREWORD

This final technical report was prepared by ASTRO, an Office of The Marquardt Corporation, Van Nuys, California, on contract AF 33(616)-8120 for the Aerospace Research Laboratories, Office of Aerospace Research, United States Air Force. The work reported herein was accomplished on Task 7116-03, "New Energy Conversion Techniques," of Project 7116, "Energy Conversion Research," under the technical cognizance of Everett D. Stephens of the Thermomechanics Research Laboratory of ARL. The research reported herein was conducted from April 1961 through January 1962 and from May 1962 through January 1963. The work done in this period was a continuation of research initiated under contract AF 33(616)-6844 from October 1959 through May 1960.

The assistance of Leo Wagner, Linda Gardener, Marcia Muzzillo, Sally Pate, Joyce Chamberlain and Pamela Carr is greatfully acknowledged.

ABSTRACT

Phenomena associated with the interaction of high energy ions and solid surfaces under conditions relevant to ion rocket operation have been investigated. The number of target atoms removed per incident ion, or sputtering ratio, has been determined for xenon and argon ions incident on copper, tungsten, molybdenum, silicon and titanium with energies from 1,500 to 39,000 electron volts and at incidence angles from 2° to normal incidence. The effect of target temperatures, both high and low, on the sputtering ratio has been investigated. The ratio of secondary particles produced to incident ions, along with their energy and angular distribution, has been investigated as functions of ion energy and incidence angle. Areas investigated for the first time in this program include:

(1) Sputtering and secondary emission for very low angles of ion incidence, and effects of surface roughness.

(2) The energy and angular distributions of secondary particles as a function of beam incidence angle.

(3) Sputtering and secondary emission of surfaces at reduced temperatures.

Analysis of theoretical concepts of sputtering and existing empirical data have led to recommendations of likely materials for ion rocket use. A bibliography of relevant papers has also been compiled.

TABLE OF CONTENTS

LIST OF ILLUSTRATIONS

LIST OF ILLUSTRATIONS (Continued)

LIST OF ILLUSTRATIONS (Continued)

LIST OF ILLUSTRATIONS (Continued)

I. INTRODUCTION

Any ion engine will suffer to some degree from electrode damage due to ions striking the accelerating electrodes and "sputtering" away material. This program was oriented toward providing data to allow this sputtering damage to be estimated and toward providing data useful for a fundamental understanding of the sputtering phenomena. Sputtering produces secondary electrons and secondary ions which may interfere with the efficient operation of an ion engine. These secondaries also complicate the study of sputtering phenomena where the incidence angle between the incoming particle's path and the target surface is very low. For example, it is usually necessary to know the amount of beam current reaching the target. If no secondaries were produced, this current would be exactly that measured by an ammeter connected to the target. If secondary electrons leave the target, however, the current measured by the meter will be too large. In general, secondaries of both positive and negative charge will be produced, both at the target and at any other surfaces struck by the primary beam or high energy secondary particles, and these must all be accounted for. Therefore, these secondary particle's were also investigated. This program was particularly concerned with low incidence angle (near grazing) sputtering in the energy range of interest for ion rocket applications, i.e. ion energies of greater than 1000 electron volts.

Heavy ions, and particularly cesium, are preferred for ion rocket use. The ion source available for this program was only suitable for handling gases, preferably noble gases. Xenon was used for most tests in order to simulate cesium. The masses of the two elements are nearly identical and they appear to produce very simular sputtering ratios.

The sputtering test stand used with xenon is shown in Figure 1 and is thoroughly discussed in the equipment section. The points to be noted particularly are that the beam is analyzed to separate particles according to charge-to-mass ratio so as to insure that sputtering is done only with the ion species desired and that the target is surrounded by a cup to prevent the escape of secondary charged particles. In order to investigate sputtering with cesium a test stand employing a contact ionizer was constructed as shown schematically in Figure 2. A more complete description of this equipment is contained in the equipment section. No sputtering data was obtained with this equipment due to various developmental problems. A well focused beam of satisfactory current density was eventually obtained, but there was not sufficient time remaining to run any sputtering experiments with cesium.

The plan of the remainder of this report is as follows. Section II, Discussion, begins with a subsection II A, reviewing the history and present knowledge of sputtering phenomena. The next subsection II B, Experimental Equipment, discusses the experimental and measuring equipment and probable errors. Section II C, Experimental Procedure and Results, begins with a short description of sputtering and experimental procedures to make it self-contained for the reader familiar with sputtering. This short introduction is followed by a detailed presentation and discussion of the experimental results of this program. The Summary, Section III, is followed by Section IV, Conclusions, where some recommendations for future work are made. In addition to the references cited in the text, Section V, a bibliography of books and articles found helpful is included in Section VI. A table of all sputtering ratios obtained is included in the Appendix, Section VII, along with further discussion of the equipment.

"Manuscript released by the author(s), April 12, 1963, for publication as an ARL Technical Documentary Report."

SPUTTERING TEST STAND

(PHILIP'S IONIZATION GAUGE SOURCE)

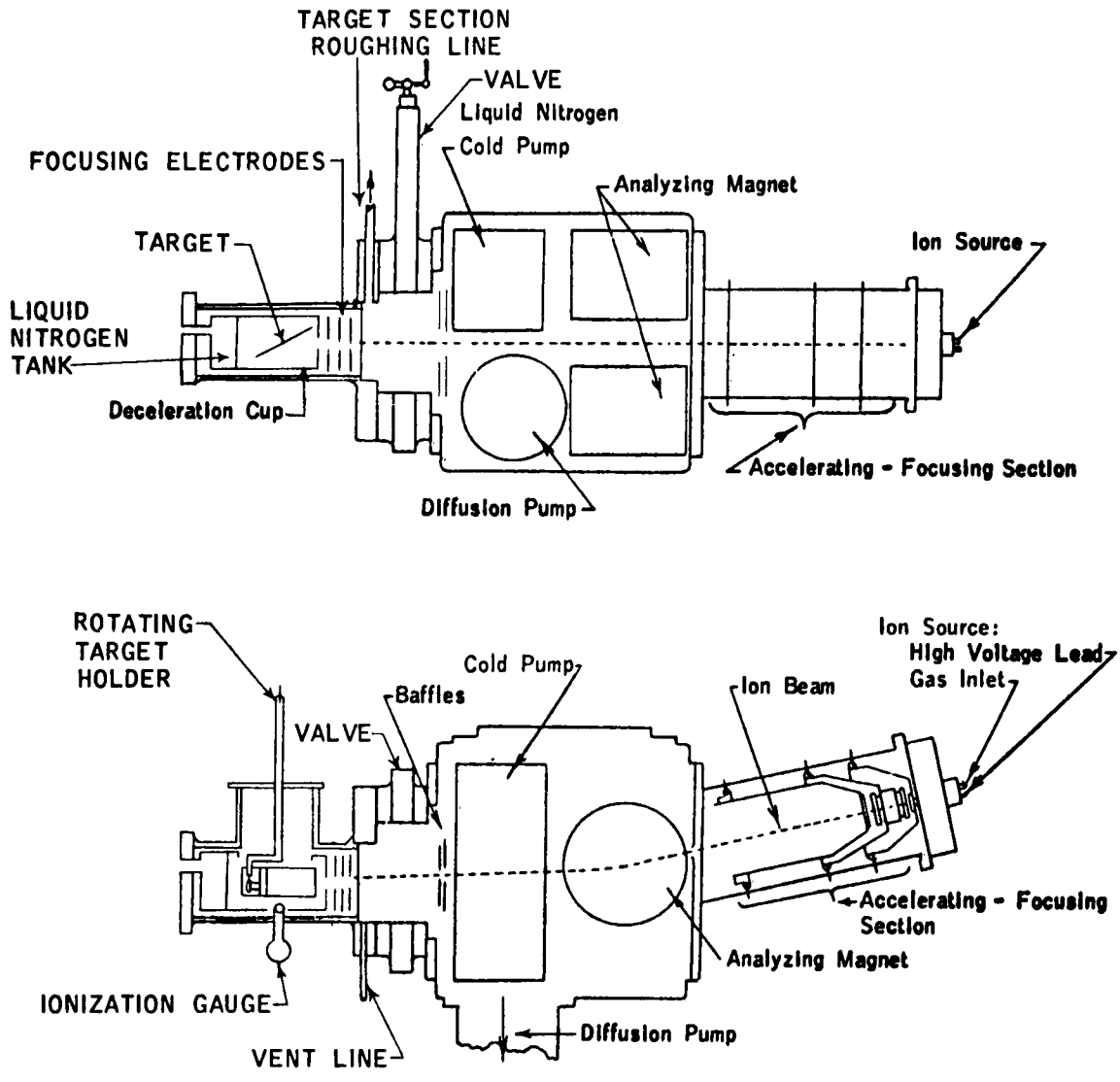

CESIUM ION SPUTTERING APPARATUS

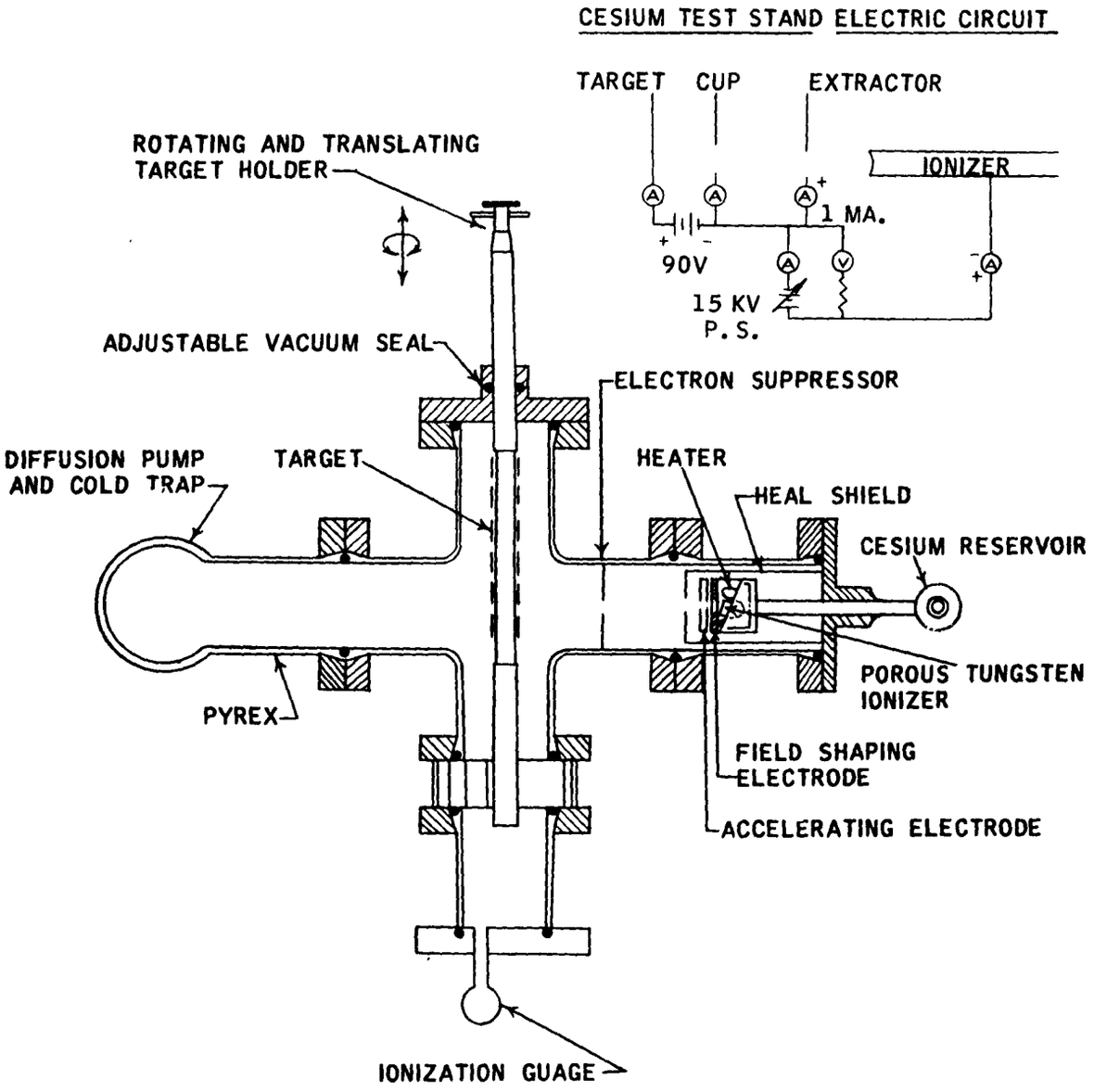

FIGURE 2

II. DISCUSSION *

A. Theory

1. Historical Background

In 1858 J. Plucker, working with the gas discharge tubes constructed by Geissler, a glassblower at Bonn, observed that "the metal of the electrodes, particularly of the negative one, becomes transferred to the glass of the tubes. This is even the case with platinum electrodes, and the blackening of the tube in the neighborhood of the hot pole is ascribed predominantly to platinum, which at the same time combines with traces of other substances in the tubes" (1). Plucker referred to this transfer of cathode material as "zerstaubung". This was then translated into English as "sputtering". The word does not accurately describe the atomic character of the process, but is the name almost universally applied to this phenomenon. "Impact evaporation", as used by another early investigator, does indicate that transfer is by individual atoms but suggests that escape from the cathode is a thermal process; this simple concept is not now believed to be adequate either.

In 1891 Sir William Crookes published a paper "On Electrical Evaporation" (2) in which he gave the relative rates of sputtering of a number of metals in a discharge in air at six mm Hg pressure. He reported that "the current influenced the normal vibrations of the metal molecules, so that several of them could be caused to escape the field of attraction of the metal and be carried away by the gas molecules. This electrical volatization or evaporation is very similar to ordinary evaporation by the agency of heat".

These and other early researchers were seriously limited by the experimental environment used. The ordinary glow discharge was used as a source of ions and the metal targets were placed directly in the discharge vessel. The glow discharge operates at pressures of a few mm Hg, so that the mean free path of the sputtered atoms is much shorter than the distance between the cathode and the collector of sputtered material. Consequently, the atoms undergo many collisions on their way toward the collector, and many of them never reach that goal but are returned to the cathode. In other words, the collection of sputtered material becomes controlled by diffusion.

It was not until 1923 that experiments were done under more suitable conditions, at the General Electric Co., Ltd (3) and by K. H. Kingdom and Irving Langmuir (4). Electrons from a hot filament were used to ionize the gas, and its pressure was kept too low to interfere with the escape of sputtered atoms. Kingdom and Langmuir studied the sputtering of monatomic layers of thorium on tungsten, and devised a clever mechanism. As the first step in the sputtering process "a surface atom of thorium is struck by an ion and driven into the underlying tungsten, forming a depression. When this depressed thorium atom is struck by a second ion, the ion is elastically reflected and, on its way back, may strike one of the surrounding thorium atoms and dislodge it, provided the energy which it can communicate to the atom, according to the laws of momentum transfer, exceeds the atomic heat of evaporation".

---

* The principle results of this program are discussed in Section II C, the reader acquainted with sputtering phenomena may prefer to begin reading there.

E. S. Lamar and K. T. Compton (5) suggested that momentum transfer to a surface atom might occur when an ion penetrated the surface, was reflected from a lower layer, and recoiled to strike the surface atom in the outward direction. This model is close to that now used in theories based on momentum transfer, except that the recoil particles that cause the sputtering are believed to be displaced target atoms.

Until recently, however, it was quite widely accepted that sputtering was due to the formation, at the points of ionic impact, of localized hot spots from which ordinary evaporation of target atoms occurred. This mechanism had been given a fairly quantitative treatment by C. H. Townes (6). According to his equation, the sputtering ratio (atoms of target sputtered per incident ion) should depend on the energy of the ion, but not on the ratio of its mass to that of the target atom.

There is now good evidence that such simple energy transfer does not suffice to explain sputtering.

2. Introduction To Contemporary Theory of Sputtering

In 1954, Frank Keywell (7) devised a model of sputtering based upon a succession of random collisions between target atoms, beginning at an atom displaced by a bombarding ion and ending at the surface of the target. Further calculations based upon this model were made by D. E. Harrison (8) and R. S. Pease (9). However, these calculations all ignore the ordered lattice structure of solids.

Present theories of sputtering are based on such a transfer of energy through collision processes. The efficiency of energy transfer by collision is a function of the masses of the two particles concerned and the scattering angle. The collision cross section, giving the apparent sizes of the particles involved, is a function of the nuclear charge, the energy of particles, and the number of screening electrons that each particle has. Clearly, in order for sputtering to occur, the momentum vector of the incoming particle must somehow be reversed before the momentum is transferred to a surface atom. In the case of a light ion striking a surface composed of heavy atoms, this momentum reversal could be accomplished in one collision. However, generally several collisions are required and the momentum reversal takes place fairly deep inside the crystal. It appears probable that instead of the crystal atoms going directly to the surface and escaping, they transfer their energy down chains of atoms, cf. Figure 3, finally transferring the energy to a surface atom which can escape. With this chain mechanism it is assumed, in contrast to previous theories, that momentum is transferred in a direction in which there exists a chain of crystal atoms. Also sufficient energy must reach the surface to permit an atom to overcome the surface binding energy and escape.

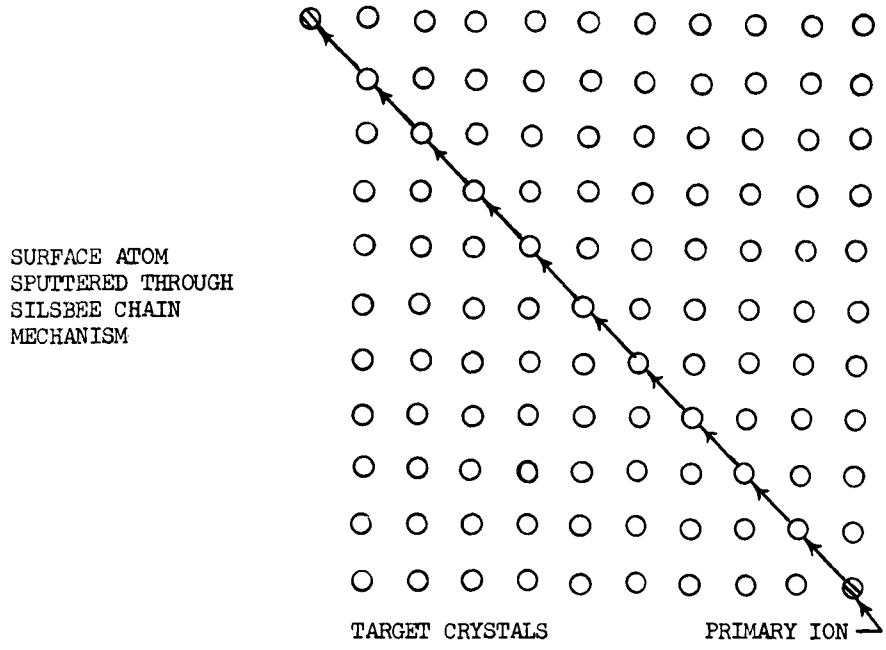

SPUTTERING BY SILSBEE CHAIN MECHANISM

FIGURE 3

Silsbee (10) first proposed this chain mechanism and subsequently considerable experimental evidence has come to light to support it. Most strikingly, spot patterns on glass collectors surrounding the target have been produced in the direction of close packing in crystals. For instance, Thompson (11) produced spot patterns on the near side of a sputtered surface. Additional, somewhat more indirect, evidence supporting the chain mechanism was pointed out by Harrison (12), who showed that the maximum energy of atoms sputtered off a surface is quite close to the maximum energy which can be transferred down a chain of atoms in a crystal. A third observation which seems to support the chain mechanism is that defects appear in relief on sputtered surfaces, i.e., the perfect crystal surface is eroded faster than the defects in the lattice structure. This result is easily explained by the chain mechanism since energy transfer cannot take place across defects, as the chain of atoms is broken by a defect. Therefore the erosion of surface atoms protected by a defect is much slower than those on the surface of a perfect crystal.

Experiments by Rol (13) on single crystals suggest that conditions which permit the deep penetration of ions are conducive to low sputtering ratios. One of these experiments involves sputtering three crystal planes of copper, as illustrated in Figure 4. The (111)-crystal-plane produced a sputtering ratio at normal incidence of 8.2 atoms per ion. The (100)-surface produced a sputtering ratio of 3.2 and the (110)-surface produced a sputtering ratio of 2.8, while a polycrystalline sample of copper produced a sputtering ratio of 6.3. Another suggestive experiment by Rol (14) is illustrated in Figure 5. The sputtering ratio at various angles on a (100)-surface of a copper crystal rotated about the

SINGLE CRYSTAL SPUTTERING

COPPER; FACE CENTERED CUBIC

SPUTTERING RATIO FOR 20 Kev ARGON IONS, ROL[14]

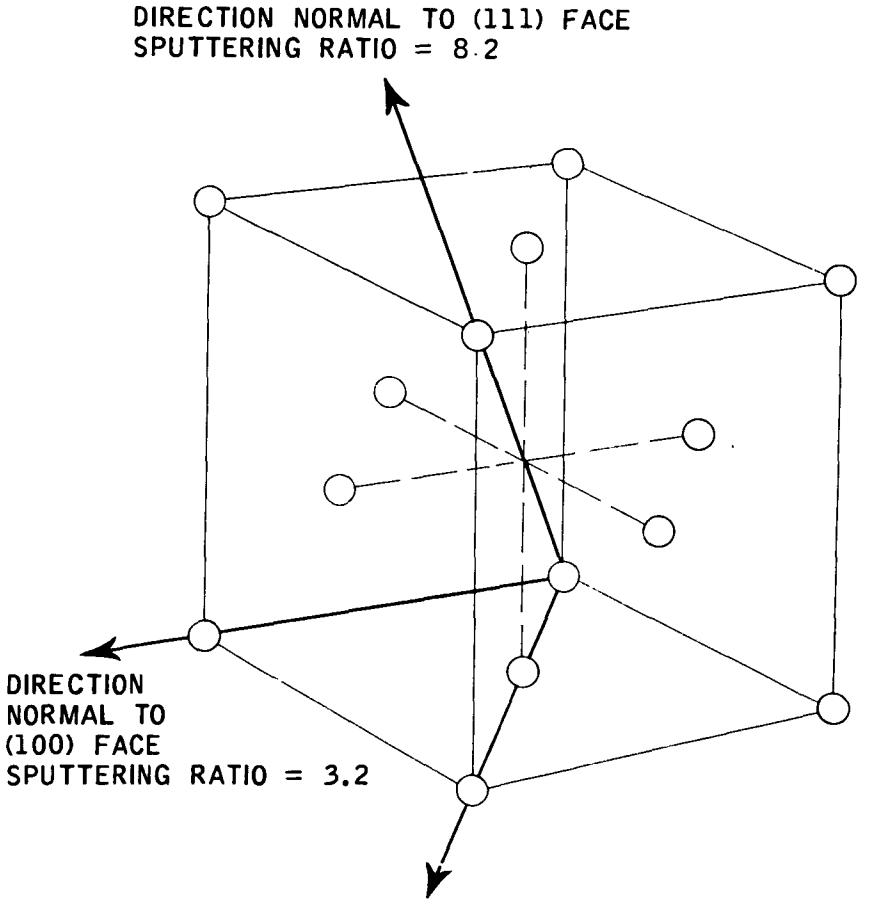

POLYCRYSTALLINE COPPER SPUTTERING RATIO = 6.3

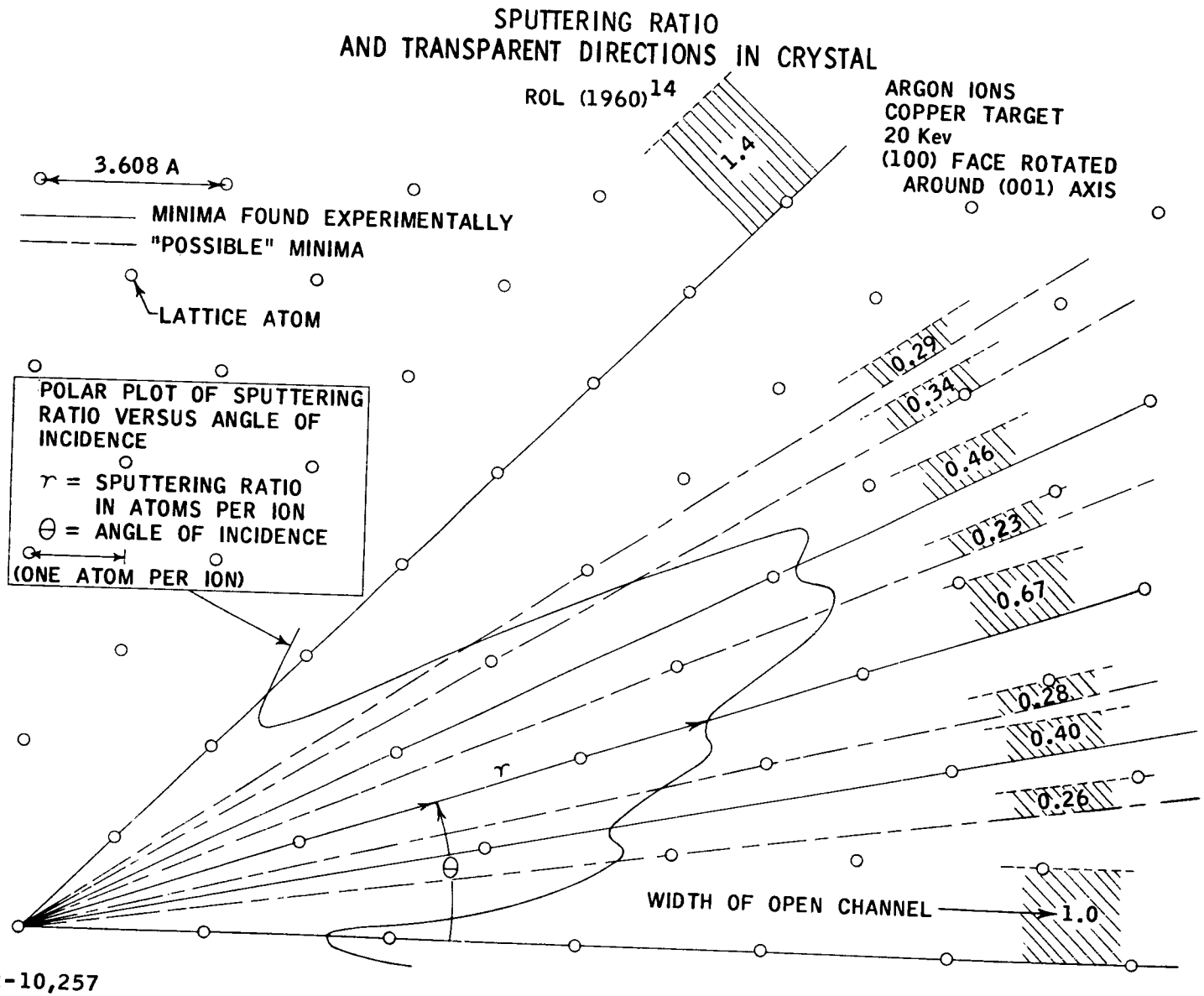

FIGURE 5

R-10,257

(001)-direction is plotted on a polar diagram, over a schematic diagram of the crystal. The sputtering ratio tends to have minima in the directions for which an incoming ion encounters a relatively open crystal. In fact, sputtering ratio minima occur for all five of the most open directions.

In opposition to the evidence just presented in favor of the Silsbee chain mechanism, other investigators have found that ion bombardment destroys the lattice structure at the surface of a target. Schlier and Farnsworth (15) reported that "Surfaces that have been subjected to positive ion bombardment, but not annealed, are so disturbed that no low-energy electron diffraction beam can be observed, even if the ion energies were as low as 150 ev". Haneman (16) later confirmed this using freshly cleaved Bi_2Te_4; bombardment by 400 ev Ar^+ at 30 ua/cm^2 for 30 minutes reduced the intensity of the diffraction pattern to a few percent of that for the annealed surface. Still, the fact remains that sputtering is closely related to the microscopic orientation of a single crystal target.

Another method of energy transfer has been proposed which is strikingly similar to the Silsbee chain mechanism. In 1950 H. Paneth (17) proposed a new type of defect, called the "crowdion". The crowdion results from the introduction of an extra atom or ion into a close-packed line in a crystal, followed by the relaxation of the atoms along the line to accommodate it. The crowdion possesses curious and unusual properties. It is free to move in one dimension only, namely, along the close-packed line, but it can have an extraordinarily high mobility in this direction, for the region of maximum compression along the line can move rapidly with very little motion of the individual atoms.

A practical aspect of sputtering which is often overlooked is the relationship between the sputtering ratio of a material in atoms per ion and the actual volumetric rate of erosion at the sputtered surface. The erosion of the surface in terms of volume or mass lost per incident ion is the product of the sputtering ratio in atoms per ion and the atomic volume or atomic mass respectively.

A diagram has been prepared to indicate the relative resistance to sputtering damage of a large number of elements. This is presented in Figure 6, with the coordinates specifying sputtering ratios in mass per ion and volume per ion. Those elements which are at the lower left show the greatest resistance to sputtering. Notice that some elements with very low sputtering ratios in terms of atoms per ion (e.g., tungsten) show poor resistance to sputtering because of their high atomic masses and atomic volumes.

3. Implications of the Theory

Sputtering is expected to be great where there is:

a. A large transfer to energy from the ion to the crystal lattice, occurring reasonably near the surface.

b. A rapid reversal of the momentum of the ion.

c. A mechanism for the transfer of energy back to the surface of the crystal.

d. An easy escape of surface atoms from the crystal.

SPUTTERING RATIOS OF ELEMENTS IN MASS PER ION AND VOLUME PER ION

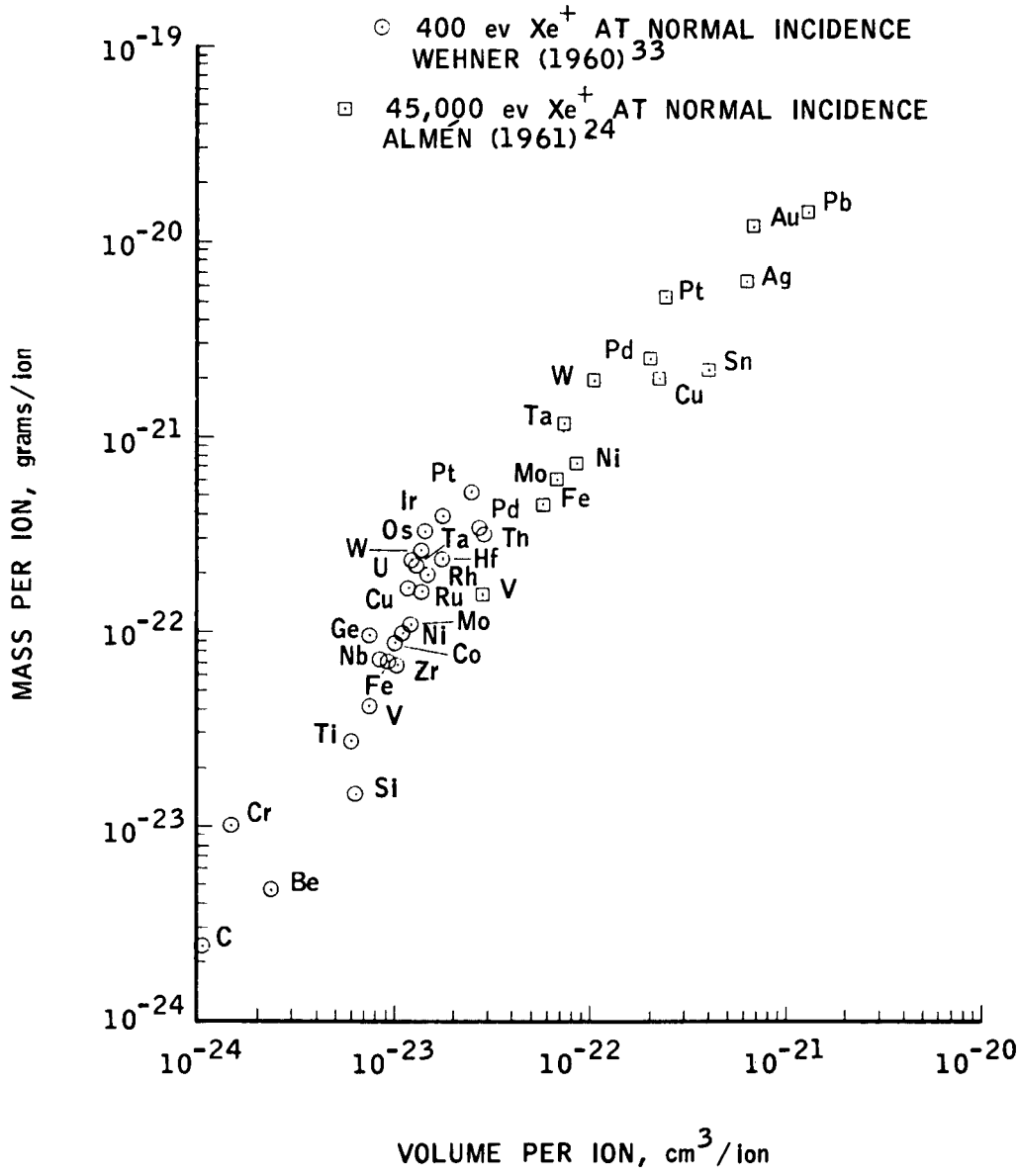

R-13,980

FIGURE 6

e. A comparatively large atomic volume, or atomic mass.

Conditions conductive to low sputtering are then:

a. Relatively open crystal structure to permit deep penetration of the ion before it strikes the crystal atom.

b. Sputtering conducted at an appropriate angle to a single crystal, i.e., an angle where the crystal has relatively open, transparent structure.

c. Small atomic volume or atomic mass; this is most characteristic of elements of low atomic number.

d. Any condition which frustrates energy transfer to the surface by the chain mechanism should lower the sputtering ratio.

An example of the latter is given by alloys of metals with widely different masses, since energy transfer is poor in this case. Another example is a thin film applied to the surface, and not ordered relative to the lattice structure of the underlying material, cf. Figure 7. A high energy particle will not have difficulty penetrating a thin film such as this, however energy transfer from the interior of the target to the surface atoms will be prevented because of the disordered condition at the interface between the interior and the surface film. The maximum energy transfer down the chain is of the order of tens of electron volts. Therefore any interference with the momentum transfer will completely prevent the escape of surface atoms. Finally, a material which is thoroughly disordered, with a very high defect density would probably not sputter much.

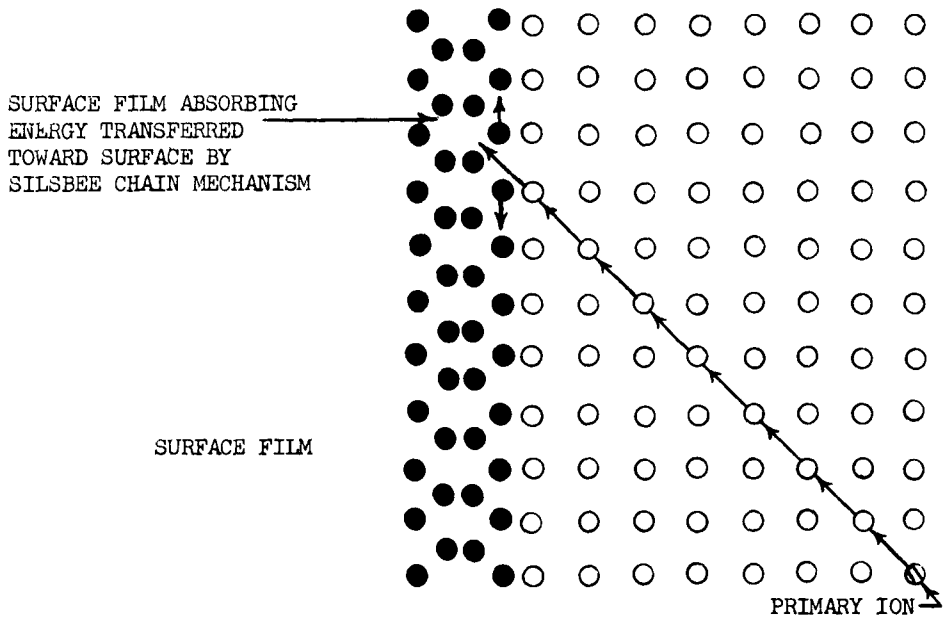

SPUTTERING INHIBITED BY SURFACE FILM

FIGURE 7

4. Theory of Angle Effect in Sputtering

If one assumes that the energy transferred to a crystal lattice by collision of an incident ion is dissipated symmetrically about the point of collision, then it can be shown that for energies at which the ion range is substantially greater than the maximum length for a Silsbee chain, the sputtering ratio is inversely proportional to the sine of the angle that the ion beam makes with the surface.

The number of sputtered particles resulting from collisions that absorb energy dE may be expressed by

$$dS = f\left(\frac{dE}{d\ell}, r\right) dE$$

where $dE/d\ell$ is the density of energy transferred to the lattica per unit length of ion path, r is the distance of the ion from the surface, and f is the appropriate function for the ion and target considered. Of course $dE/d\ell$ may in turn be expressed as a function of the ion energy, etc.

The sputtering ratio is then

$$S = \int_{E_o}^{o} f\left(\frac{dE}{d\ell}, r\right) dE \ ,$$

where E_o is the initial ion energy, and the ion is assumed to stop in the target.

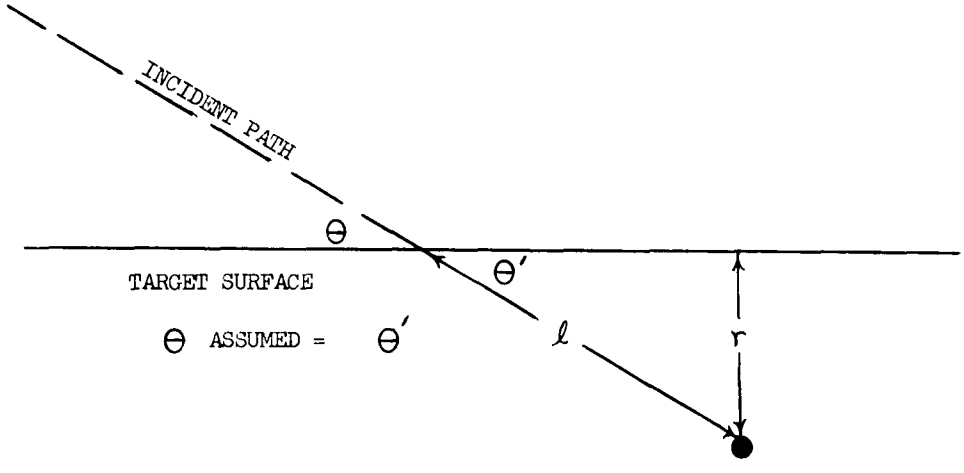

RELATIONSHIP OF NORMAL RANGE TO ANGLE OF INCIDENCE

FIGURE 8

But

$$dE = \frac{dE}{de}\, de = \frac{dE}{de}\, \frac{dr}{SIN\Theta} .$$

Since Θ is constant (the track of an ion in a solid is found to be rectilinear for the conditions considered here), sin Θ can be removed from the integration, yielding -

$$S = \frac{1}{SIN\Theta} \int_0^{r_o} f\left(\frac{dE}{d\ell}, r\right)\, \frac{dE}{d\ell}\, dr$$

where r_o is related to the range, r, by

$$r_o = R\ SIN\Theta$$

If the function f $(dE/d\ell, r)$ is such that it becomes very small for $r > r_c$, where $r_c << R$ (e.g., the Silsbee chain length is substantially less than the range), then -

$$S \simeq \frac{1}{SIN\Theta} \int_0^{r_c} f\left(\frac{dE}{d\ell}, r\right)\, \frac{dE}{d\ell}\, dr$$

Designating the integral by $S_\perp$ the sputtering ratio at normal incidence, this may be written.

$$S = \frac{1}{SIN\Theta}\, S_\perp .$$

This relationship is valid under the conditions described, and for those angles where the assumption holds that $\Theta' \simeq \Theta$.

For small angles (grazing incidence), the effect of the surface on an ion trajectory becomes much greater. Experimentally, this is evidenced by a sharp drop in the sputtering ratio for angles of incidence of less than 15°. As previously mentioned, there is evidence that specular reflection occurs at low angles of incidence. For the case that R is not greater than r_c, the upper limit of integration, R sin Θ, decreases with Θ so that -

$$S < \frac{1}{SIN\Theta}\, S_\perp .$$

An expression for $S_\perp$ has been calculated by R. S. Pease (9):

$$S_\perp = \frac{\bar{E}}{4E_D}\left[1 + \left(\frac{\ell n\, \bar{E}/E_S}{\ell n\, 2}\right)^{1/2}\right] \sigma_p\, n^{2/3} .$$

E is the average energy transferred from an ion to a target atom in a collision, E_D is the energy required to displace an atom from a lattice site, E_S is the energy necessary to remove an atom from the target surface, σ_p is the displacement cross section (for collisions), and n is the number of atoms per unit volume.

5. Previous Experiments on Sputtering

a. Angular Data

Although a number of curves can be drawn to demonstrate effect of incidence angle on the sputtering ratio, as in Figures 9, 10, and 11, the usefulness of these curves is limited in general to angles above 30°. Wehner's curves and some of Pitkin's curves go down to angles of incidence as low as 10°. However, as Wehner (18) pointed out, his angle data below 30° is quite questionable due to the experimental conditions. Also very little of this data is in the energy range of interest here. In particular, Wehner's data only goes up to 800 electron volts of energy.

b. Relationship of Sputtering by Xenon and Cesium

On the basis of measurements of sputtering ratios by Rol (13) for the alkali metal ions, sodium and potassium, and for the corresponding noble gas ions, neon and argon, presented in Figure 12, one concludes that the sputtering ratio of a noble gas ion is approximately the same as that for the alkali metal ion of approximately the same mass.

Data by a single investigator comparing sputtering by Xe^+ and Cs^+ are not available; little information is available on sputtering by cesium. Kuskevics (19) has recently reported approximate sputtering ratio for several materials, bombarded normally by 2 Kev cesium ions. The table below shows how these compare with results of The Marquardt Corporation for sputtering by Xe^+ at the same energy and angle. The correlation is quite good, and vindicates the use of Xe^+ in this program.

SPUTTERING BY 2 Kev CESIUM AND XENON IONS AT NORMAL INCIDENCE

Target	Xe^+ (TMC)	Cs^+ (EOS)
Copper	4 ± 1 atoms/ion	5.5 ± 1 atoms/ion
Tungsten	2.9 ± 0.3	0 to 1.2
Molybdenum	0.8 ± 0.3	0.8 (±?)

c. Neutral Atoms and Multiply Charged Ions

The state of knowledge of the sputtering effect of neutral and multiply charged atoms is probably best described as confused. There is a certain amount of data, however these data are neither self-consistent nor do they seem to bear any relation to any of the theories of sputtering. According to Wehner (20) ions are neutralized somewhat before they strike the surface of a crystal.

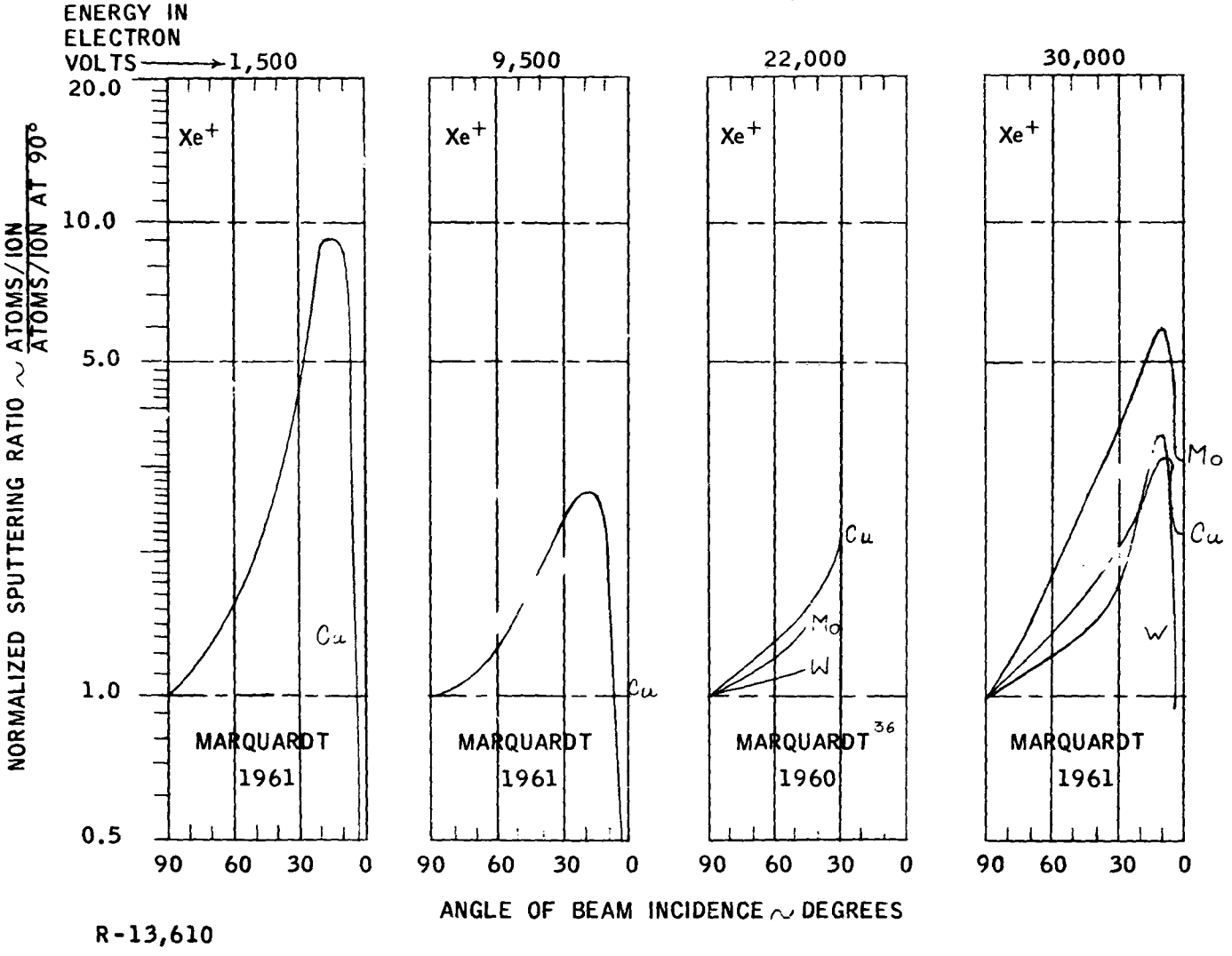
NORMALIZED SPUTTERING RATIO VERSUS ANGLE OF INCIDENCE
AT VARIOUS ION ENERGYS, Xe+
ENERGY IN ELECTRON VOLTS
1,500
9,500
22,000
30,000
NORMALIZED SPUTTERING RATIO ~ ATOMS/ION / ATOMS/ION AT 90°
20.0
10.0
5.0
1.0
0.5
Xe+
Cu
Mo
W
MARQUARDT
1961
1960
90
60
30
0
ANGLE OF BEAM INCIDENCE ~ DEGREES
R-13,610

FIGURE 9

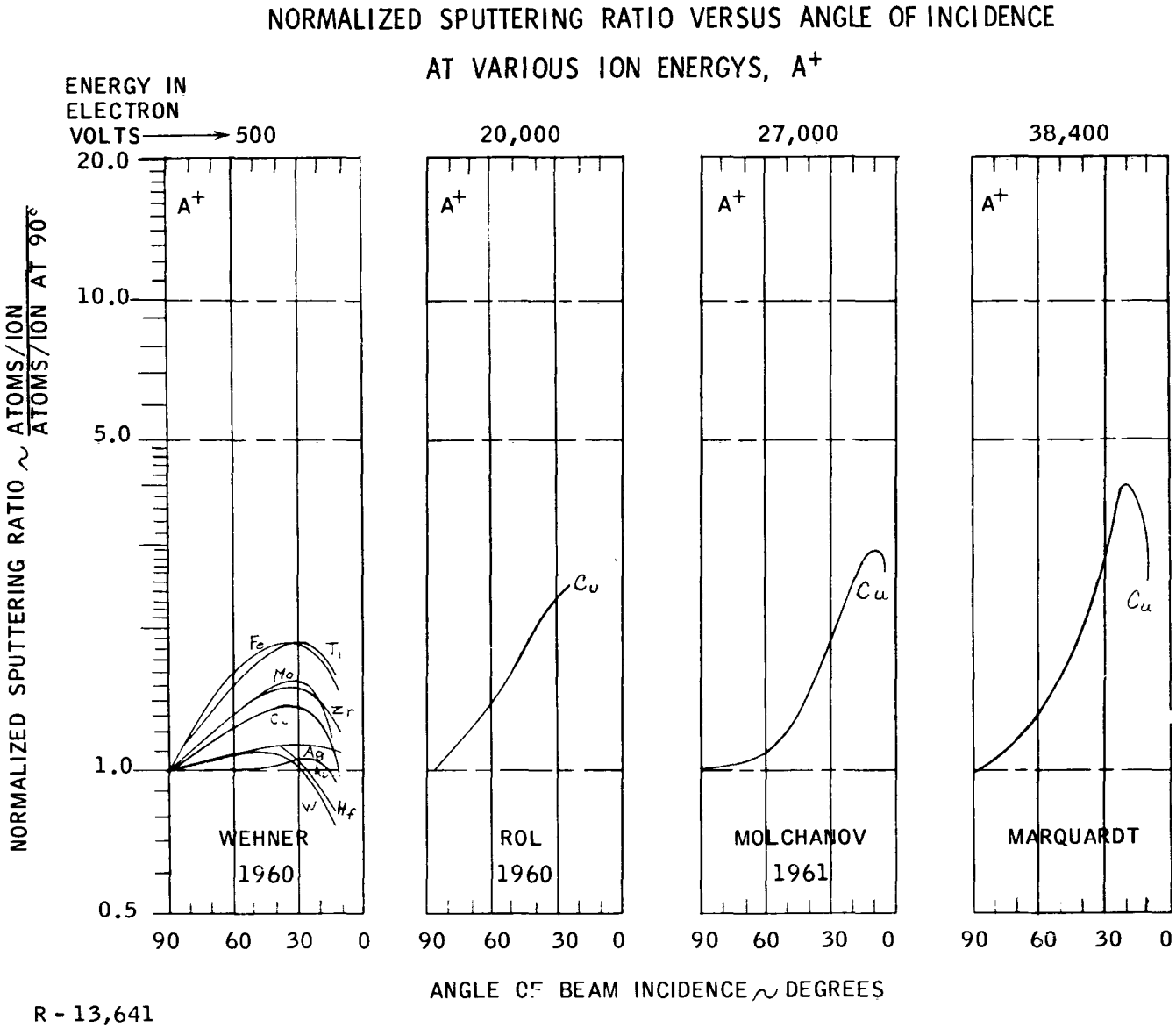

FIGURE 10

R - 13,641

NORMALIZED SPUTTERING RATIO VERSUS ANGLE OF INCIDENCE
AT VARIOUS ION ENERGYS, Hg^+ and N^+

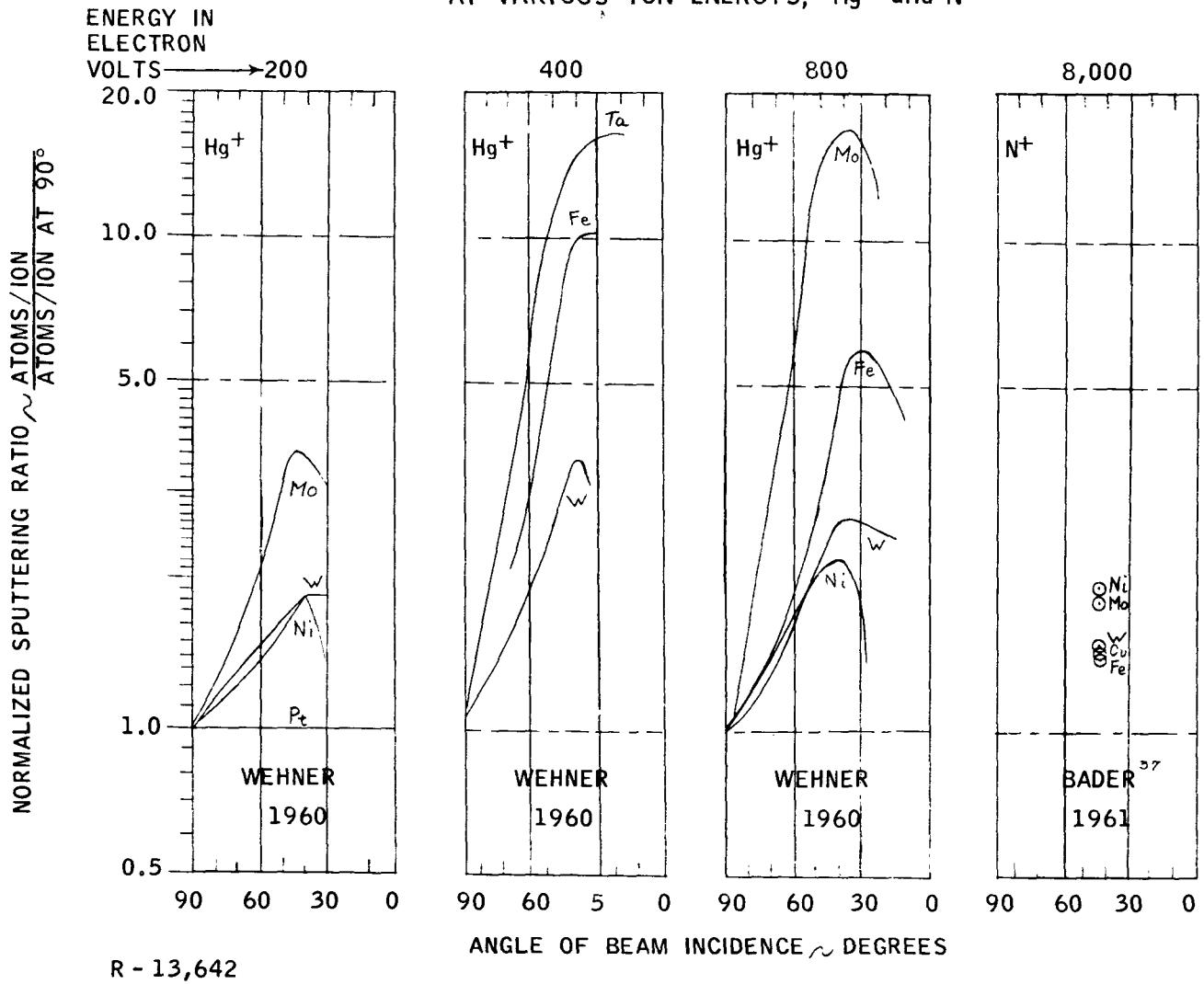

R - 13,642

FIGURE 11

SPUTTERING BY Ar^+, K^+, Ne^+, Na^+
AT NORMAL INCIDENCE ON COPPER

ROL (1960)[13]

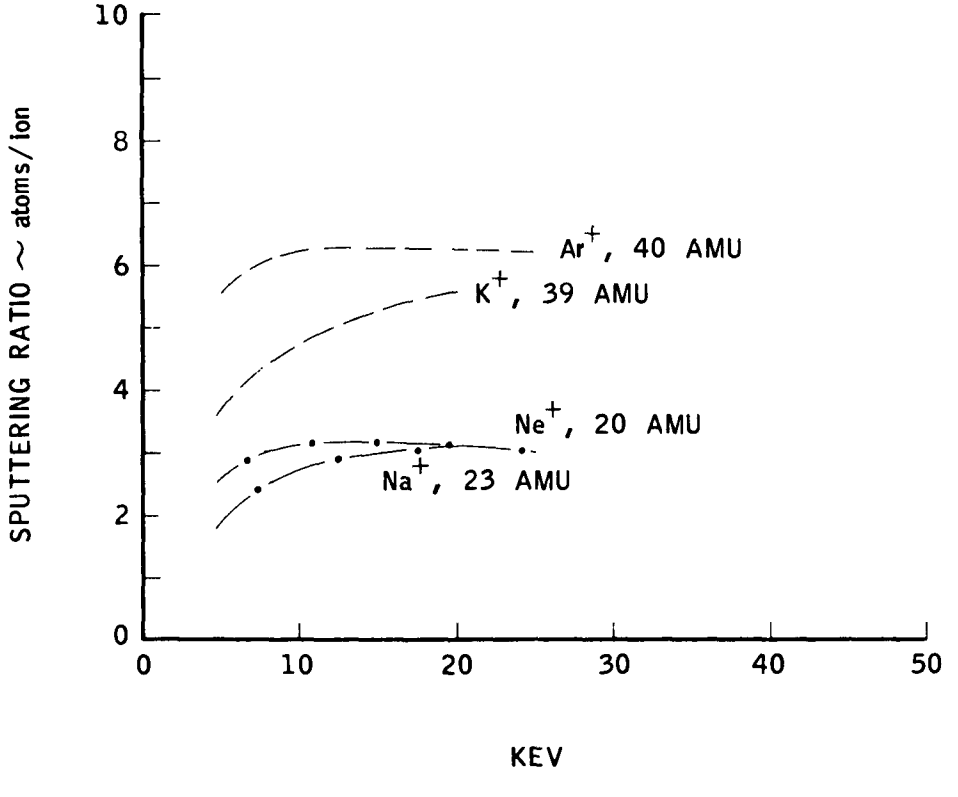

Therefore the sputtering ratios of an ion and a neutral should be identical. Also, the sputtering ratios of singly and multiply charged ions should be identical. However this charge independence is not verified by experiment.

There does not seem to be any direct experimental evidence on the sputtering ratio of neutrals. However Weiss (21) performed an experiment in which he compared the sputtering ratio of a mixed beam of hydrogen atoms and ions with the sputtering ratio of the same beam with the charged particles removed by a magnetic field. He concludes that the sputtering ratio of hydrogen atoms is much greater than the sputtering ratio of hydrogen ions. Wehner, on the other hand, concludes from somewhat indirect evidence that the sputtering ratio of neutrals is lower than the sputtering ratio of ions.

Wolsky (22) has experimented with the sputtering ratio of doubly charged argon ions versus the sputtering ratio of singly charged ions and found twice that expected on kinetic energy grounds. Bader (23) has investigated the relative sputtering ratios of nitrogen atomic ions (N^+) and molecular ions (N_2^+) and has found very little correlation. It would be expected that the sputtering ratio of an N_2^+ ion would be identical to that of $2N^+$ ions of the same energy, since the N_2^+ ion should dissociate on impact. He found, however, that the relative magnitudes of the sputtering ratios varied with energy, target material, and angle of incidence. There are several possible effects which might be responsible for Bader's results. First, the N_2^+ ion might not dissociate immediately on impact. Second, the N_2^+ ion might dissociate into an ion and an atom, or third, the two chains of collisions caused by the dissociated particles might interact.

d. Temperature Effects

Temperature can modify the structure of a material, and hence the sputtering ratio, in several ways. Three such ways are: variation of the lattice vacancy concentration, variation of the impurity concentration, and annealing of the lattice structure. The first two effects are reversible, while the last is not. Vacancy concentration and impurity concentration increase with temperature, and would tend to shorten Silsbee chains because of the increased frequency of defects in a close packed line. Hence, these two effects would cause the sputtering ratio to decrease with increasing temperature. Annealing, on the other hand, reduces the concentration of lattice defects that arise from ion bombardment, so that at temperatures for which annealing is rapid, this effect would cause sputtering to increase with temperature.

Experimental work has confirmed these predictions. Almén and Bruce (24) reported a sharp increase in the sputtering ratio of silver above 600°C, which is approximately the "annealing temperature" of that metal. For nickel and platinum, which have higher melting points, sputtering was found to decrease with increasing temperature. Snouse and Bader (23) measured the sputtering ratio, for N_2^+ bombarding copper, at temperatures from 60°C to 475°C. They also found a decrease of sputtering at the higher temperature, which is still too low for annealing.

6. Work on Secondary Particles

It appears that no one has carried out a comprehensive study of the number, atomic species, charge state, direction of emergence, and energy of secondary particles as a function of incident ion energy and angle of incidence for over one ion-target combination. However, several complementary studies have been made and are outlined below. R. Bradley (25) and R. Honig (26) used mass spectrographs to study the nature and energy of secondary particles for angles near 45°. H. Hagstrum (27) made a very detailed study of the magnitude of the reflected current for perpendicular incidence. V. Molchanov and V. Telkovskii (28) studied the energy carried away by secondary particles at angles down to 6°. The Marquardt Corporation has obtained extensive results on secondary particle currents versus angle of incidence, angle of emission, target temperature, and ion energy.

R. Bradley studied charged particles leaving a sputtered surface. He used ion energies of less than 1000 ev and, judging from figures, angles of incidence and emergence of 45°. His results indicated that a very small percentage (on the order of 0.01%) of the sputtered particles were charged, that they were invariably singly ionized, and that they had energies on the order of 10 e.v. or less. For 500 e.v. argon ions incident on molybdenum, the number of reflected ions was slightly less than the number of sputtered molybdenum ions. His incident ion beam contained multiply charged argon ions, and doubly charged argon ions were observed to reflect from the target. The fact that the only doubly charged ions observed were those of the same element as the beam strongly indicates a true reflection mechanism. Bradley and Ruedl (29) obtained evidence that the emission of positive ions of target material for a copper target only occurs under particular surface conditions, e.g., the presence of an oxide layer. For 1 kev Ar^+ bombarding a copper single crystal, which was 99.999% pure, electropolished, and carefully rinsed, the secondary positive particles detected were predominantly Ar^+, Ar^{++}, Cu^+, and CuO^+. The crystal was then annealed at 650°C in the vacuum. In subsequent sputtering of the surface, no Cu^+ or CuO^+ particles were detected.

R. Honig studied sputtered particles using incident ions with energies between 30 and 400 e.v. and again, judging from the figure, incidence and emergence angles near 45°. He found a great variety of secondary particles with a large proportion of reflected singly and doubly ionized ions. The energy of the sputtered ions was quite small, almost all less than 10 e.v.

The most thorough treatment of reflected ions is that by H. Hagstrum. He used noble gas ions with energies up to 1000 e.v. directed at normal incidence to the target. Under these conditions the ratio of reflected ions to incident ions was found to be quite low, 0.04% to 0.2% and independent of energy.

Hagstrum (30) has studied secondary electron emission for bombardment of metals by very low energy ions, and presented a remarkable theory to account for those phenomena. The electronic processes involved, however, are not those which obtain at ion energies considered here.

The striking point of the results above is the very small number and energy of the reflected or secondary ions. In the light of The Marquardt Corporation's experience and the results of Molchanov and Telkovaskii (28), it appears that there is a fairly sudden, and very large, rise in the secondary positive ratio between 15° and 10°. Molchanov and Telkovskii, using 27 Kev argon ions bombarding copper, found no observable energy in the reflected beam for angles down

to 20°, six percent at 12°, 17 percent at 8°, and 22 percent at 6°. Secondary particle effects observed at The Marquardt Corporation are in agreement with these results.

The secondary ion emission is composed primarily of ions of the bombarding and target elements. For those of the bombarding element, an electronic interaction with the target occurs that is dependent upon the relative values of the ionization potential of the bombarding element and the work function of the target surface. For the case that the ionization potential of the bombarding element is lower than the surface work function, an ejected atom is expected to yield its electron to the surface and leave as an ion. Cesium has a very low ionization potential, so that bombardment by cesium often satisfies this condition. The noble gases, on the other hand, have very high ionization potentials, much higher than the work function of any surface. For this reason, ionization of an ejected noble gas atom would not occur in the way described above. Then in contrast to the close comparison between sputtering ratios for Cs^+ and Xe^+, one expects that secondary ion emission for these bombarding ions would be quite different. U. A. Arifov et al. (31) have compared measurements of secondary ion emission for bombardment of nickel by Cs^+ (where the ionization potential is substantially less than the work function) to those for bombardment of molybdenum by Ba^+ (where the ionization potential is greater than the work function). They found secondary ion emission to be much less for the latter case, as expected.

B. Experimental Equipment

Equipment directly involved in acquiring data is discussed below. A more extensive discussion of equipment is included in Appendix B.

1. Equipment for Sputtering with Noble Gases

The test equipment for sputtering with noble gas ions is shown in Figures 1, 2, 13, and 14. Ions of the gas employed are produced by a Penning type ion source. Along with an extractor electrode, the machine is equipped with two accelerating-focusing electrodes. Best operation requires a net energy of 30 to 40 thousand electron volts for ions leaving the acceleration section. The ion beam next enters the vacuum box where it is analyzed (components separated according to charge/mass ratio) with a six-inch electromagnet shown in Figures 1 and 15.

The target assembly, cf. Figure 16, is contained in a pyrex tube which isolates the assembly electrically. A positive voltage may be applied to the deceleration cup and target, reducing the ion energy to the desired value. The cup may be biased relative to the target in order to return secondary electrons to the target or, alternately, to collect secondary electrons on the cup.

The vacuum system consists of a six-inch diffusion pump equipped with a freon cooled baffle, a cryogenic pump in the form of a liquid nitrogen filled container, Figure 15, located inside the vacuum box, and for many runs, a liquid nitrogen cooled cup surrounding the target, cf. Figure 1. Base pressure in the low 10^{-7} mm Hg range and running pressures in the low 10^{-6} mm Hg range are usual.

XENON TEST STAND

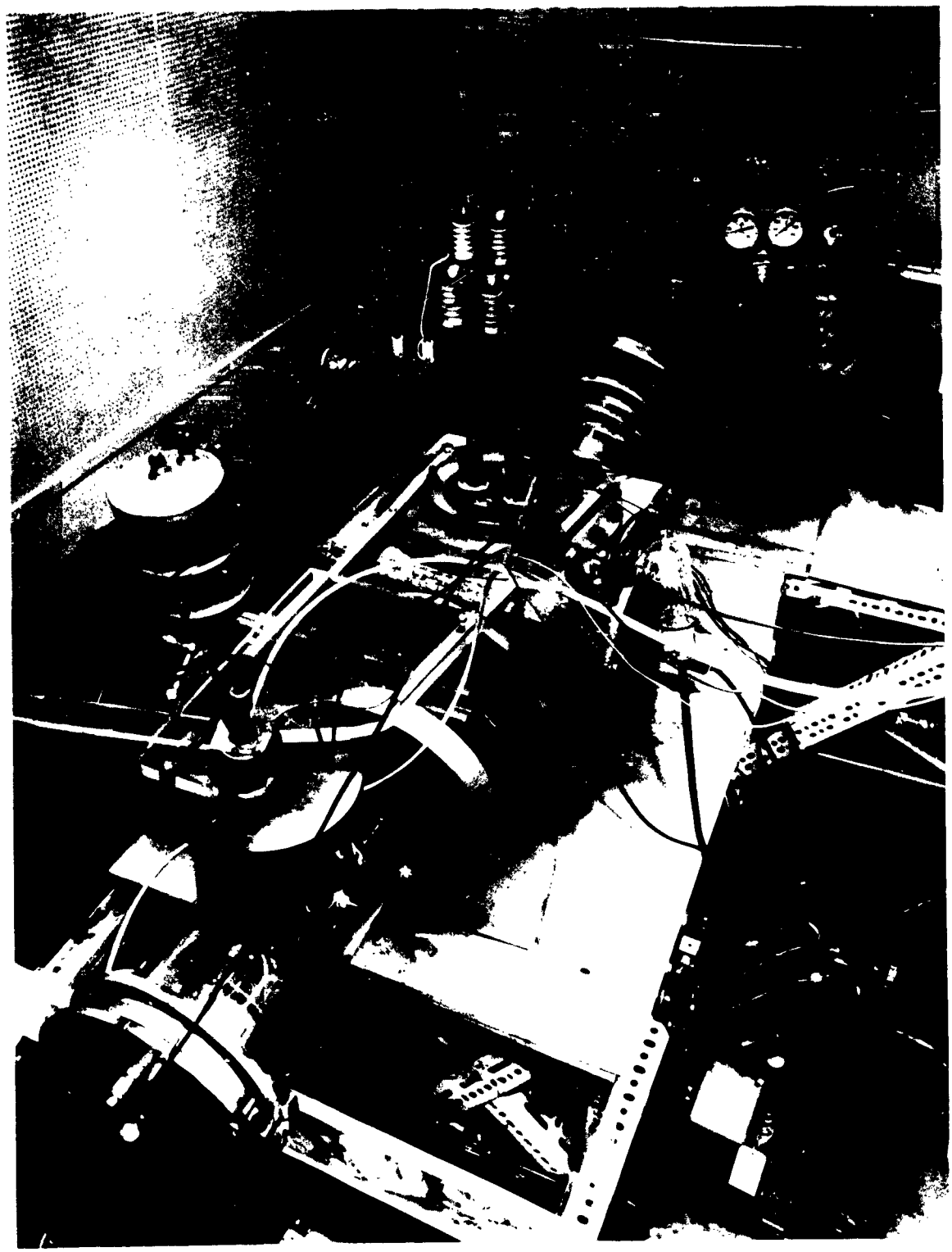

FIGURE 13

SCHEMATIC OF NOBLE GAS TEST STAND

ELECTRIC CIRCUIT

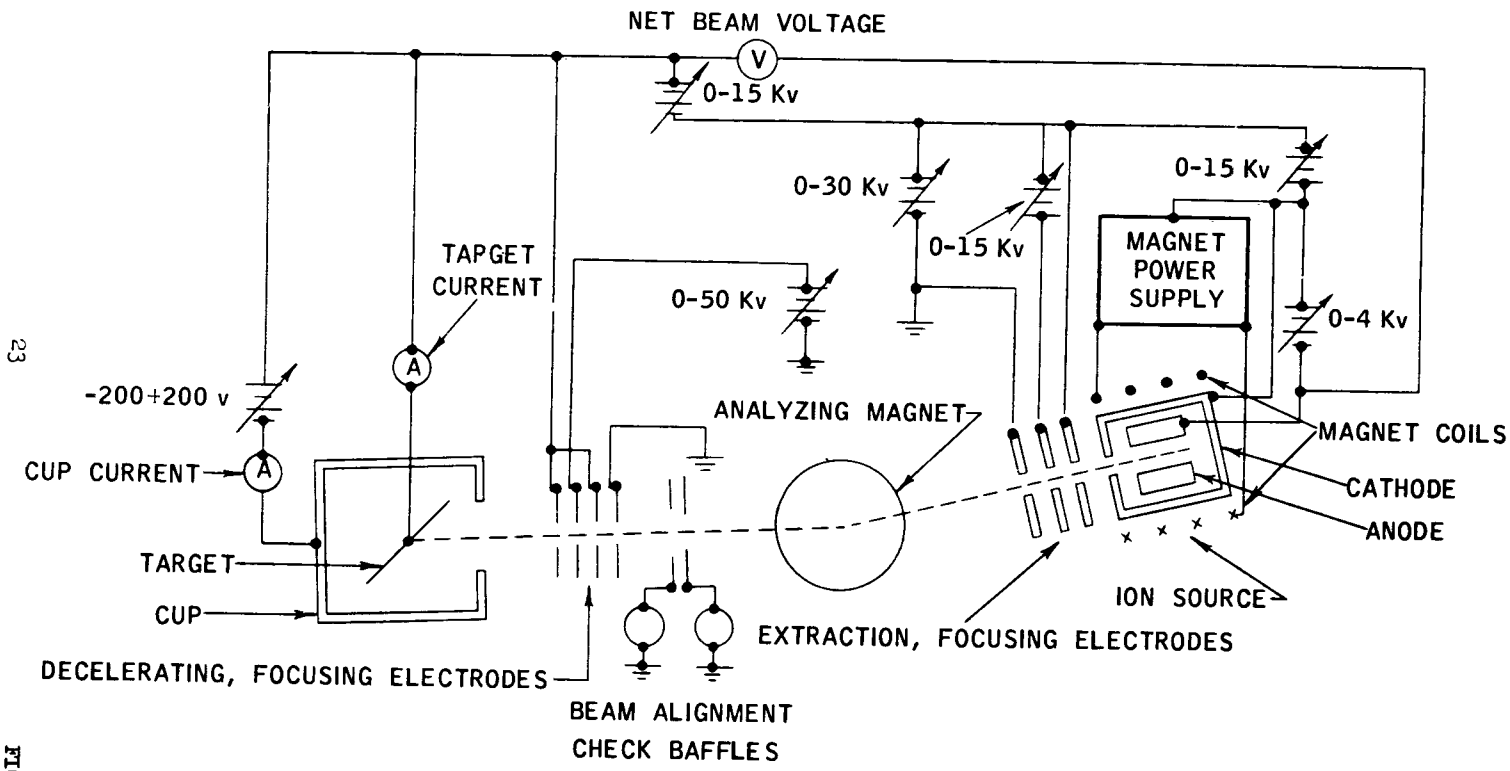

FIGURE 14

TYPICAL CONFIGURATION FOR DECELERATED BEAM

R-13,923

INTERNAL VIEW OF SPUTTERING TEST STAND

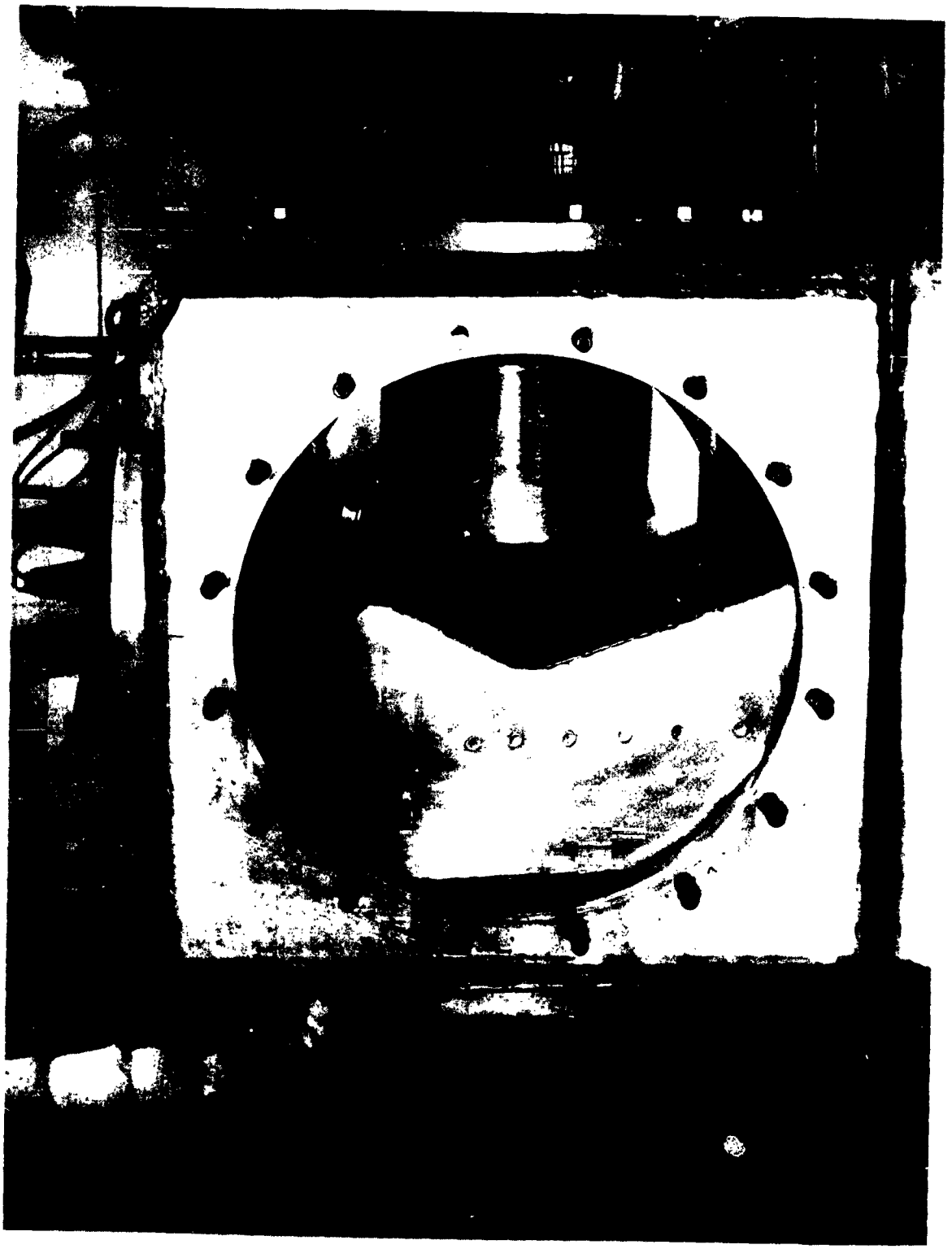

FIGURE 15

ROTATING TARGET HOLDER AND SECONDARY PARTICLE DETECTOR

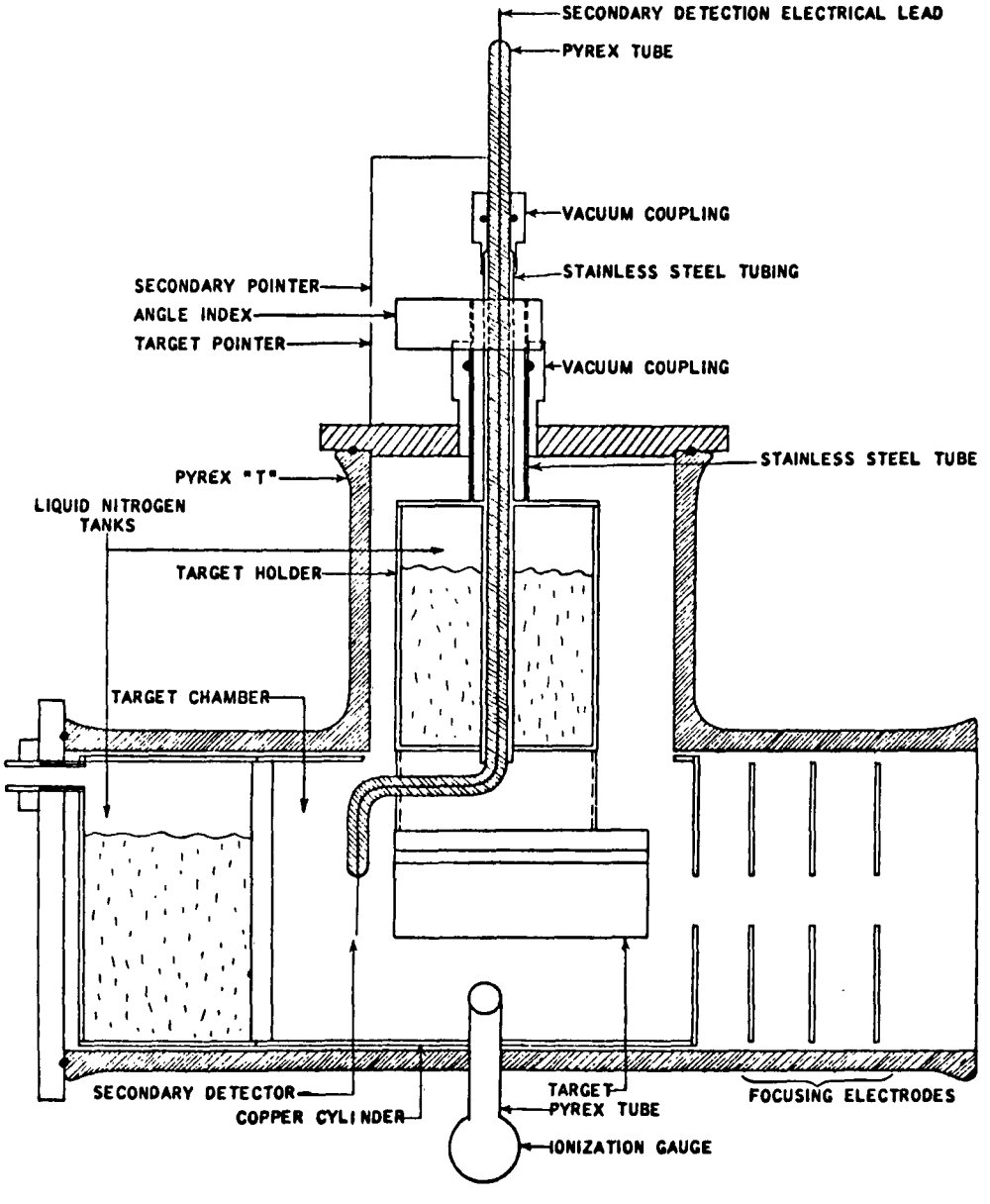

R-12,385A

FIGURE 16

A series of target holders and target chambers have been designed to permit increasingly accurate and flexible data gathering. The original target chamber along with a typical target holder is shown in Figure 17. This system was used for all the krypton and argon runs and some of the high incidence angle xenon runs.

The original deceleration cup did not have enough room for single targets of sufficient length for use at incidence angles less than 30°. A new deceleration cup was constructed which permitted the use of a long target. Sputtering ratio data for angles between 2° and 10° were obtained, with a few exceptions using this target holder, a sketch of which is shown in Figure 18. At very low angles, part of the ion beam misses the target; this portion of the beam must be isolated if the current carried by the ion beam striking the target is to be measured. Downstream of the target chamber proper, a second chamber was constructed as illustrated in the figure, with a collecting plate biased positively with respect to its surroundings. Any portion of the ion beam which misses the target strikes the collecting plate in the second chamber and any secondary electrons produced there are returned to the collecting plate. The mark produced on the collecting plate by the ion beam grazing the edge of the target was used to provide a direct measure of the angle of incidence of the beam on the target.

The cup and the target holder used for low temperature sputtering runs and secondary particle runs is shown in Figure 16. The cup is designed to surround the target with liquid nitrogen cooled surfaces, which will act as a cryogenic pump for the system as a whole, and more important, reduce the pressure seen by the target below the over-all system pressure. According to Yoda and Siegel (32), a system of this type may reduce the effective pressure at the target by two orders of magnitude. For low temperature runs, the tank of the target holder was filled with liquid nitrogen. The entire target assembly can be rotated during a run, this feature was particularly valuable in determining the zero beam-target angle as a reference in measuring other angles. Angles obtained from this holder were reproducible to + 1/2°. The secondary particle detector feed-through rotates with the target holder but permits the detector to be moved independently.

The detector shown schematically in Figure 19 was used to determine the angular distribution of secondary particles. The detector and target rotated independently around a common axis and could be rotated during a run. The detector proper was surrounded by a grounded shield to minimize the perturbations introduced by a biased detector on the angular distribution of the secondaries. An electrode between the detector and shield was included to permit further control of the secondaries reaching or leaving the detector.

A bare wire, as shown in Figure 16 was used in place of the shielded detector for preliminary tests. This unshielded detector could be used much closer to the primary beam than the more bulky shielded detector, and detected particles coming from any direction.

2. Errors and Measuring Instruments

The limiting factor in the accuracy of the results of the sputtering ratio measurements was in all cases the measurement of the mass change. The mass changes were small and the time required to obtain them was large. A nominal error

TARGET HOLDER AND CUP

FIGURE 17

LOW ANGLE TARGET HOLDER

FIGURE 18

SECONDARY PARTICLE **MEASURING CIRCUIT**

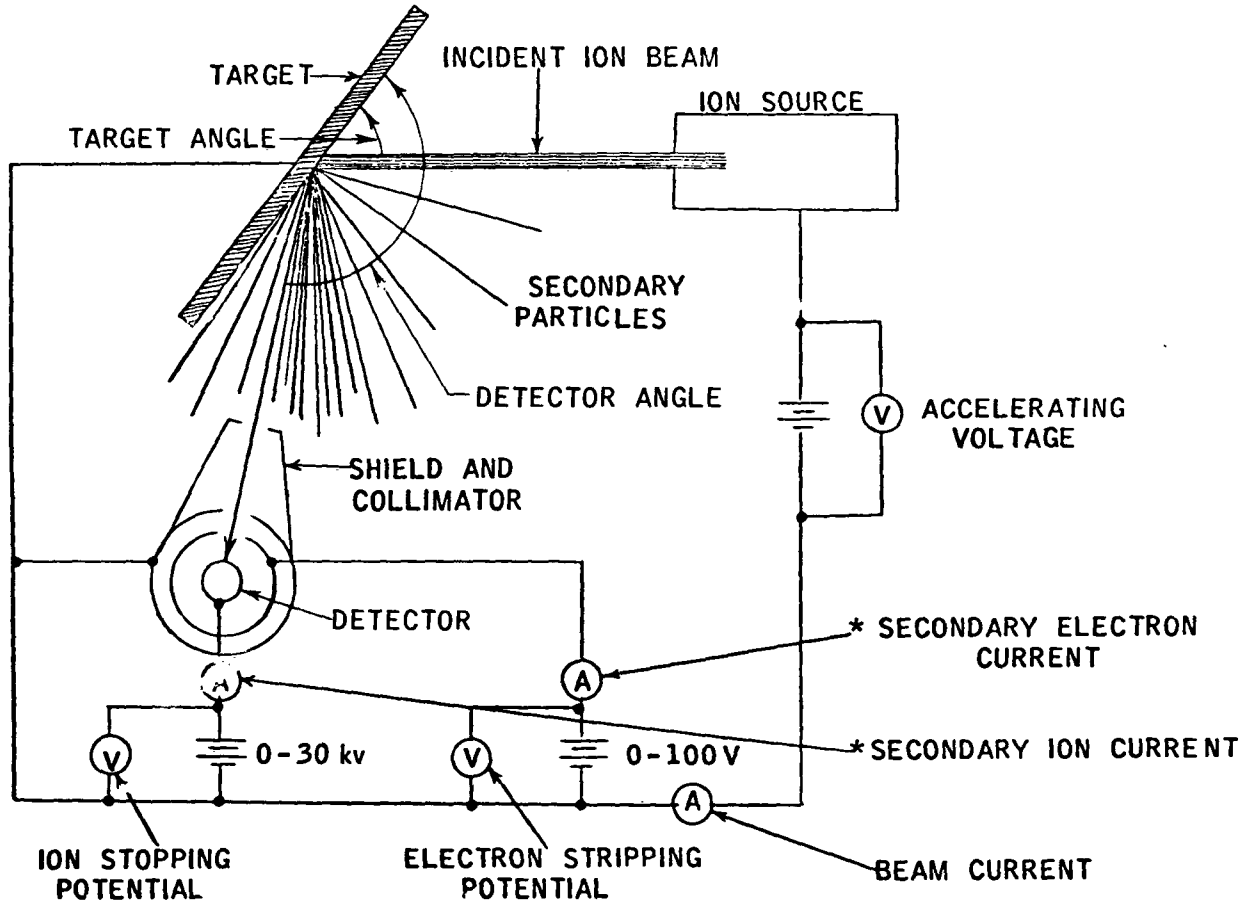

FIGURE 19

* ONLY A SAMPLING AT A PARTICULAR ANGLE OF TOTAL LEAVING THE TARGET

R-12,384 A

of 10% was chosen as striking a reasonable balance between time consumed and results obtained. No effort was taken to obtain current or voltage measurements more accurately than 5% although the instruments, when calibrated, were always found to be accurate to 2-3%.

The limiting factors in the secondary measurements were not the instruments at all but the surface condition of the targets and the experimental difficulties involved in collecting charged particles. The instrumental error was in the 5% range but the real errors were probably much larger. Every effort was made to take data regarding a specific effort (i.e. angular distribution of secondaries) in such a fashion that it was internally consistent even if the absolute values were in error.

All errors quoted are estimated experimental errors with the exception of 30 Kev xenon bombarding copper at normal incidence at room and liquid nitrogen temperatures, which are standard deviations.

Mass changes due to sputtering were determined by weighing the targets before and after each run. Most of the weighing was done on an Ainsworth "Right-A-Weight" with a precision of $\pm$ 0.1 milligrams. A Mettler M5 microbalance with a precision of $\pm$ 0.001 milligrams was used in the latter part of the program, in particular for all low and high temperature runs.

Current measurements were generally made with 5% panel meters. For the latter sputtering runs and almost all secondary measurements, Hewlett-Packard Model 425A microampere meters were used, these meters are also rated as 5% instruments. The output of one of these microampere meters, used as an amplifier, was recorded on a Honeywell 906C Visicorder for all angular distribution measurements of secondary runs.

The beam-target angle for most low incidence angle runs was determined by observing the spot sputtered on the collector (cf. Figure 18). This spot showed a straight edge where the beam was cut off by the target. The right triangle formed between this mark, the edge of the target and the intersection of an extension of the target and the end plate had an acute angle very close to the beam-target angle. The error was taken at a nominal 1° although it was probably smaller in most cases. The rotating target holder greatly simplified the problem of determining the beam-target angle. The target was rotated until only the edge was exposed to the beam, then adjusted until the target current was a minimum. This setting was easily reproducible to $\pm$ 1/2°.

When a bare wire was used for a secondary detector its angle relative to the target could be accurately determined by setting the target edgewise to the beam then locating the detector in the center of the shadow produced downstream of the target. The shielded detector proved to be somewhat of a problem to align, primarily because it could not be rotated significantly past 180° (cf. Figure 18). Only half of the target shadow could be observed, and the center could not be estimated precisely. Finally, a profile of the beam was obtained with the target removed and the center of this profile taken as 180° when the target was at 0° (see Figure 19). The angles obtained with the detector are internally consistent to $\pm$ 1° for the copper and tungsten runs individually but the copper and tungsten angles may differ from each other (and the correct angle) by as much as 5°.

C. Experimental Procedures and Results

1. Introduction

a. General Aspects of Sputtering

The motivation for various experimental procedures and the significance of the results obtained will be best understood by referring to some empirical results and their interpretations presented below. A more complete discussion of sputtering theory is given in Section II-A. Sputtering may be pictured as following from collisions between the primary ion and target atoms and the collisions subsequantly induced between target atoms.

The typical sputtering ratio vs. ion energy plot rises with energy to a peak in the tens of thousands of electron volt energy region, then begins to level off or even decrease, as shown in Figure 20 below:

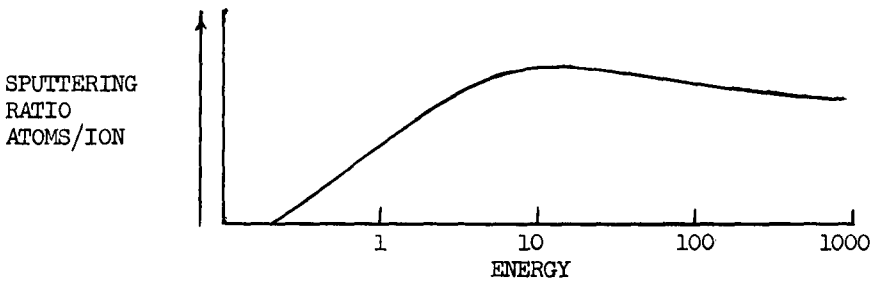

SPUTTERING RATIO VERSUS ENERGY FIGURE 20

The rise of the sputtering ratio is simply the result of more energy becoming available to remove target atoms, while the decrease at higher ion energies occurs because the ions penetrate farther into the target and give most of their energy to atoms too deeply buried to escape from the surface.

As the angle of ion incidence decreases from 90° to grazing incidence, the sputtering ratio first increases, then decreases, dropping rather abruptly in some cases (cf. Figure 21). The increase in sputtering with decreasing incidence angles probably results from the ions remaining nearer the surface and directing more energy toward the surface. The decline in sputtering ratio at low incidence angles seems to result from ions escaping from the target while retaining most of their energy, after a single collision for example. Alternately, an ion can give a large percentage of its energy to a single target atom which immediately escapes without communicating a significant amount of energy to adjacent atoms.

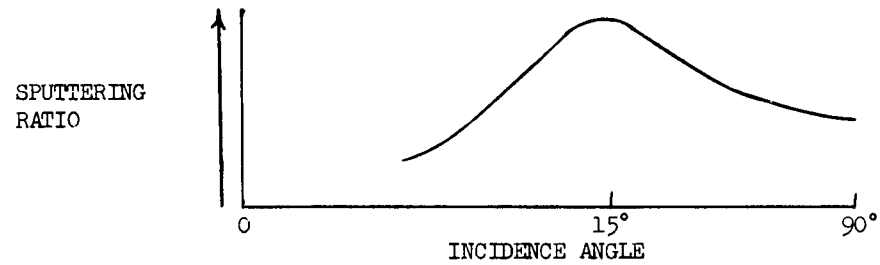

SPUTTERING RATIO VERSUS ANGLE OF INCIDENCE

FIGURE 21

The mechanism of the production of secondary ions and electrons seems to be largely unknown and at high energy the experimental data is sparse and unreliable. That the number of secondaries produced, positive and negative, increases with ion energy is well-established. The number and energy of positive or neutral secondaries increases as the incidence angle goes toward grazing incidence. There is some evidence that the secondary electron ratio may decrease at very low angles. The secondary ratios are extremely sensitive to contamination of the target; therefore, great care is required to acquire data applicable to the clean metal surface.

Sputtering ratios were calculated from the measured mass change of the target and the total number of ions which struck the target, as measured by the beam current. Electric current measurements were complicated by the presence of secondary particles, both positive and negative. There are often a great number of secondary electrons, and usually a small percentage of positive secondaries. The method of determining the target current was to insure, when possible, that all the ion beam struck the target, which was biased positive relative to a surrounding cup (cf. Figure 14) and to assume that the sum of the indicated cup and target current readings was the true target current. It was found that despite every precaution, it could not be insured that none of the secondaries accelerated toward the cup would escape through the hole necessary to admit the incoming ion beam. This procedure did however insure that this lost current was only a small percentage of a secondary current which was itself much less than the beam current. Therefore it could not seriously affect the beam current reading.

At very low incidence angles the beam was wider than the projected width of the target and provisions had to be made to handle the portion of the beam missing the target. The low angle target holder shown in Figure 22 was therefore designed. The portion of the beam missing the target was isolated and any secondary electrons were suppressed by the positive bias of the downstream ion collecting plate relative to the cup.

Some objection might be raised on the uncertainty in the measurement of the mass removed from the target due to the possibility of bombarding ions remaining in the target and decreasing the apparent mass change. Almen and Bruce (24) have shown, however, that for metal targets, this effect is negligible compared to the mass change considered here.

LOW-ANGLE TARGET HOLDER

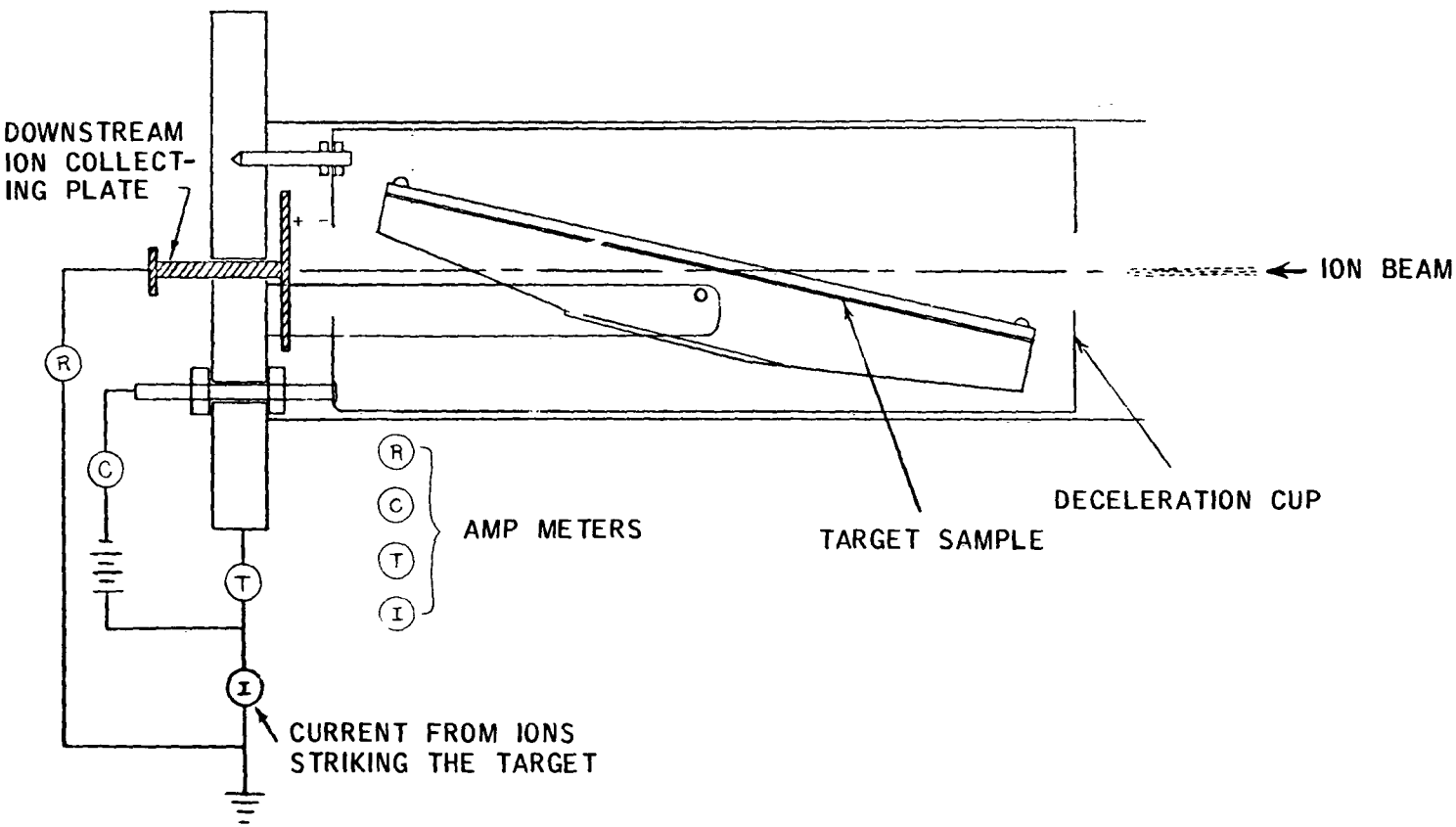

R-10,394A

FIGURE 22

2. Sputtering Ratios

a. Argon Ions

The effect of incidence angle on the sputtering ratio of argon ions incident on non-electropolished copper is illustrated in Figure 23, which compares The Marquardt Corporation's data with a curve from Molchanov (28), along with similar curves for xenon on electropolished and non-electropolished copper. The fact that these argon curves were obtained at a variety of ion energies should be kept in mind when comparing them. Molchanov's data were taken at 27 Kev while The Marquardt Corporation's data were taken over a small range of ion energies, centering around 37.3 Kev. It is well-known that the sputtering ratio of argon on copper is relatively insensitive to ion energy in this energy range, therefore the curves should be at least roughly comparable. The fact that the maximum of the 37.3 Kev curve appears to occur at 20° may be due to the absence of an experimental point between 10° and 20°. The comparatively sharp descent of the 37.3 Kev argon curve with decreasing incidence angle starting from a higher angle than the 27 Kev curve could be either an energy dependent effect or the result of different surface smoothness of the targets used in the two series of tests. The last explanation seems to be favored by the evidence of the xenon curves. Here the curve for the smoother targets drops off sharply from a higher angle (15°), as theory (cf. Section II-A) would predict.

b. Xenon Ions

In order to simulate the sputtering of cesium as closely as possible with a noble gas (the Penning ion source operates well only with noble gases), xenon ions were employed for most tests. The mass of xenon is 131.3 amu and that of cesium is 132.9 amu, therefore, all mass dependent sputtering effects should be nearly identical. This assumption has received experimental support through the published sputtering ratio data of Kuskevics (19) for cesium on various metals at 2 Kev energy, which matched closely with those of The Marquardt Corporation for xenon. These data were compared in Section II-A and the sputtering ratios were found to be quite similar.

Almost all of the tests were intentionally designed to investigate a specific effect. The tests for dependence of the sputtering ratio on the target temperature, for example, were conducted with copper targets and with ions having 30 Kev energy. The 30 Kev energy was chosen strictly for experimental reasons: high sputtering ratio, high current density, due to good focusing, and the fact that the target assembly could be maintained at ground potential. The latter fact facilitated handling the rotating target and detector and measuring the very low currents. The reasons for the choice of copper for the target material were: 1. its high sputtering ratio, 2. the large body of knowledge on its sputtering characteristics, and 3. the interest in the low boiling point materials of this type for the electrodes of contact ionization sources.

Several other materials were investigated. Tungsten and molybdenum were sputtered over a wide range of energies and angles while titanium, silicon and tungsten carbide were sputtered at 30 Kev and normal incidence.

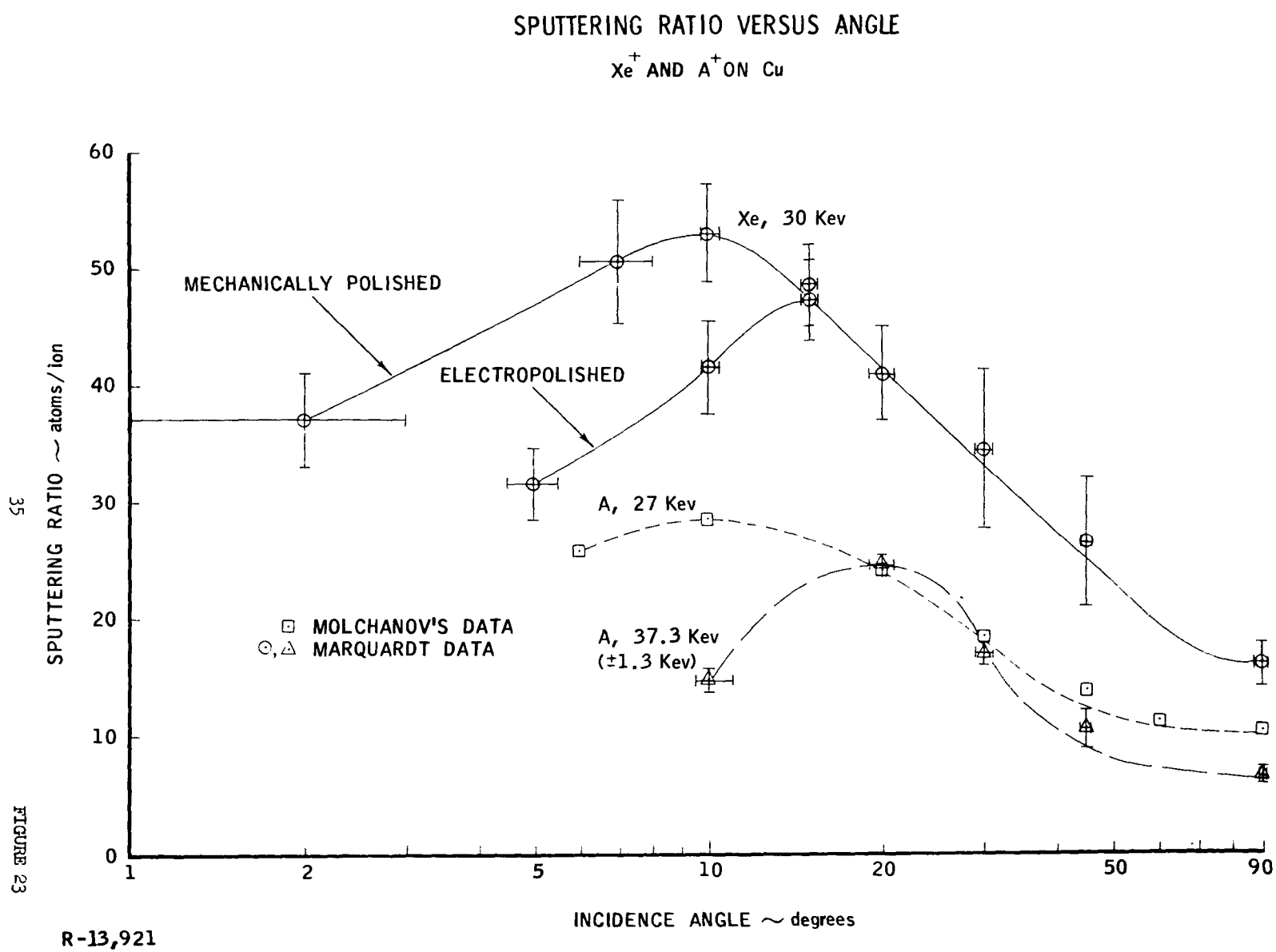

FIGURE 23

R-13,921

i. Copper

Electropolished copper targets were sputtered at ion incidence angles from 2° to 90° and at energies from 1.5 to 30 Kev. The range of values considered is best illustrated by the equi-sputtering ratio graph, Figure 24. Here contours of equal sputtering ratio are plotted with ion energy and angle of incidence on the coordinate axes. The experimental points obtained in this program are circled. The base vacuum for these runs was in the low 10^{-7} mm range and the running pressure was in the 10^{-6} mm range. Beam current was 10-20 microamps, and beam diameter was 1-2 cm.

The effect of target surface condition on sputtering at low angles is illustrated in Figure 25. The sputtering ratio of electropolished copper is found to drop off at larger angles and much more steeply with decreasing incidence angle than that of mechanically polished copper.

The effect of incidence angle on the sputtering ratio vs. energy curves is shown in Figure 26; data points have error bars, interpolated points (from Figure 25) do not. It is clear that the angular dependence of the sputtering ratio becomes much more striking above 10 Kev and below 15°. This same effect can be seen in Figure 24, the equi-sputtering ratio graph.

ii. Molybdenum and Tungsten

These metals were sputtered under the same conditions of vacuum, beam current, and beam size as was copper; however, the surface condition of these targets was much rougher than that of the copper because electropolishing was not successful. This surface roughness probably accounts for the peaking of the sputtering ratio curves at 10°, in Figure 28. This is a smaller angle than that found for copper while a larger angle might have been expected. This roughness would account for the leveling off of the sputtering ratios below 5°, since as illustrated in Figure 27 the ratio based upon the effective angle of incidence would remain relatively constant at very low apparent incidence angles.

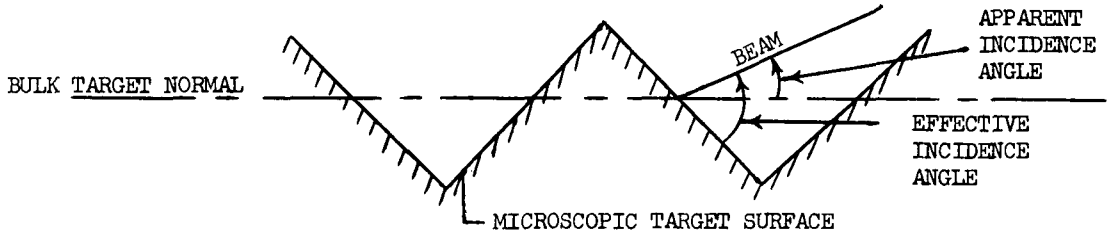

EFFECTIVE ANGLE OF INCIDENCE

FIGURE 27

A striking feature of Figure 28 is the reversal in the relative magnitudes of the tungsten and molybdenum sputtering ratios between 9.5 and 30 Kev; evidently molybdenum is much more sensitive to energy changes in this region than is tungsten. This effect is also evident in Figure 29 which shows the energy dependence explicitly. It seems probable that molybdenum is approaching a maximum in its sputtering ratio vs. energy curve while tungsten will reach its maximum at a much higher energy.

ENERGY versus ANGLE

WITH CONSTANT SPUTTERING RATIO CONTOURS

Xe^+ into Cu

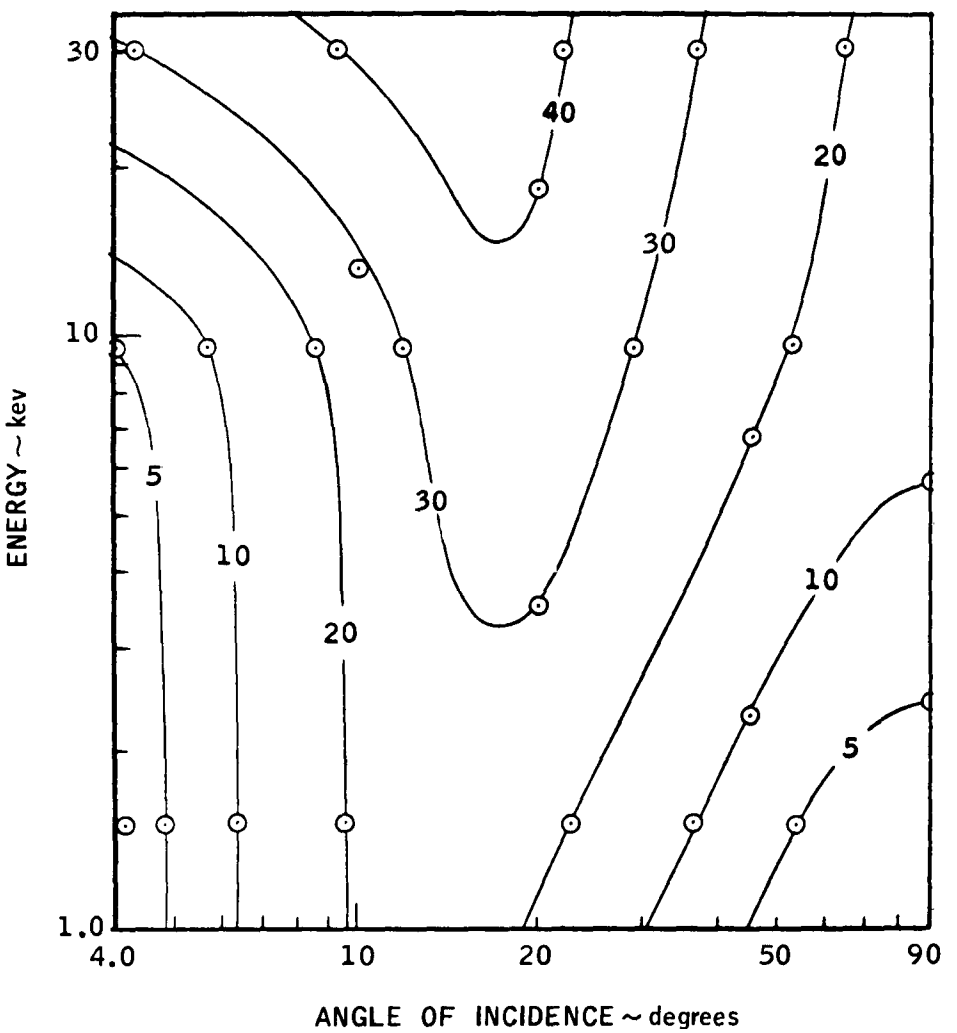

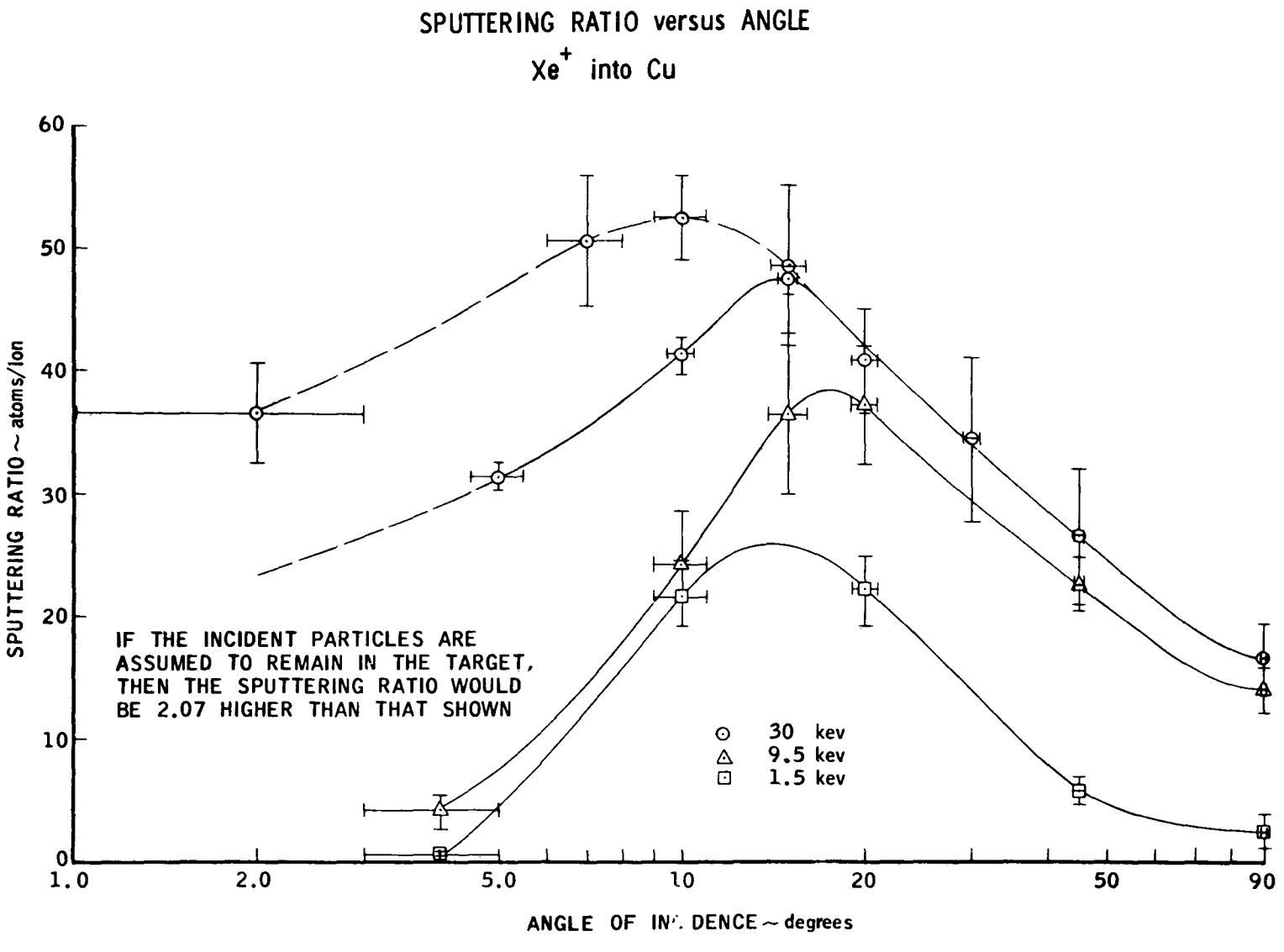

FIGURE 25

R-11,512B

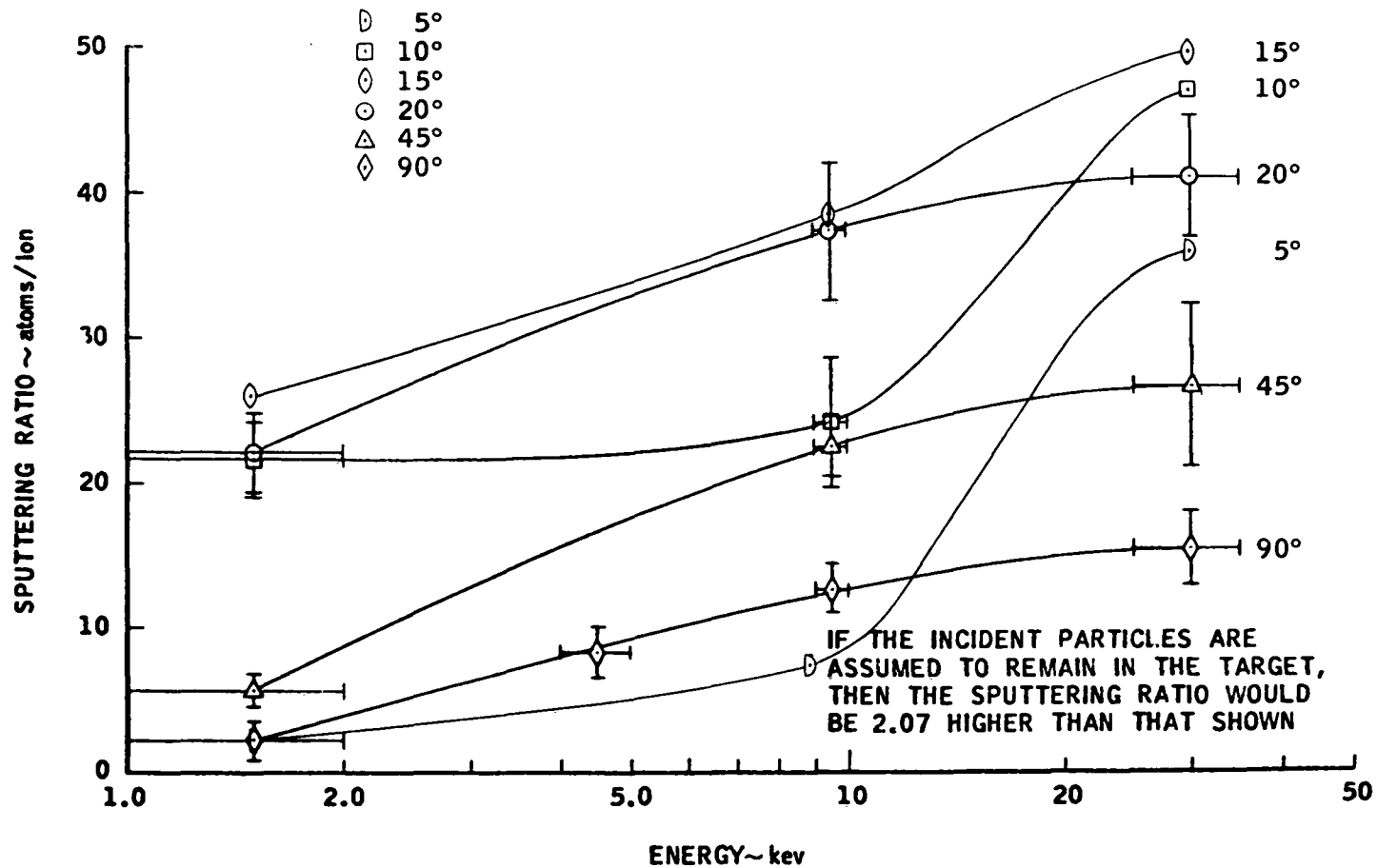

FIGURE 26

R-11,514B

SPUTTERING RATIO versus ANGLE

Xe^+ into Mo and W

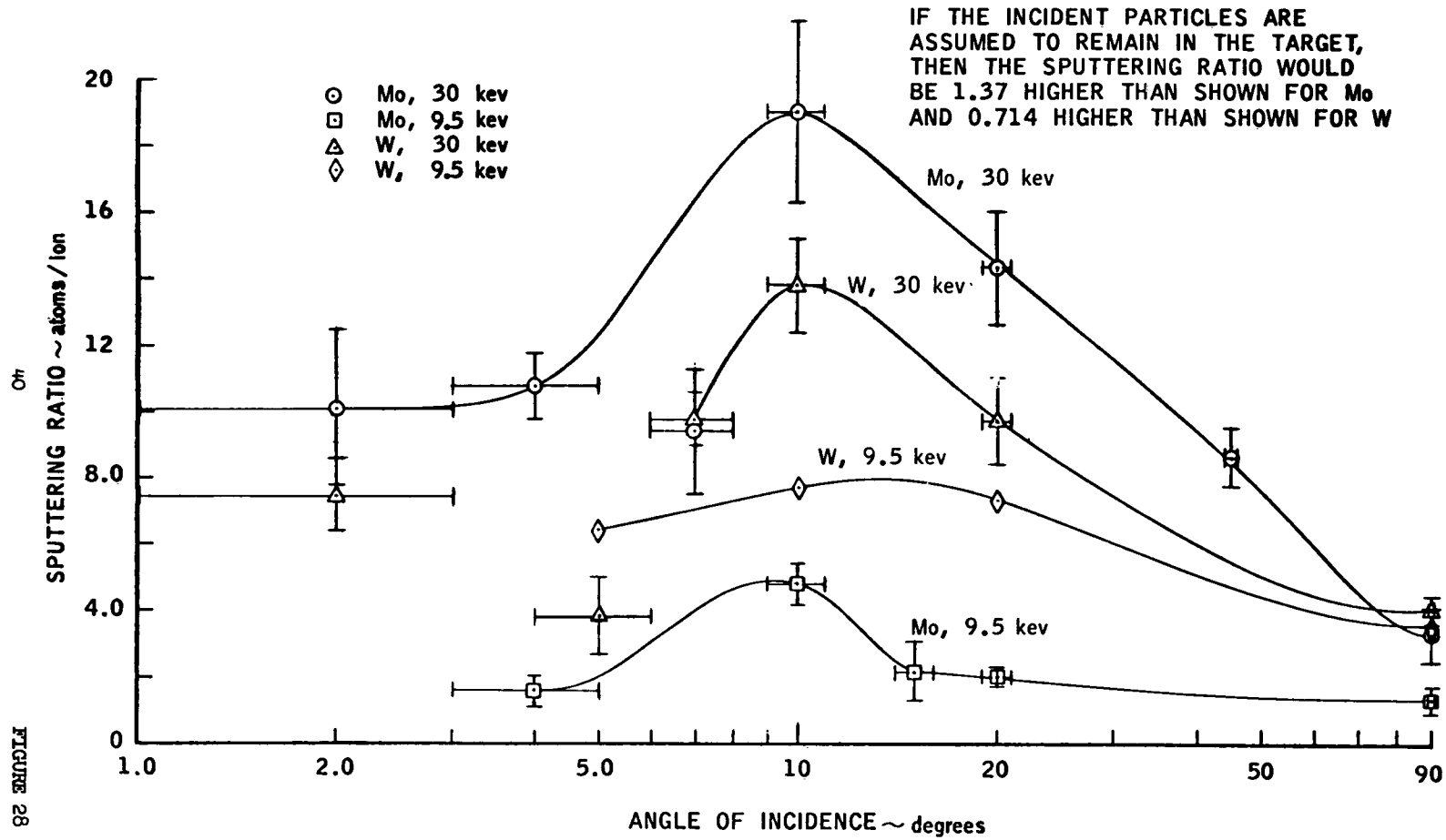

FIGURE 28

R-11,513B

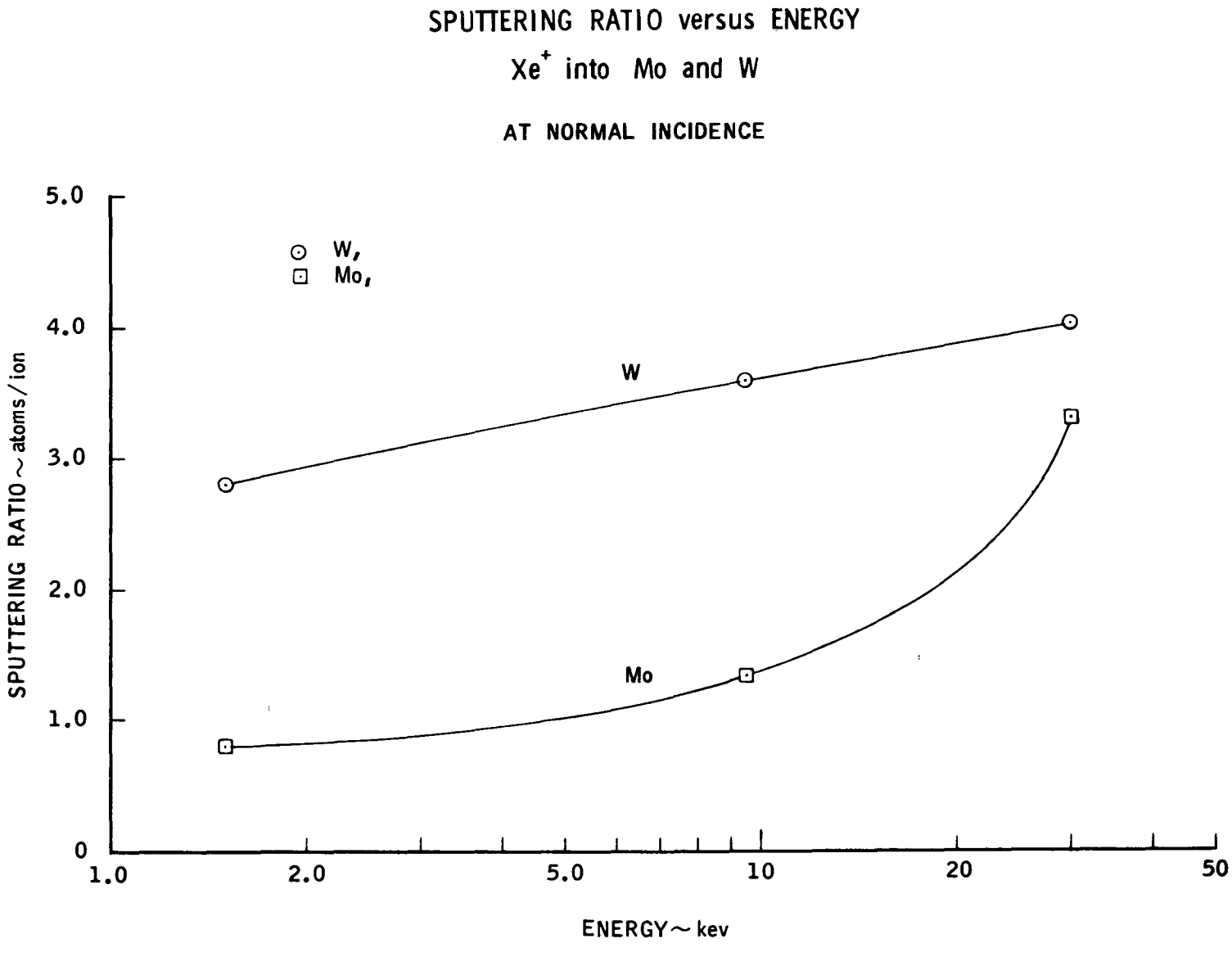

FIGURE 29

R-11,750

iii. Tungsten Carbide

Two differently prepared samples of tungsten carbide were sputtered and gave surprisingly similar sputtering ratios. A plasma sprayed sample yielded a sputtering ratio of 6.0 while a target in which the tungsten carbide was contained in a nickel matrix yielded a sputtering ratio of 8.7, both with xenon ions normally incident with 30 Kev energy. These values are considerably greater than the corresponding sputtering ratio for tungsten of 4.0 ± 0.4. The beam current was about 10 microamps on a spot of approximately 0.5 cm diameter. The target was surrounded by the liquid nitrogen cooled cup.

iv. Titanium

One run was made with titanium under conditions exactly as described above for tungsten carbide; the sputtering ratio was 13.5 ± 1.3.

v. Non-Metallics

Lithium hydride, sodium chloride and single crystal silicon were sputtered with xenon ions at normal incidence and 30 Kev energy but only the silicon yielded any results, a sputtering ratio of 24.8 ± 2.6. In view of the very low sputtering ratios reported by Wehner (33) for silicon even this result appears questionable. Wehner obtained 0.5 atoms/ion at 600 ev with xenon while he obtained a sputtering ratio of 2.5 with a copper target. Almén (24) found this same general ratio using krypton ions at 45 Kev on silicon and copper. Since carbon and silicon have similar sputtering ratios at low energies this reasoning implies that silicon would also have a low sputtering ratio at high energies.

Any of three factors may have contributed to the problems encountered with these materials. First, they are all much lighter than xenon, therefore if an appreciable percentage of the xenon remains in the target the target could actually gain weight. Second, the sputtering ratio may have simply been too low to be detected under the conditions of these runs. Third, since these materials are insulators there were experimental difficulties involved with charge buildup on the surface.

This surface charge could decelerate the beam or possibly entirely repel it. The lithium hydride and silicon targets did not seem to give any trouble of this type, at least the beam remained focused, as evidenced by the mark sputtered on the target, and the current measurements were stable. On the other hand, small arcs from the crystal surface to a wire stretched across to provide neutralization continually appeared with the sodium chloride. The beam did, however, appear to remain focused on this case also.

The most striking feature of the lithium hydride runs was the attractive orange-violet glow the beam produced on the target, but no reasonable sputtering ratio data was obtained. The sodium chloride target also glowed, though not as vividly as the lithium hydride one. After sputtering, violet color centers also appeared in the previously colorless crystal.

3. Cold Target Sputtering

As was discussed in detail in the theoretical section (II-A), it was felt that there was reason to expect a reduction of sputtering with temperature. In order to test this hypothesis, a series of tests were made with copper targets at temperatures near 77°K, liquid nitrogen's boiling point. The target was surrounded with a liquid nitrogen cooled cup, cf. Figure 16, and the runs were made at a relatively high energy in order to reduce the possibility of enhanced surface contamination due to the low target temperature. Four satisfactory runs were obtained at normal incidence, and also one at 45°. The average sputtering ratio at normal incidence was 12.6 ± 1.9 atoms/ion as compared with a room temperature average of 15.9 ± 1.7 atoms/ion. The ± are standard deviations here. The 45° sputtering ratio was 18.6 or a factor of 1.5 times that at normal incidence; the corresponding increase in sputtering ratio was by a factor of 1.7 at room temperature. These ratios are very close, in fact essentially the same, when the experimental errors are considered.

A measure of surface conditions much more sensitive than the sputtering ratio is the secondary electron ratio. By this test, at least, the conditions involved were far from reproducible; the range of measured secondary electron ratios had a spread of over 50% and the ratio varied as much as 25% during many runs.

A real reduction in sputtering ratios seems to exist here although a more extensive investigation, particular of the effect of beam intensity, would certainly be of value. The beam density varied by a factor of 3, from 20 to 60 microamps/cm^2 for different runs and, within this range, did not affect the sputtering or secondary electron production appreciably.

4. Hot Target Sputtering

A short series of experiments concerning the effect of temperature on the sputtering ratio of copper was conducted. A small heater employing a tungsten resistance element inside an alumina case was used to heat the target. The target and heater were surrounded by the cup illustrated in Figure 1. Here water was used instead of liquid nitrogen to cool the cup for these experiments. This arrangement proved very satisfactory.

The results were consistent with those of Almén and Bruce (24) (as discussed in the theory section (II-A)), in that no significant deviations from room temperature sputtering ratios were found up to 600°C. Almén and Bruce point out that significant weight losses due to sublimation begin to occur at higher temperatures. A program designed to separate the effects of sputtering and sublimation would be required to examine this region in detail.

5. Secondary Particles

The number, charge, direction and energy of secondary particles have been investigated as functions of ion energy, incidence angle, target element and target temperature. Information has been obtained as to the order of magnitude of the effect of most of these variables but in almost no cases was the data reproducible to any better accuracy. This lack of reproducibility can be attributed to the extreme sensitivity of secondary production rates to surface contamination. Every effort was made to obtain the largest primary current density along with the best

vacuum possible. The data was reproducible when a focused beam was incident on a target inside the liquid nitrogen cooled cap. Due to experimental difficulties, these conditions could not be maintained for many runs. The data obtained under poorer conditions are best regarded as indicating the direction of trends and the order of magnitude of the effect.

a. Total Number of Secondaries

i. Angle

The first thing to be investigated was the total number of secondaries produced under given conditions. For the xenon on copper at 30 Kev case, these data were reasonably reproducible. A typical secondary ratio vs. incidence angle result is shown in Figure 30. The secondary current leaving the target is shown for the target biased positive and negative and for no bias. The "no bias" curve illustrates a somewhat unexpected effect which strongly influenced the secondary current vs. bias measurements discussed below. It is easily seen that the "no bias" current is not the sum of the positive bias and negative bias currents as might be expected. It appears that the "no bias" current is space-charge limited. A rough calculation indicates that the biased currents at ($\pm$ 300 v) can not be severely affected by space charge. These data were taken with a beam density of approximately 50 micro-amps/cm^2, the background pressure in the vacuum system was 2.8 x 10^{-7} mm Hg and the target was surrounded with a cooled cup. The beam remained entirely on the target down to 4° - 5°. The target was mechanically polished.

ii. Energy

All experiments have indicated that secondary particle production goes up with energy. The most graphic, and reliable, illustration of this is a curve of secondary electron ratio versus ion energy. Figure 31, taken as the energy of ions incident on a near 45° copper target was varied from 3 to 10 Kev. The points fall on a virtually straight line.

iii. Temperature

At liquid nitrogen target temperatures the secondary electron to incident ion ratio (xenon, copper, 30 Kev, normal incidence) was generally between 1 and 1.5 while the secondary positive ratios ran from 0.1 to 0.3, the order was the same for both, i.e., if a given run had a relatively high secondary electron ratio it also had a high secondary positive ratio. The secondary ratios were in the same range as those found at room temperature.

iv. Surface Condition

In some experiments mechanically polished samples were used because of the unavailability of electropolished targets; it was found that the sputtering ratio was unaffected at angles above 20°. The secondary positive production also seems to be independent of this variation of surface condition, at least at 90°, however, the secondary electron ratio for 30 Kev Xe^+ ions normally incident on copper was almost exactly twice as much for mechanically polished samples as for electropolished ones. This result might simply reflect the fact that electropolishing leaves a cleaner, less contaminated surface. It appears more probable

NORMALIZED SECONDARY CURRENT VERSUS ANGLE OF INCIDENCE

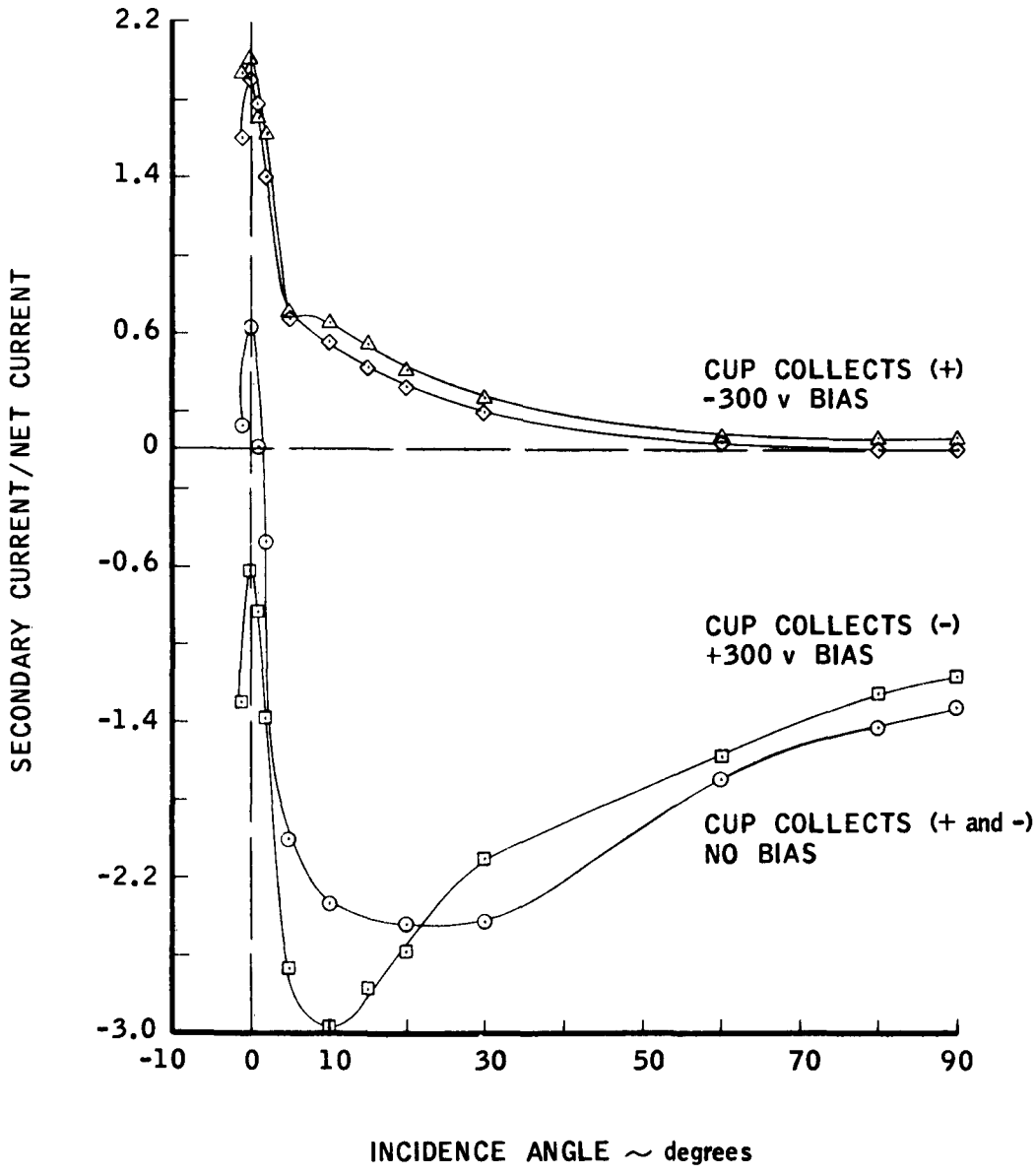

SECONDARY ELECTRON RATIO VERSUS ION ENERGY

Xe^+, Cu TARGET

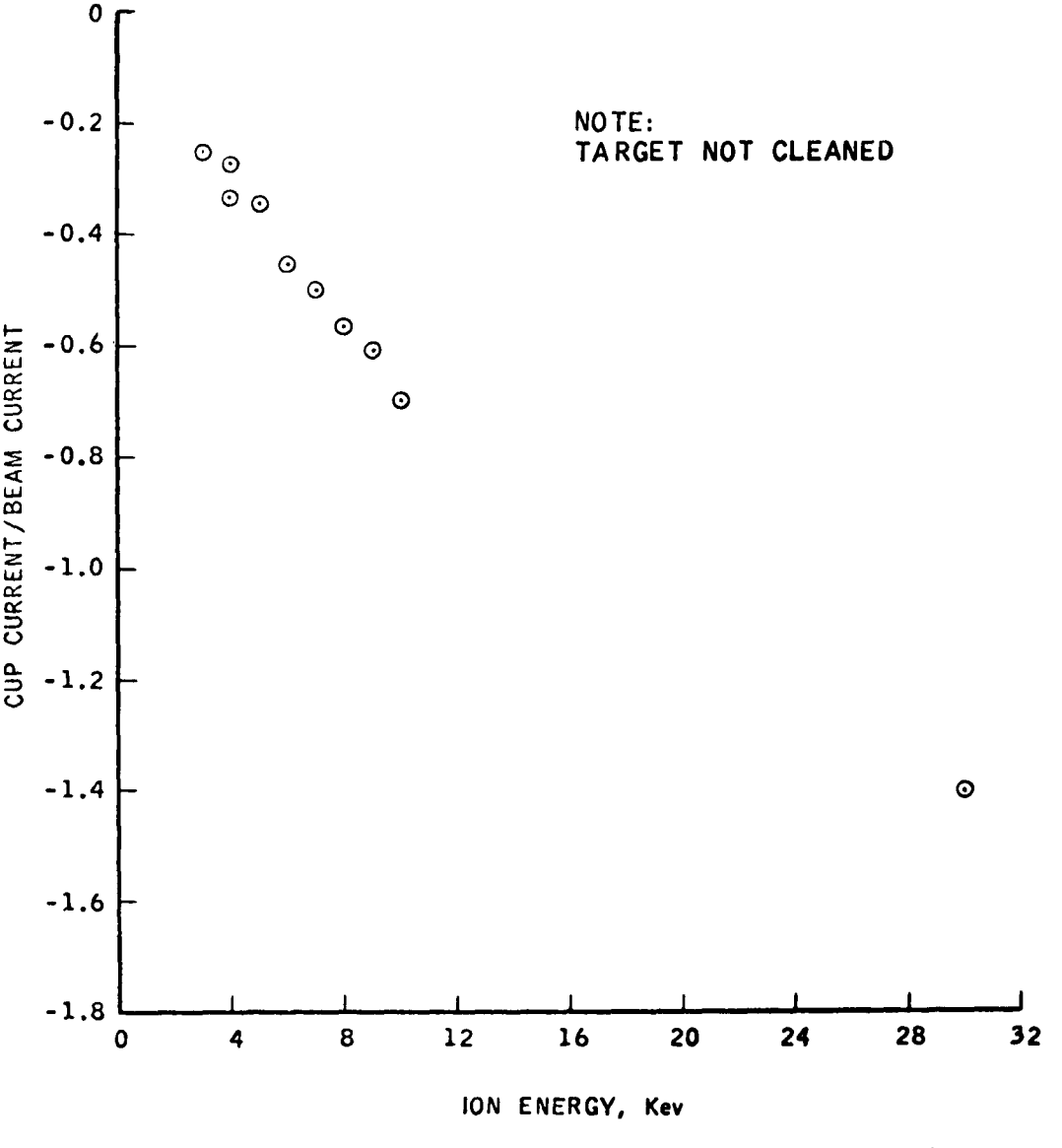

R-13,301A

FIGURE 31

that the different secondary ratios were due to variations in surface roughness since the targets were generally sputtered sufficiently to remove any surface contamination. The reproducibility of the results obtained with a mechanically polished target were very good, the spread was less than a third that of a group of electropolished targets.

b. Energy Distribution

i. Target Bias

An attempt to determine the energy distribution of secondary particles by means of a retarding potential was made, and the secondary current ratio versus retarding potentials which resulted are shown in Figure 32. A mechanically polished copper target surrounded by a cooled cup was used. The first thing to be noted is that these curves do not give a true picture of the energy distribution of secondaries, due to space charge limitations on the maximum current which could be emitted. Calculations of potentials in a "beam" of electrons and ions with energy distributions are difficult at best; here, in addition, the external fields were not well-defined due to the complicated geometry of the cup and target holder. A rough calculation indicated that the curve from approximately -50 to +50 v was almost entirely due to space-charge limitations, therefore no further experiments were conducted along these lines. There is a further limitation on this type of experiment in that many of the secondaries may not be injected directly toward the collector and may not reach it even though they possess sufficient energy. This effect and methods of dealing with it are discussed by Lukivsky (34) and Ganichev (35), to obtain a first approximation of the energy distribution, the errors due to this effect could have been ignored; however, those due to space-charge could not be tolerated. There is some information available from the curves obtained even under these rather poor test conditions. First, the secondary particle ratios are clearly established at 90° and 10°. Second, it can be seen that there are an appreciable number of charged particles present with energies as high as 100 ev.

ii. Detector Bias

An estimate of the distribution of energies of secondaries emerging at a particular angle can be made by comparing the various "Angular Distribution of Secondaries" plots. The conditions under which these data were taken and the hazards involved in their use are discussed in Section c below.

c. Angular Distribution of Secondaries

The investigation of the angular distribution of secondaries was motivated by two different observations. In one case the glow that the beam made on the target was being observed in a darkened room while the beam was being focused. It was observed that the pyrex pipe surrounding the target was glowing over a small area. When the target was rotated the glowing area moved so as to remain approximately normal to the target.

The second set of observations have to do with the decline of sputtering ratio at low incidence angles, and particularly the observations of Molchanov (28) regarding the energy carried off by sputtered or reflected particles. Molchanov observed that for argon ions incident on copper up to 22% of the energy

NORMALIZED SECONDARY CURRENT VERSUS BIAS VOLTAGE

TWO RUNS

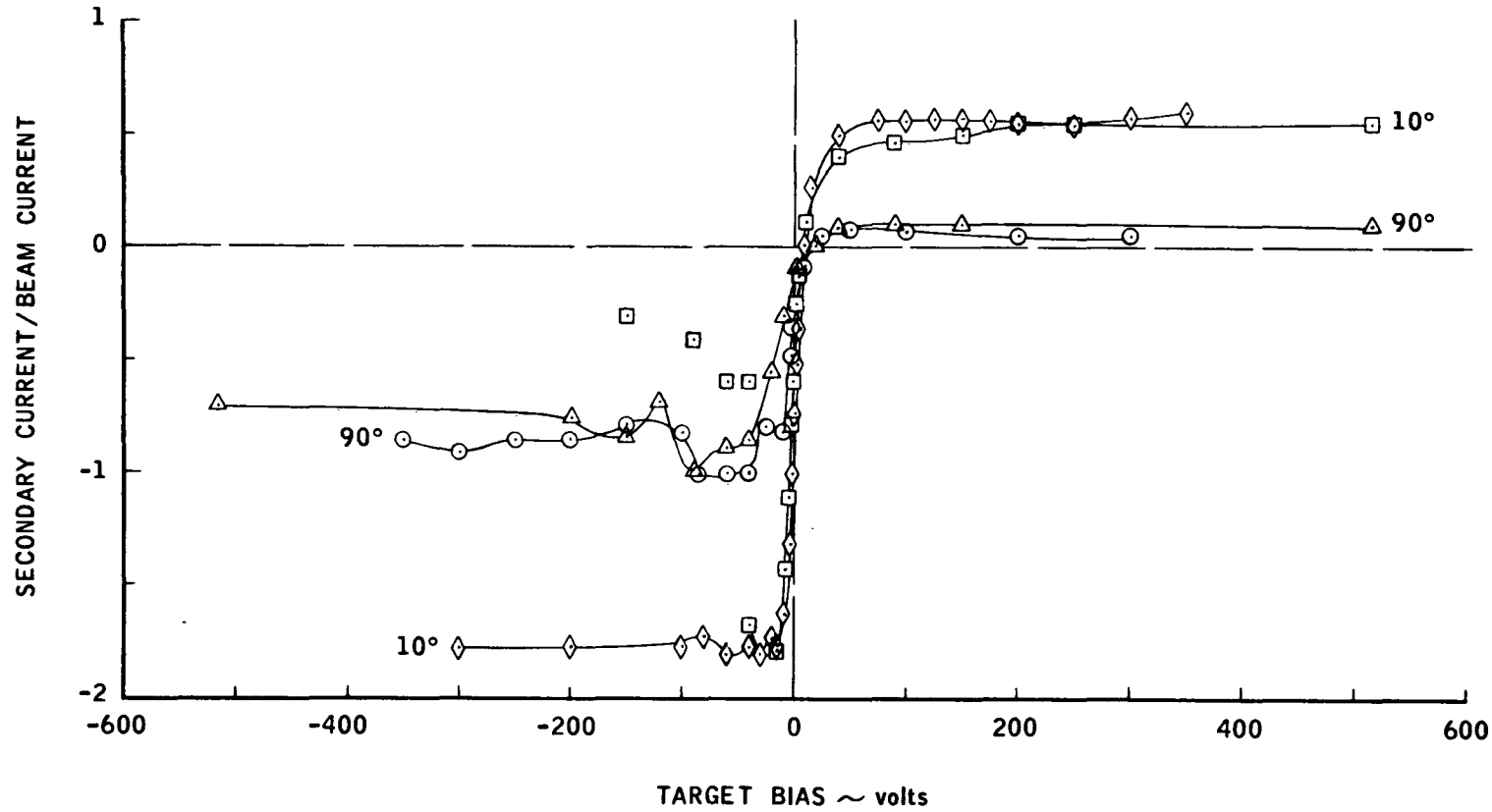

R-13,922

FIGURE 32

carried by incident ions was removed by secondary particles. It appears probable that these high energy secondaries are the result of a single collision and, as discussed in Section II-B, their angular distribution should be roughly predictable.

Three sets of experiments were conducted while investigating this distribution. A preliminary test used a highly biased (-300 v) secondary detector, cf. Figure 16, and was intended to observe high velocity positives or neutrals. The results of this test are shown schematically in Figure 33. The target is located vertically at the origin and the beam enters from the lower left. The detector currents, for beam incidence angles of 45° and 30°, are plotted in polar coordinates. The radius corresponds to the magnitude of the current and the angle is the angle at which the current was observed. The high bias on the detector attracted low energy positives and repelled secondary electrons, therefore, no significance can be attached to the absolute value of the current. The schematic plot has had a good deal of this background current removed to illustrate the structure more clearly. The results of this test were very satisfactory in that a good deal of structure was revealed.

A second series of tests was made over a much wider range of target angles using the same unshielded detector inside a bare pyrex tube. In order to be able to estimate the relative magnitude of the secondary currents observed at different target angles a half inch target entirely immersed in the primary beam was used. The primary current striking the target varied with the target angle but the results could be easily normalized. To suppress secondaries produced by the portion of the beam missing the target a screen was inserted just upstream of the end plate. The end plate was maintained 150 volts positive relative to ground, and the screen at ground potential. Any secondary electrons produced at the screen or end plate were retained by the end plate. Secondaries produced at the leading edge of the target were reduced to a minimum by beveling the edge facing the beam, cf. Figure 33. The effect of this was that secondaries from the leading edge of the target could only reach the detector when it was outside of the areas of interest and only in very small numbers even then. Figure 34 shows a typical result obtained under these conditions. Note that the detector current is not normalized to account for the amount of the beam striking the target. A feature characteristic of these unshielded detector results was the large increase in negative detector current just adjacent to the primary beam. The curve for 60° is a good example since the edge of the primary beam is shown.

The last series of runs (cf. Figures 35-47) employed a shielded detector, cf. Figure 19, and a grounded shield over the pyrex. The target (at ground) was now almost entirely surrounded by grounded conductors, therefore, the angular distributions obtained should be representative of the actual distribution uninfluenced by outside fields. It was not possible to use the liquid nitrogen cooled cup around the target so the beam density was probably not sufficient to maintain an uncontaminated target surface. The beam current density was of the order of 2 micro-amps/cm^2 and the background pressure was in the 10^{-7} mm Hg range.

SCHEMATIC - ANGULAR DISTRIBUTION OF SECONDARIES

Xe^+ into Cu, 30 Kev

BACKGROUND CURRENT REMOVED

DETECTOR BIAS -300 v RELATIVE TO TARGET

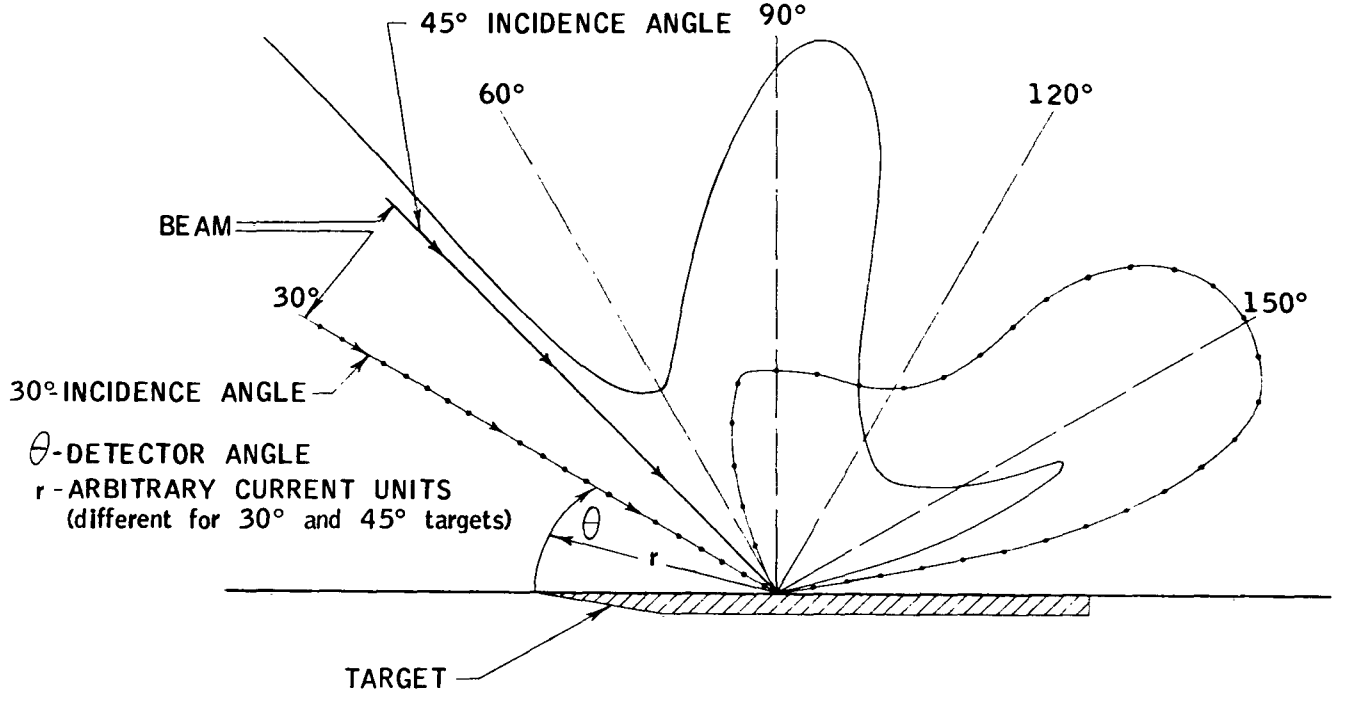

R-13,979

FIGURE 33

ANGULAR DISTRIBUTIONS OF SECONDARIES

UNSHIELDED DETECTOR, NO TARGET ANGLE NORMALIZATION
FOR ANGLES OF INCIDENCE OF ION BEAM FROM 5° TO 90°

30 Kev Xe^{+} on Cu, -1 volt detector bias

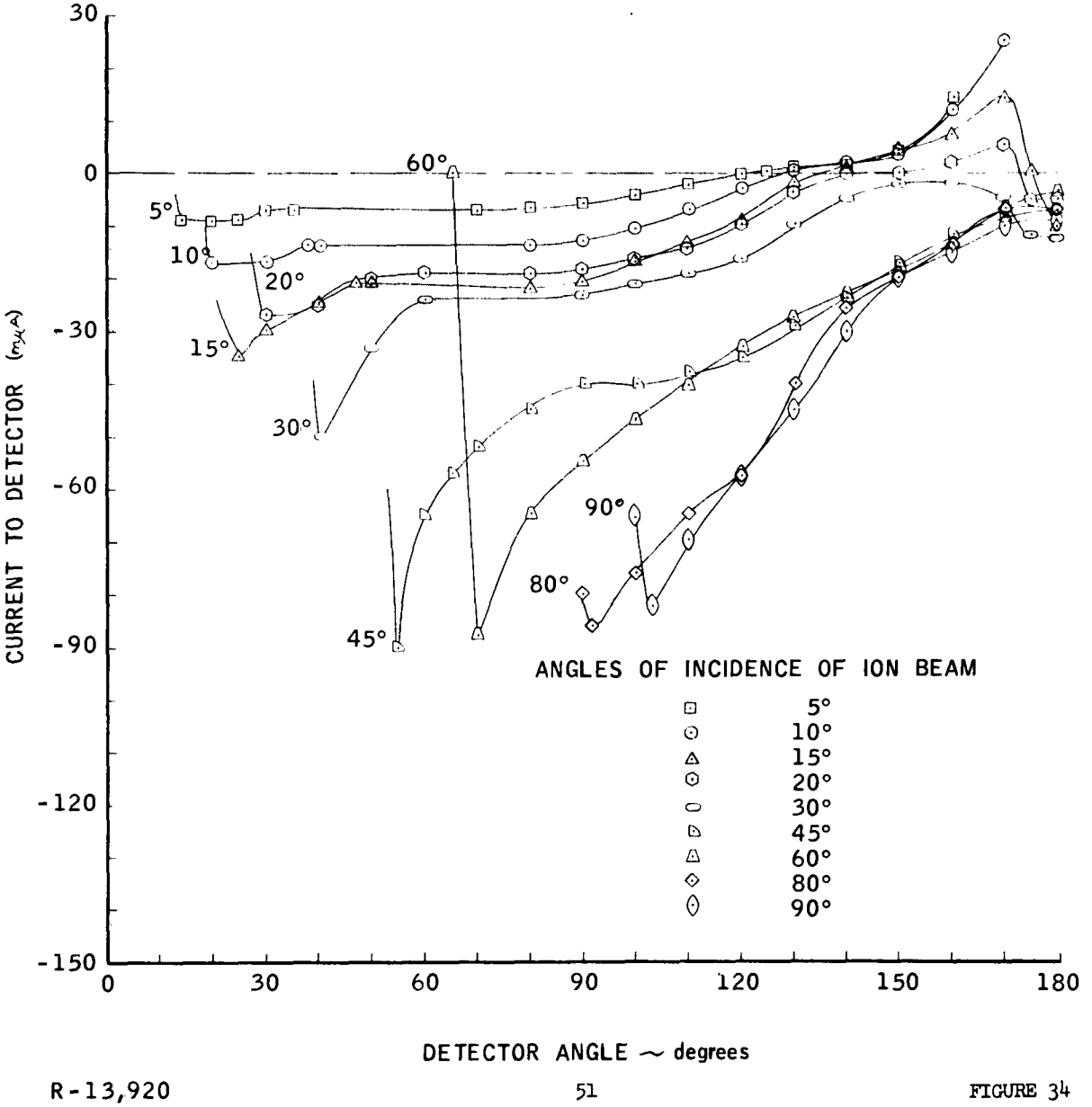

ANGULAR DISTRIBUTION OF SECONDARIES, +1v DETECTOR BIAS
Xe^{+}, Cu, 30 Kev

ELECTROPOLISHED TARGET

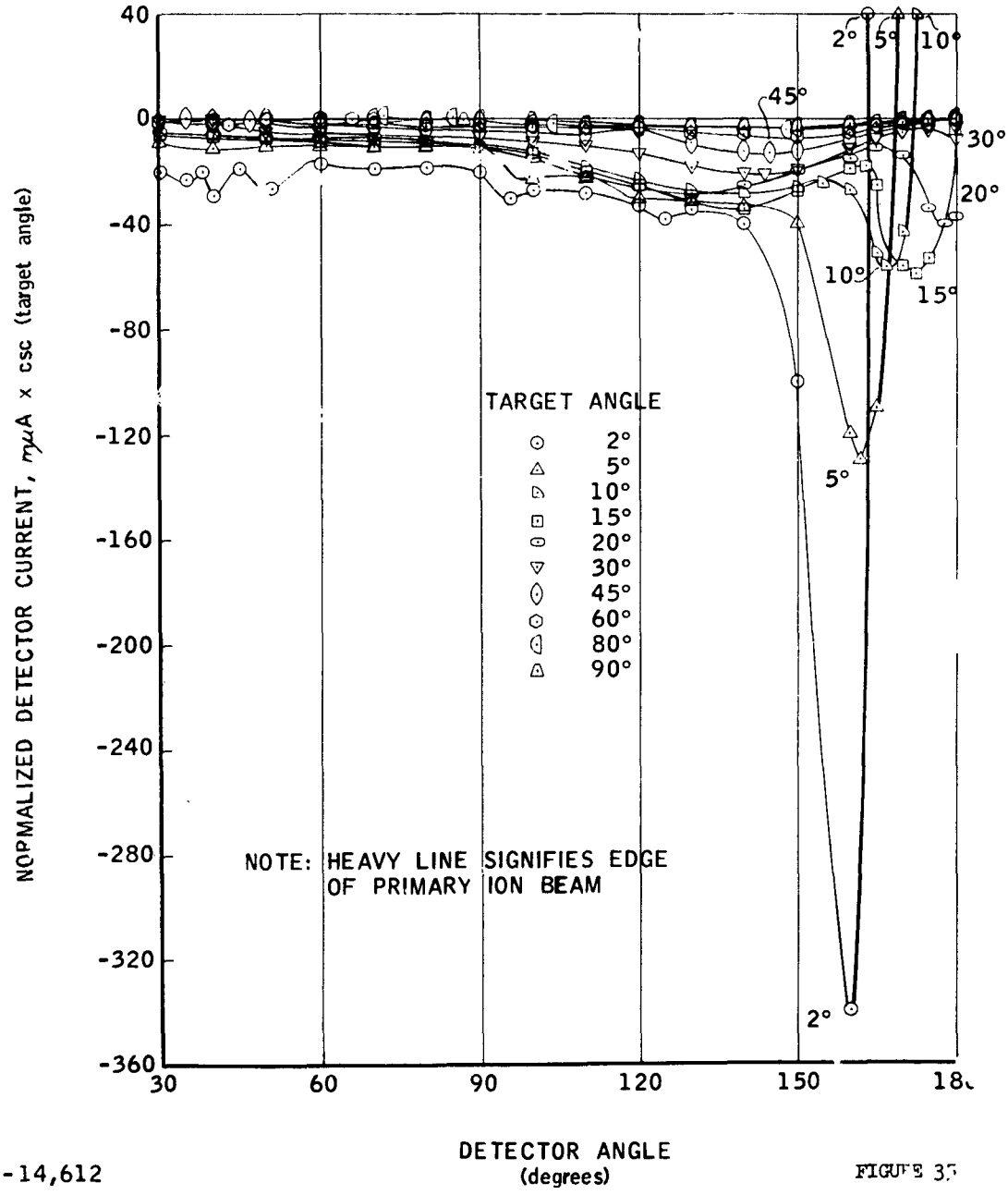

R-14,612

FIGURE 37

ANGULAR DISTRIBUTION OF SECONDARIES, NO DETECTOR BIAS
$Xe,^{+}$ Cu, 30 Kev

ELECTROPOLISHED TARGET

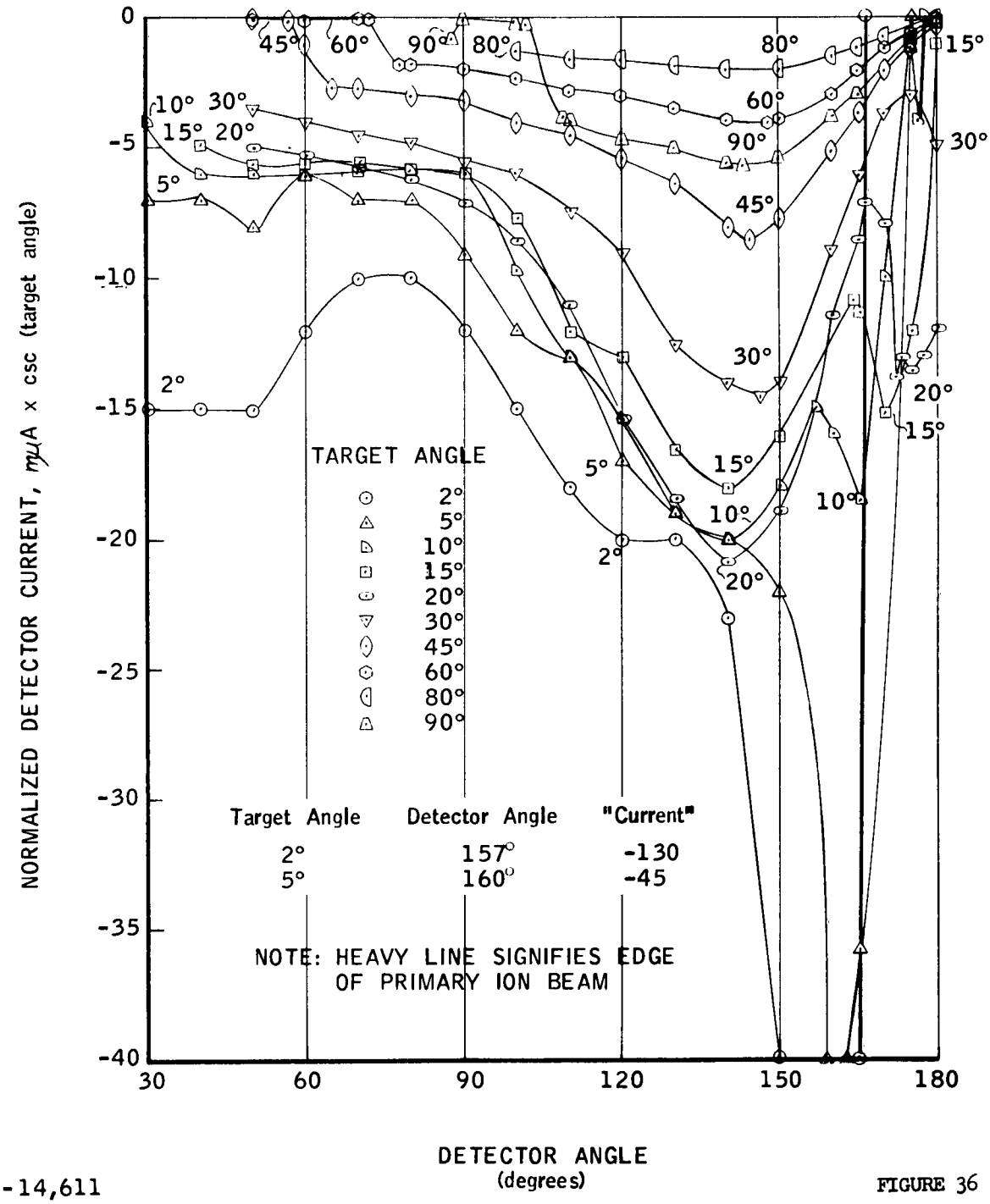

R-14,611

FIGURE 36

ANGULAR DISTRIBUTION OF SECONDARIES, -1v DETECTOR BIAS
Xe,$^{+}$ Cu, 30 Kev

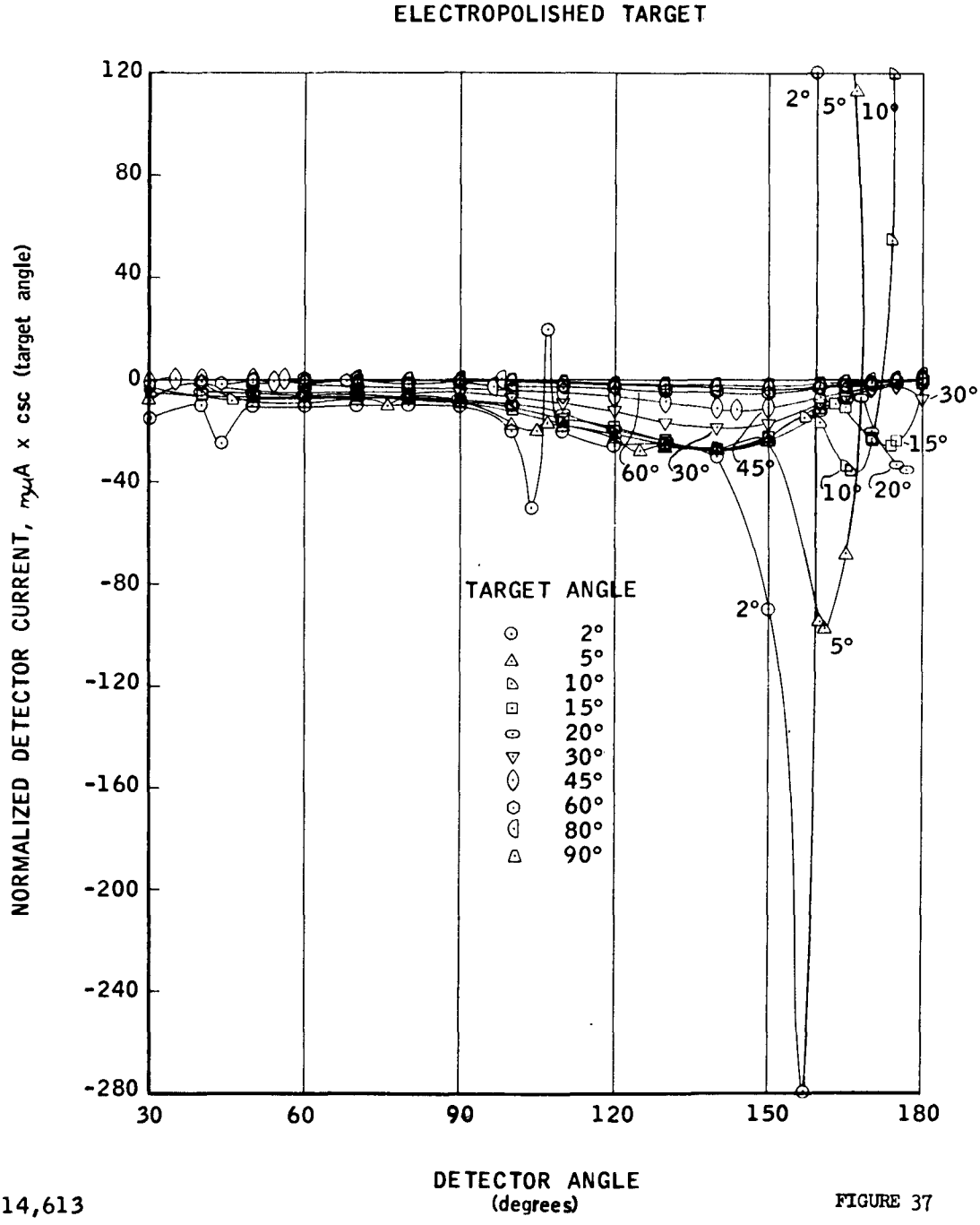

R-14,613

FIGURE 37

ANGULAR DISTRIBUTION OF SECONDARIES, -5v DETECTOR BIAS
$Xe,^{+}$ Cu, 30 Kev

ELECTROPOLISHED TARGET

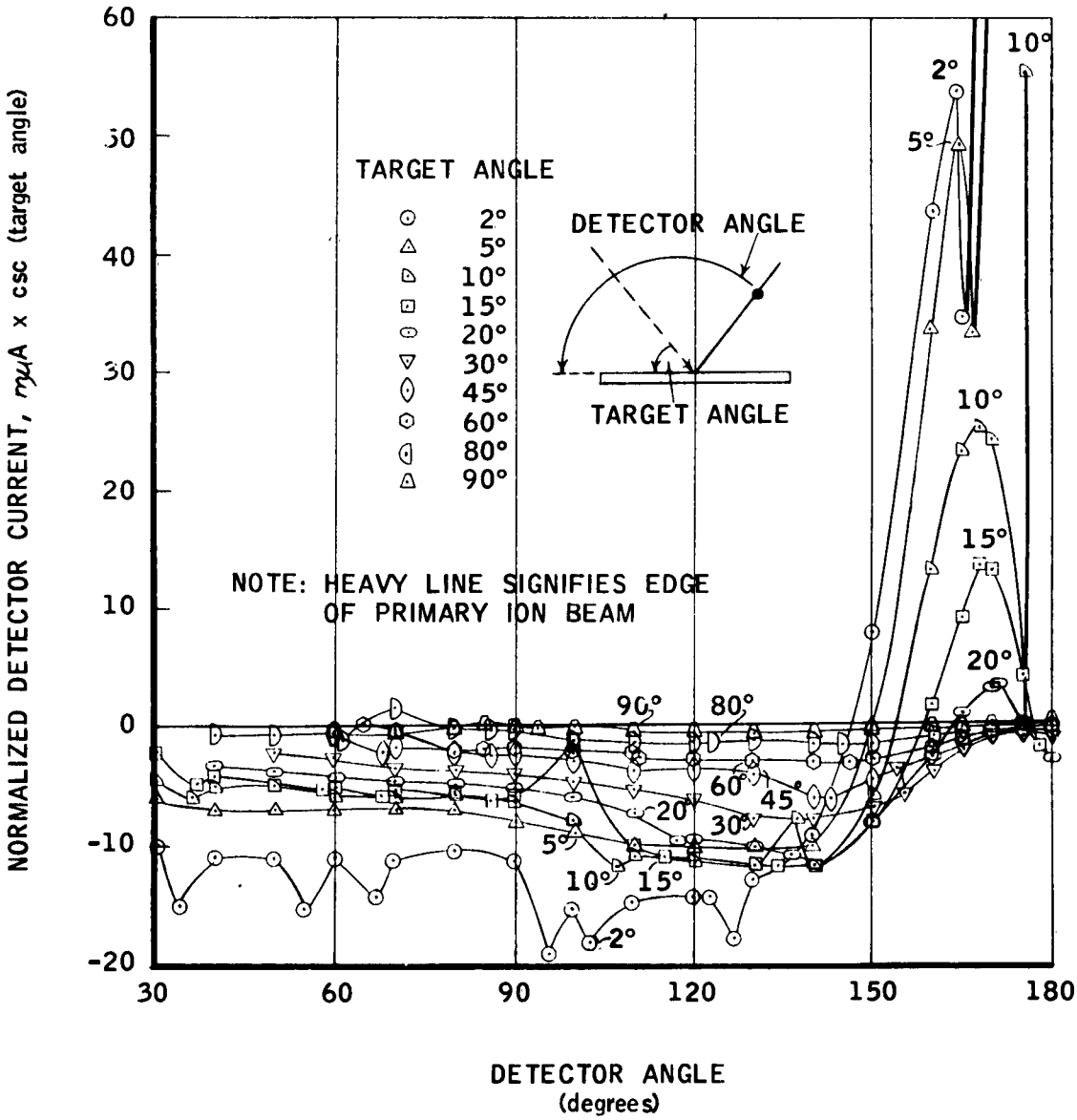

R-14,614

FIGURE 38

ANGULAR DISTRIBUTION OF SECONDARIES, -10v DETECTOR BIAS

$Xe,^{+}$ Cu, 30 Kev

ELECTROPOLISHED TARGET

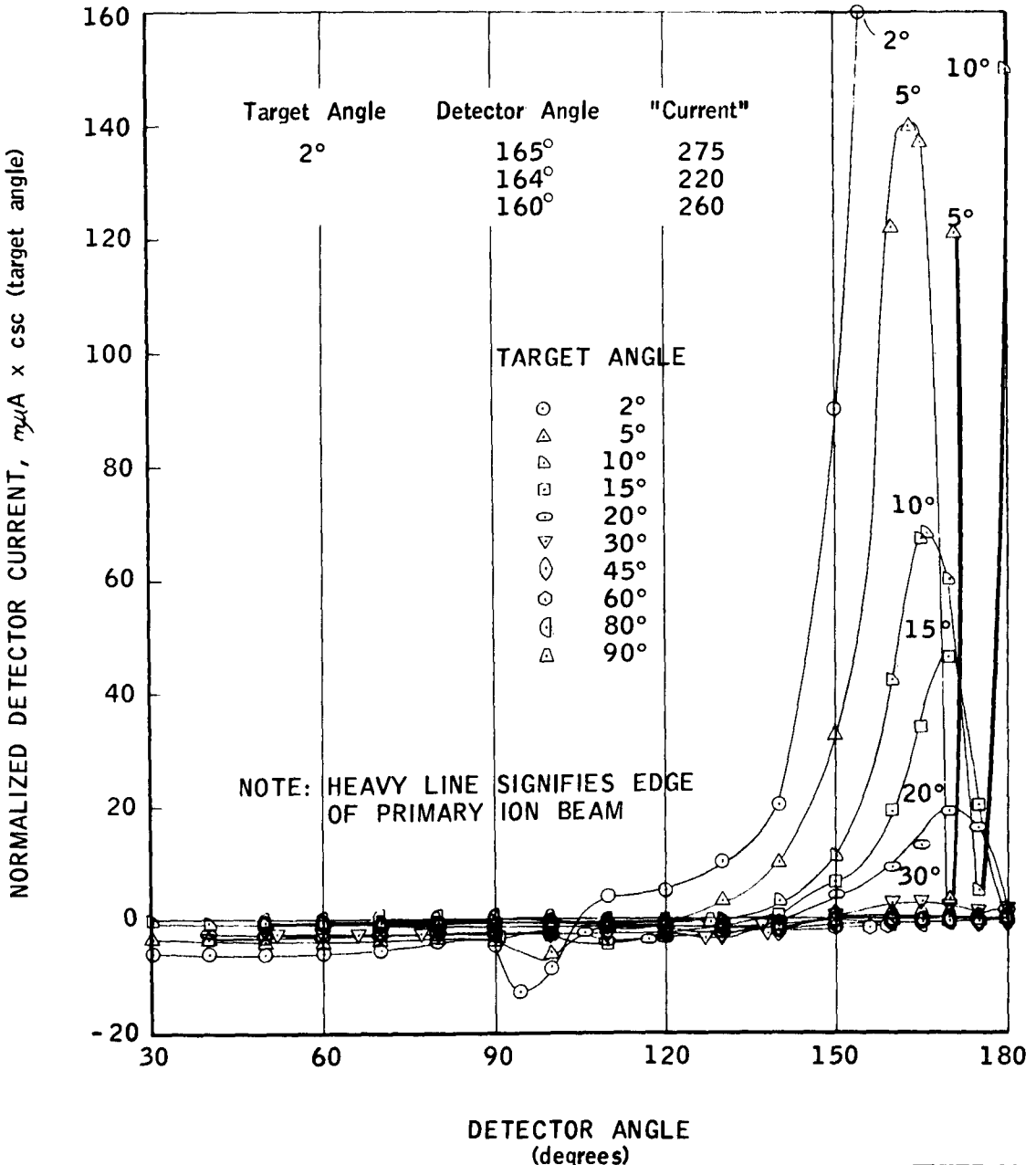

R-14,615

FIGURE 39

ANGULAR DISTRIBUTION OF SECONDARIES, +20v DETECTOR BIAS
Xe,' W, 30 Kev

UNPOLISHED TARGET

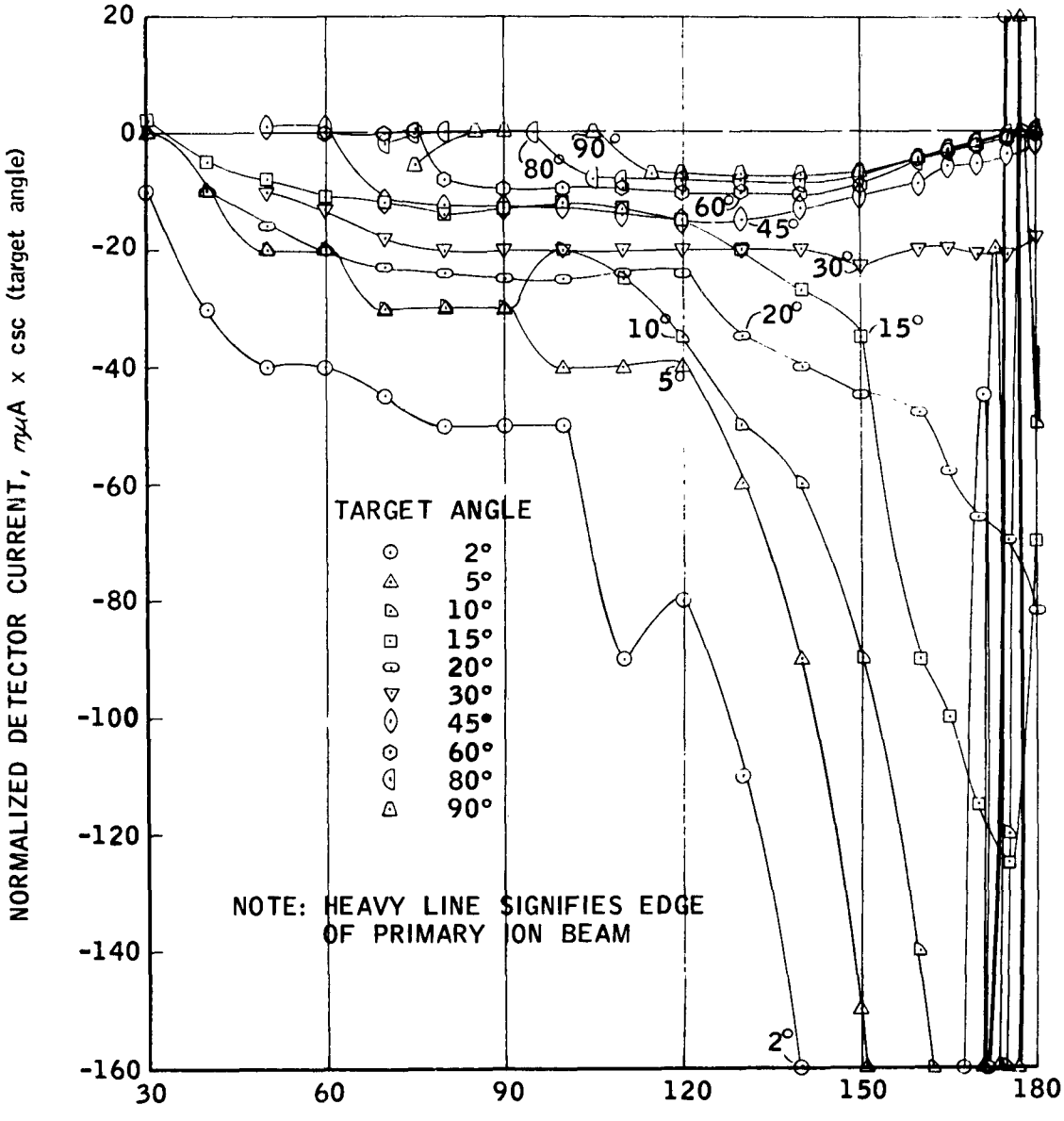

R-14,621

FIGURE 40

ANGULAR DISTRIBUTION OF SECONDARIES, +20v DETECTOR BIAS
Xe^{+}, W, 30 Kev
EXPANDED SCALE

UNPOLISHED TARGET

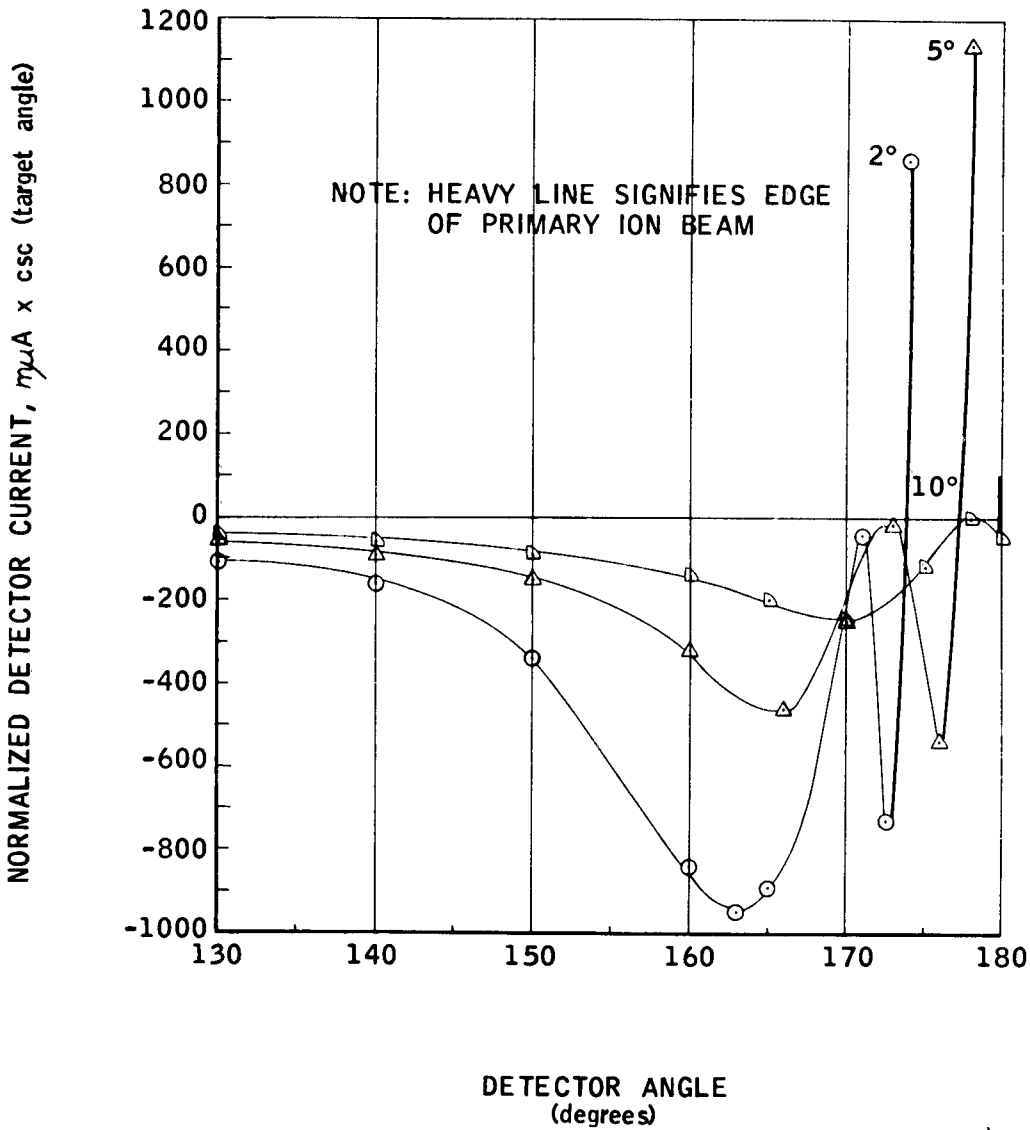

R-14,622

FIGURE 40a

ANGULAR DISTRIBUTION OF SECONDARIES, +10v DETECTOR BIAS
Xe^{+}, W, 30 Kev

UNPOLISHED TARGET

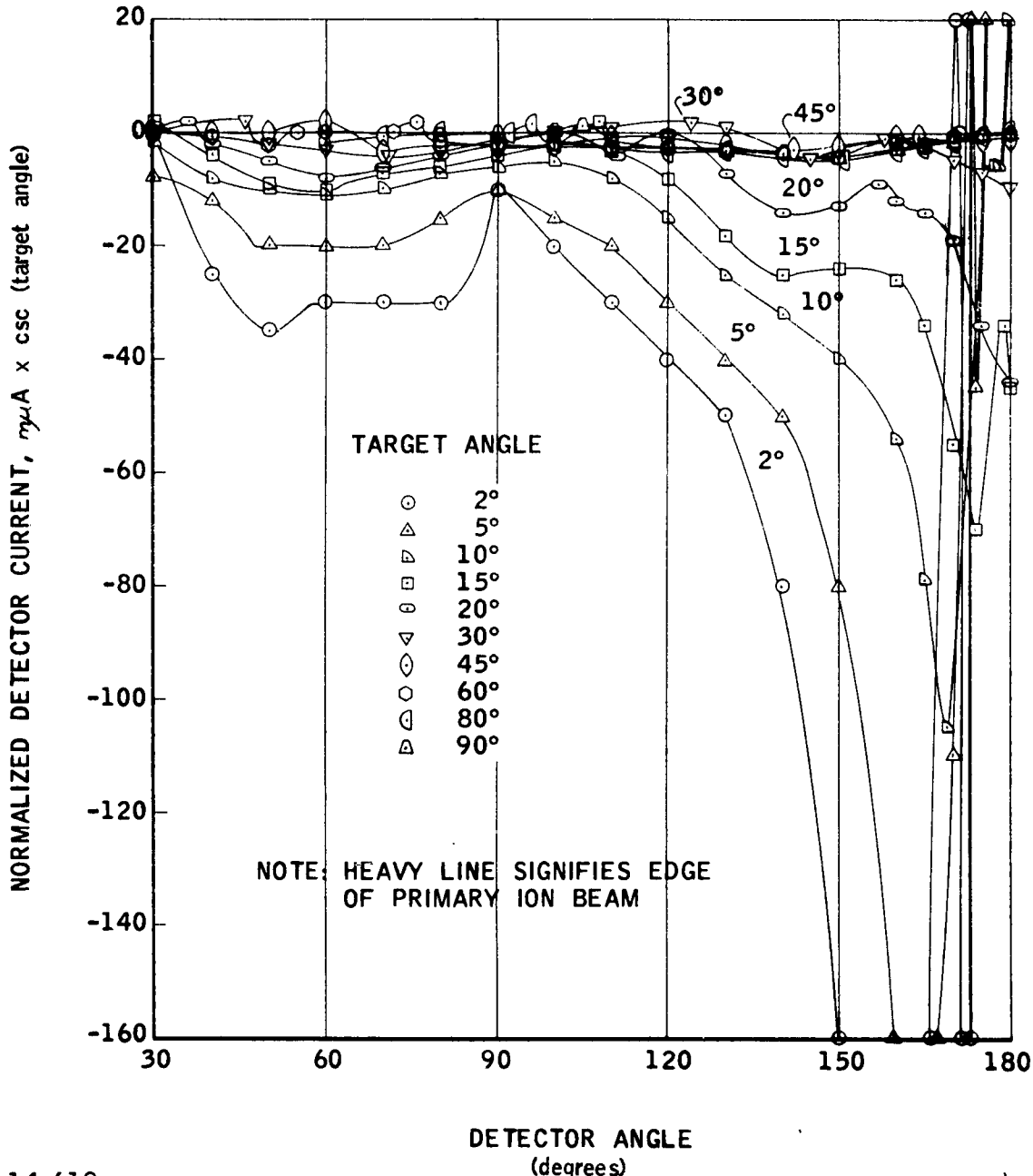

R-14,619

FIGURE 41

ANGULAR DISTRIBUTION OF SECONDARIES, +10v DETECTOR BIAS
Xe^+, W, 30 Kev
EXPANDED SCALE

UNPOLISHED TARGET

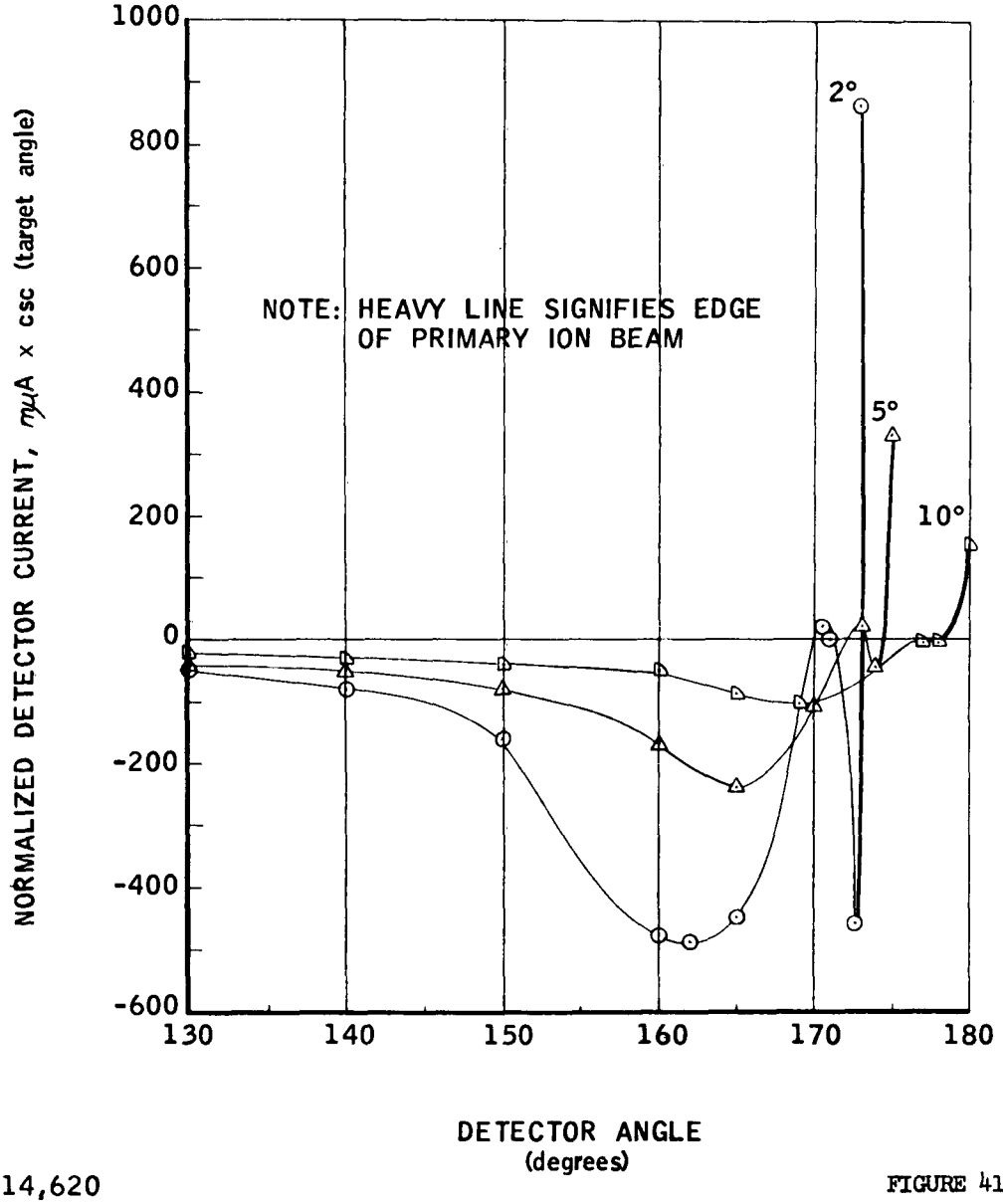

R-14,620

FIGURE 41a

ANGULAR DISTRIBUTION OF SECONDARIES, +5v DETECTOR BIAS
Xe^{+}, W, 30 Kev

UNPOLISHED TARGET

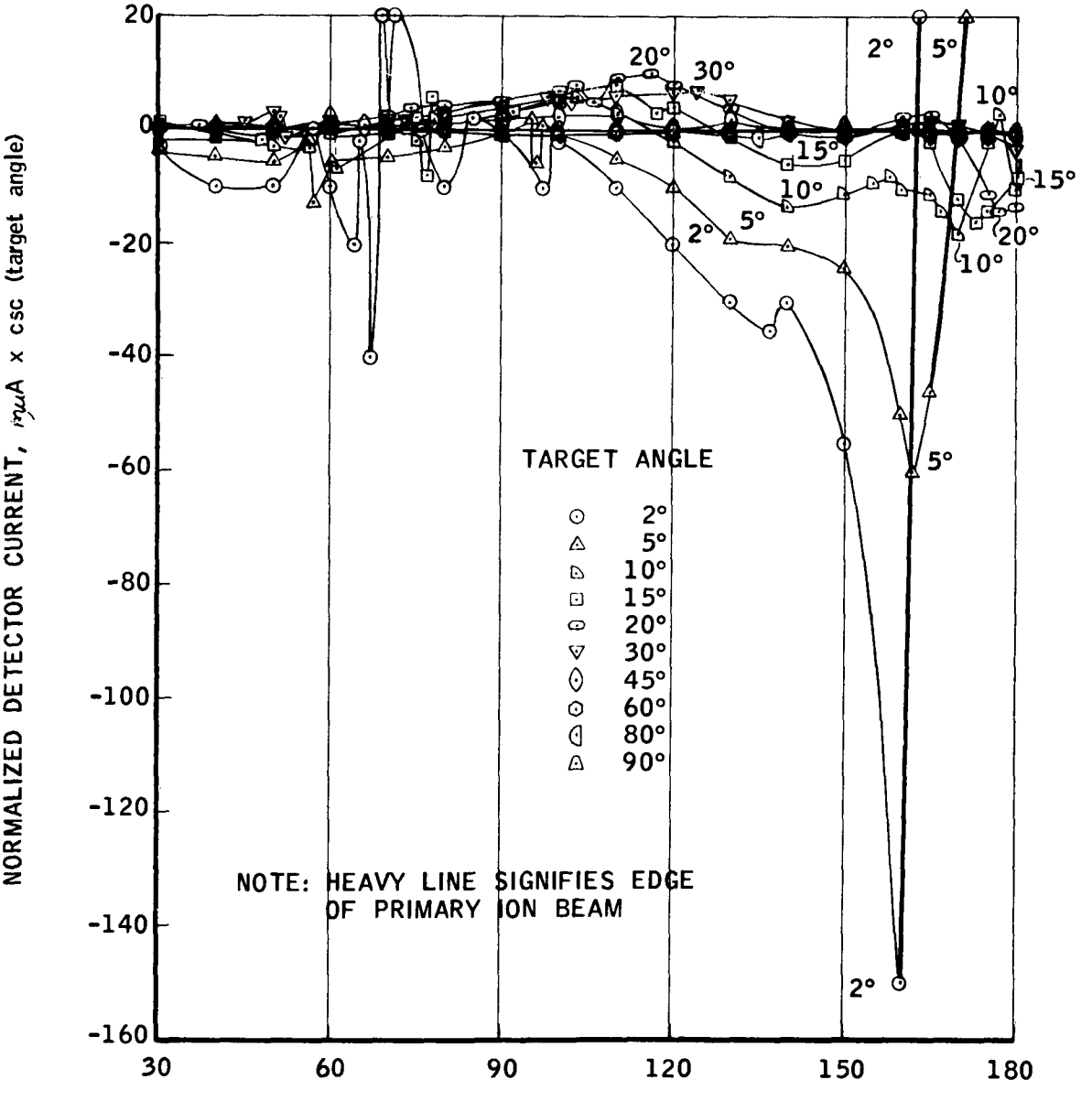

R-14,618

FIGURE 42

ANGULAR DISTRIBUTION OF SECONDARIES, +1v DETECTOR BIAS
$Xe,^{+}$ W, 30 Kev

UNPOLISHED TARGET

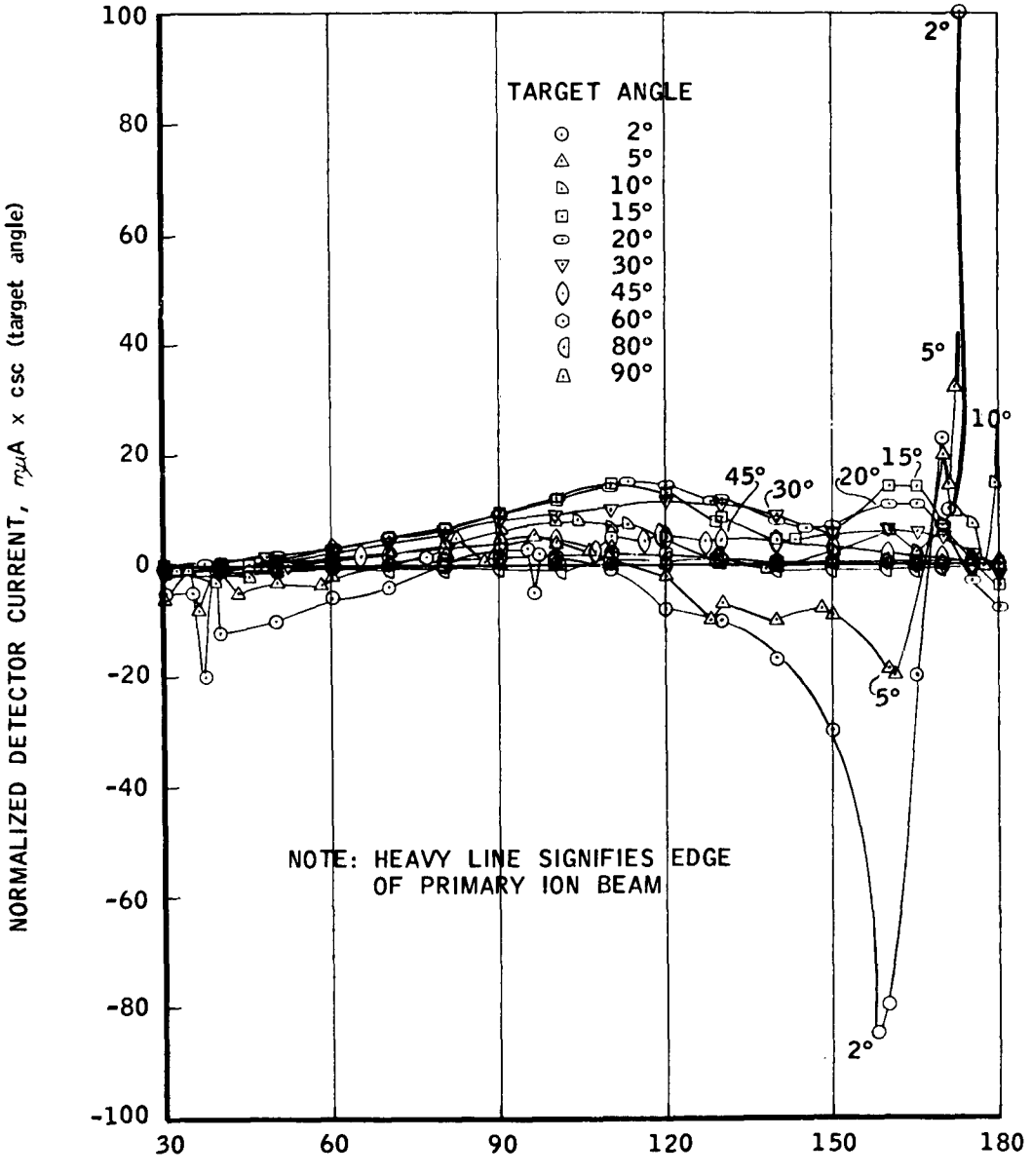

R-14,617

FIGURE 43

ANGULAR DISTRIBUTION OF SECONDARIES, NO DETECTOR BIAS
$Xe,^{+}$ W, 30 Kev

UNPOLISHED TARGET

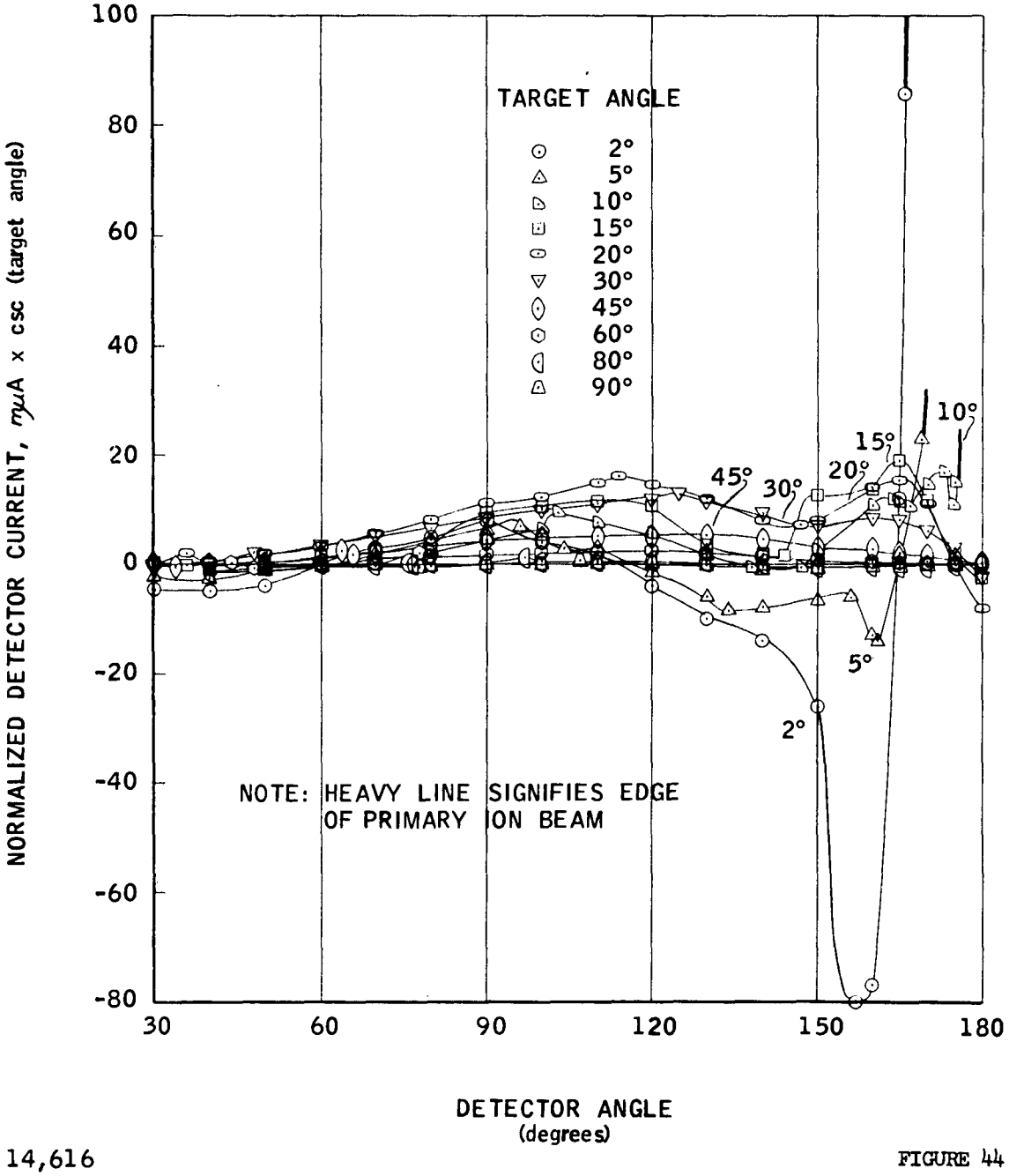

R-14,616

FIGURE 44

ANGULAR DISTRIBUTION OF SECONDARIES, -1v DETECTOR BIAS
$Xe,^{+}$ W, 30 Kev

UNPOLISHED TARGET

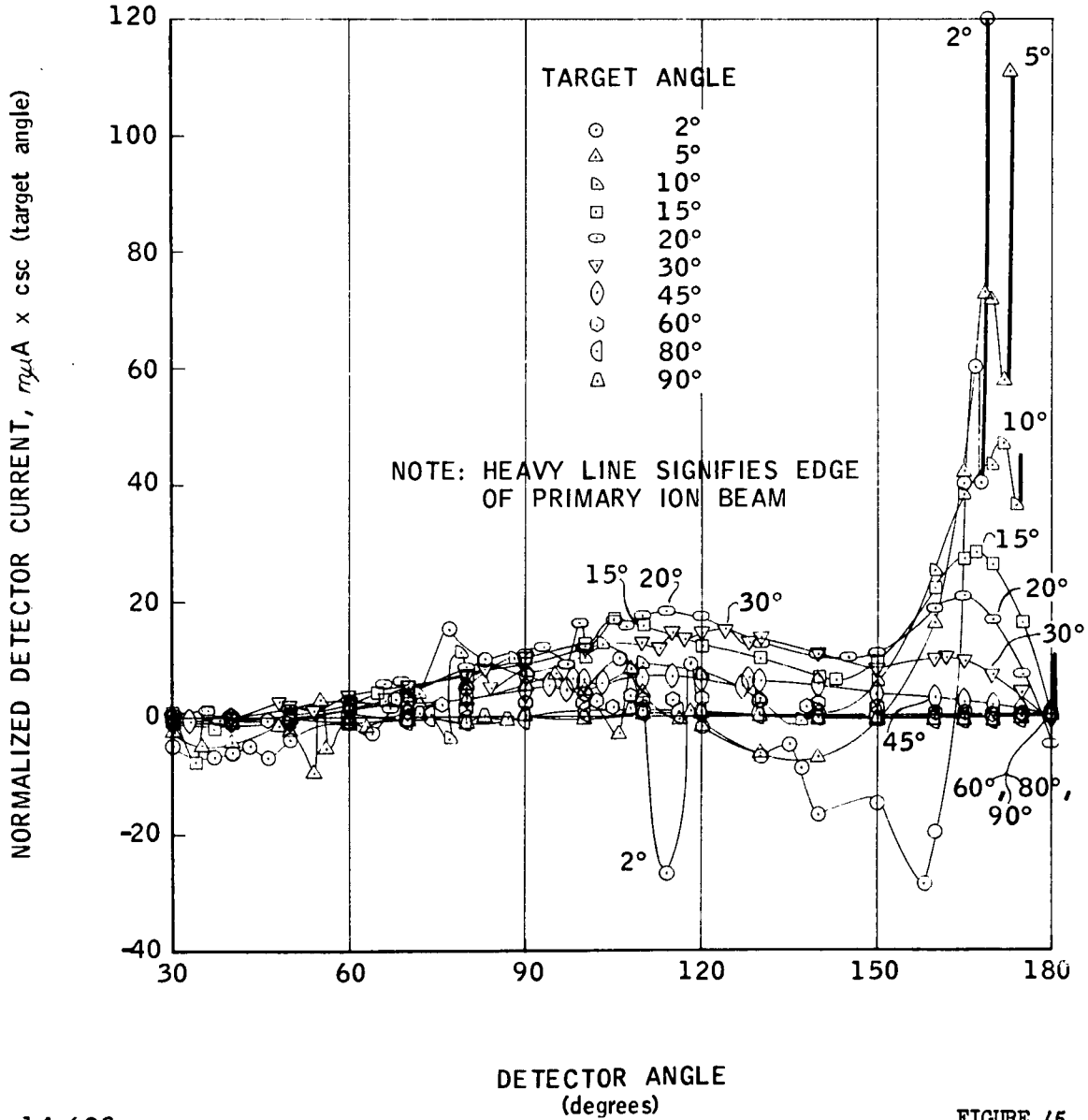

R-14,623

FIGURE 45

ANGULAR DISTRIBUTION OF SECONDARIES, -5v DETECTOR BIAS
Xe^{+}, W, 30 Kev

UNPOLISHED TARGET

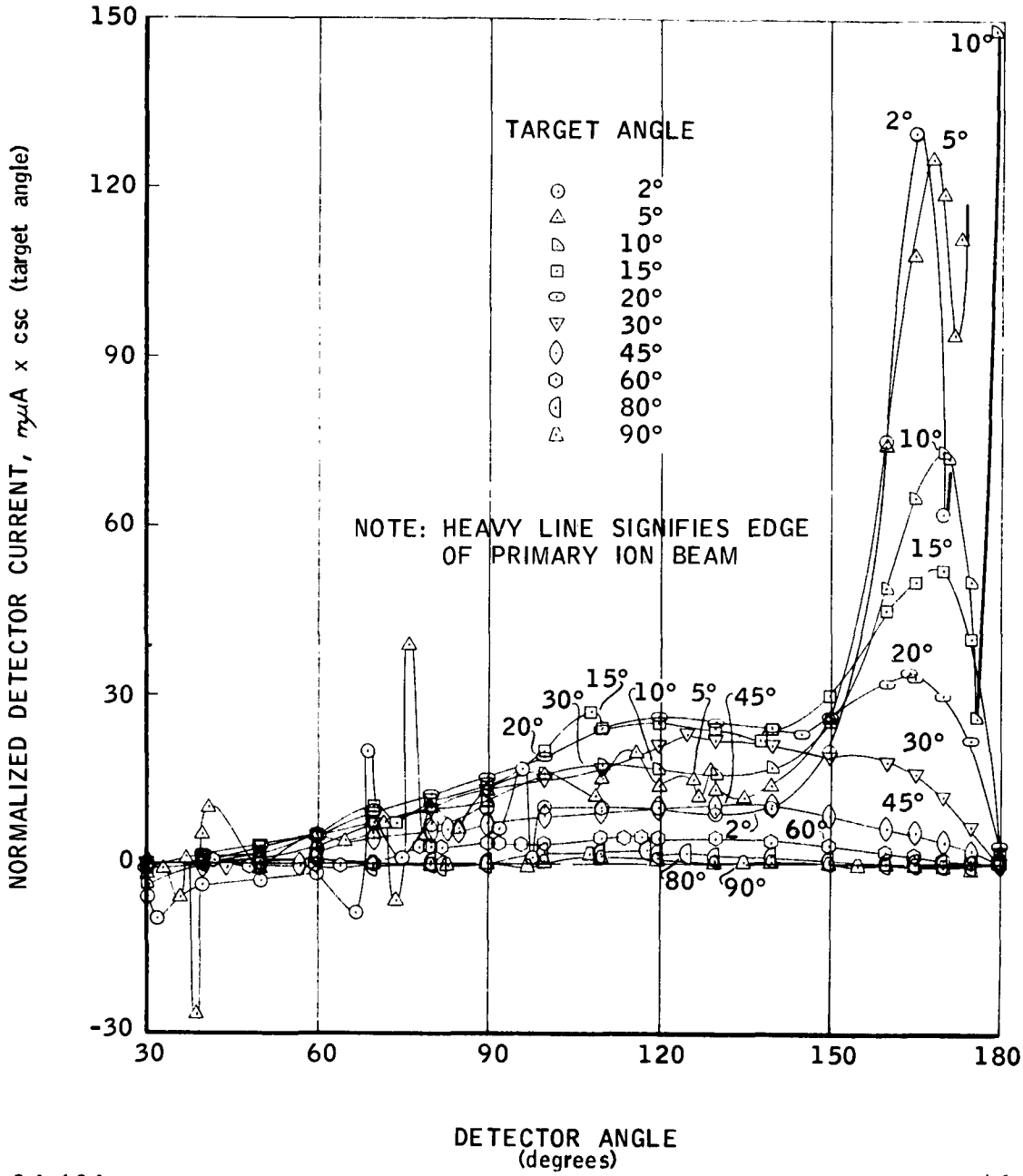

R-14,624

FIGURE 46

ANGULAR DISTRIBUTION OF SECONDARIES, -10v DETECTOR BIAS
Xe, W, 30 Kev

UNPOLISHED TARGET

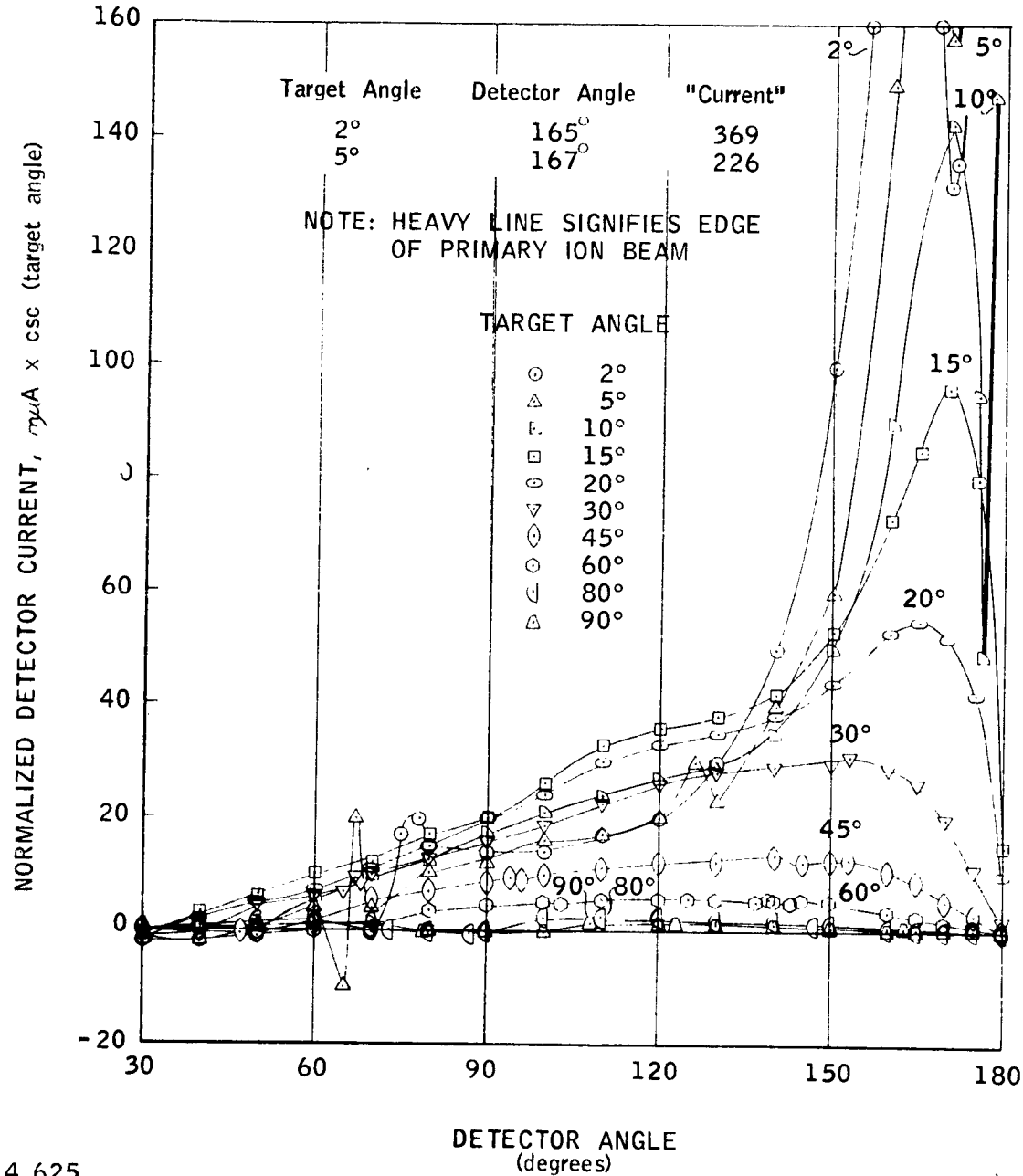

R-14,625

FIGURE 47

The targets used were electropolished copper and unpolished tungsten. The tungsten was very rough microscopically; therefore, the low angle results should not necessarily be taken to be characteristic of the nominal target angle.

The target angles are accurate to $\pm$ 1/2°. The detector angles are self-consistent to $\pm$ 1°, however, they may be as much as 5° out of proper alignment with the target.

It should be noted that none of these curves is normalized according to the actual primary beam current. If the beam intensity changed during a run the recorded results would be in error as to the relative magnitude of the secondary currents. The primary beam was steady throughout this series of tests and all runs were made during as short a period as possible so as to minimize the drift of beam intensity with time. The degree of confidence to be placed in the relative magnitudes can be listed in decreasing order as follows. First, an individual curve from a typical figure, say copper at 15° target angle, deserves the most confidence. All the data on this curve were recorded in less than one minute. Second in confidence level is the whole group of curves in a figure at the same detector bias, say -10 v. All target angles were run off in a period of 10 to 20 minutes, then any striking features in the results were examined more closely, (at target angles between those usually examined, for example). The entire collection of figures for a given target material are the next step as regards internal consistency, since these data were obtained over a period of several hours. Last, the relative secondary currents produced by copper in contrast to tungsten targets should only be compared as to order of magnitude since these tests were run on different days with a beam that was only approximately the same intensity. As was anticipated, the intensity difference between copper and tungsten secondaries is so large that this uncertainty is not important.

Where possible, the portion of a curve due to the primary beam has been darkened to distinguish it from the current due to secondary ions. In some cases (cf. Figure 48) there is a very large and sharp positive peak adjacent to the primary beam. The minimum separating the primary beam and this maximum may not have been resolved in all cases; if so, the first appearance of the current on the right side of the graphs would be the edge of this secondary maximum and not the edge of the primary beam.

The most striking feature of this set of data is the characteristic large positive peak occurring at small incidence angles when the detector was biased negative to suppress secondary electrons. It was anticipated that if xenon ions were reflected as the result of a single collision they would be confined to small angles near the surface. The angular distribution of positive secondaries generally supported this expectation. Positive secondaries from copper targets were peaked at angles rather close to that of the primary ion beam for low incidence angles, while practically no positive secondaries were observed anywhere for incidence angles above 20°. The positive secondaries from tungsten targets peaked sharply close to the beam for low incidence angles but, in contrast to the results for copper, showed broad peaks even for fairly high angles of incidence. These broad peaks were probably due in part to the roughness of the tungsten targets; however, a xenon ion can reflect in any direction from the heavier tungsten atom and might produce these peaks even on a smooth target.

Another notable feature occurs on graphs of runs where the detector was not biased strongly negative. Here there was a very large negative current detected adjacent to either the beam or the positive secondary peak. There are several factors to be considered in interpreting this result and its true significance is not yet clear. In the first place a similar dip can be seen in Figure 35 when an unshielded wire detector was brought near the primary beam. In this case the explanation seems to be that low energy secondary electrons were attracted toward the positive beam. The bare wire detector accepted electrons approaching from any direction and therefore showed a large negative current. On the other hand the case of the shielded detector, as illustrated in Figure 38 for example, is quite different. Here the detector, cf. Figure 18, could only accept electrons falling within a rather small angle as seen from the detector. The negative current in this case must then be due to electrons moving almost parallel to a line from the target to the detector.

III. SUMMARY

A. Sputtering

1. A^+, Cu:

Sputtering ratios were obtained with argon ions with energies near 37.3 Kev incident on mechanically polished copper targets at angles from 10° to 90°. The sputtering ratio went from 6.4 to 24.4 atoms/ion with the maximum between 10° and 20°.

2. Xe^+, Cu:

At room temperature, sputtering ratios for copper were obtained for incidence angles from 2° to 90° and energies of 1.5, 9.5 and 30 Kev. Electropolished samples yielded a maximum sputtering ratio at an angle near 15° while the maximum occurred for mechanically polished samples near 10° at 30 Kev. At 30 Kev the maximum sputtering ratio for electropolished copper was 47.2 atoms/ion, for mechanically polished copper 52.4 atoms/ion.

3. Xe^+, Cu: near 77°K:

The sputtering ratio of 30 Kev ions normally incident on a target held at a temperature near that of liquid nitrogen was 12.6 ± 1.9 atoms/ion as compared to 15.9 ± 1.7 for room temperature targets.

4. Xe^+, Cu: at high temperatures:

The sputtering ratio of copper at temperatures up to 600°C was found to be essentially identical to that at room temperature.

5. Xe^+, W:

Tungsten was sputtered at 30 and 9.5 Kev at angles from 2° to 90° the maximum occurred at near 10° for 30 Kev sputtering and between 10° and 20° for 9.5 Kev sputtering. The angular dependence was much more pronounced at 30 Kev.

6. Xe^+, Mo:

Molybdenum was sputtered at 30 and 9.5 Kev at angles from 2° to 9°. The maximum for both energies occurred near 10°.

7. Xe^+, WC:

Two tungsten carbide samples were sputtered, the sputtering ratios were 6.0 ± 0.6 and 8.7 ± 0.8 for normal incidence at 30 Kev.

8. Xe^+, Ti:

Titanium was sputtered by normally incident 30 Kev ions, the sputtering ratio was 13.5 ± 1.3.

9. Xe^+, Si:

Single crystal silicon was sputtered by normally incident 30 Kev ions, the sputtering ratio found was 24.8 ± 2.6, this value is much larger than would be expected from the results of other investigators.

B. Secondaries

1. Incidence Angle

The number of negative secondaries produced was found to have a maximum for an angle of incidence near 15°. The number of positive secondaries increased monotomically from normal incidence to 5° and, probably, to grazing incidence.

2. Ion Energy

The production of secondaries increased with ion energy under all conditions investigated. From 3 to 10 Kev, (xenon on copper, 45°) the increase was linear with ion energy.

3. Target Temperature

No change in the secondary ratios as a function of target temperature was observed, however, any change of less than 25% would not have been observable due to data spread.

4. Energy Distribution

Two attempts to gain an estimate of the energy distribution of secondaries were made. Some information about the net number of high energy secondaries was obtained and data indicating the relative magnitude and energy of low energy secondary currents in particular directions were obtained.

5. Angular Distribution

Data on the relative number of secondaries produced were taken under the following conditions (see Figure 37).

Xe, Cu, 30 Kev

Target Angle 2°, 5°, 10°, 15°, 20°, 30°, 45°, 60°, 80°, 90°.

Detector Bias -10, -5, -1, 0, 1 volts

Xe, W, 30 Kev

Target Angle 2°, 5°, 10°, 15°, 20°, 30°, 45°, 60°, 80°, 90°.

Detector Bias -10, -5, -1, 0, 1, 5, 10, 20 volts

IV. CONCLUSIONS

A. Sputtering Ratios

Two general conclusions can be made regarding the results of this program.

1. In the first place the dependence of the sputtering ratio on angle of incidence and energy under the conditions of interest for ion rockets has been established for polycrystalline targets. If these factors are known, the sputtering ratio can be estimated fairly closely for the target elements used in this program and to better than an order of magnitude for almost any other element. There are several complimentary directions which future applied research should take. More exact sputtering ratios, for a wider variety of elements bombarded with cesium ions should be obtained. An effort to develop materials resistant to sputtering damage might also prove fruitful. As pointed out in the theoretical section, carbon and silicon are particularly resistant to sputtering. An investigation into the cause of these low sputtering ratios would probably result in suggestions for low boiling point materials with relatively low sputtering ratios.

2. There are a number of points which have been brought to light and bear further investigation, even though they do not bear directly on sputtering as applied to ion rockets. The effect of low temperatures on the sputtering ratio is one such point. Another example is the interaction between incidence angle and ion energy, (cf. the equa-sputtering ratio graph, in Figure 25) of an ion-target pair that definitely exhibits a maximum in the sputtering ratio vs. energy curve. This last is particularly interesting in that the sputtering ratio of copper bombarded by xenon apparently does not have a maximum as a function of energy, therefore, the equa-sputtering ratio curves are not closed as they would be if this maximum occurred.

B. Secondary Particles

An outline of the characteristics of the secondary charged particles produced by xenon, particularly on copper, has been established. The data is sufficiently accurate to greatly facilitate the design and evaluation of experiments or equipment which involve secondary particles. Rather simple extensions of the experiments conducted here could produce information of great value for both the microscopic understanding of these phenomena and the design of high energy ion equipment. The simplest, and perhaps most fruitful, extension involves permitting the ratios of ion mass-to-target mass and ion ionization potential-to-target work function to obtain all possible combinations. A beam current density-to-background pressure ratio should be maintained sufficiently high to insure a clean surface. Due mainly to time limitations this was not always possible in this program. An effort should be made to determine the effect of atomic surface condition on the secondary particle effects. A search for high energy neutral particles should be made. Qualitative experiments involving relatively high energy secondaries can be conducted in the present apparatus with minor modification.

V. REFERENCES

1. J. Plucker, "On the Action of the Magnet on the Electrical Discharge in Dilute Gases," Pogg. Ann., 103, 90 (1858).

2. W. Crookes, "On Electrical Evaporation," Proc. Roy. Soc. London, 50, 88 (1891).

3. General Electric Co., Ltd., Phil. Mag. (6), 45, 98 (1923).

4. K. H. Kingdon, I. Langmuir, Phys. Rev., 22, 148 (1923).

5. E. S. Lamar, K. T. Compton, Science, 80, 541 (1934).

6. C. H. Townes, Phys. Rev., 65, 319 (1944).

7. F. Keywell, "Measurements and Collision-Radiation Damage Theory of High-Vacuum Sputtering," Phys. Rev., 97, 1611 (1955).

8. D. T. Goldman, D. E. Harrison, R. R. Coveyou, ORNL Report - 2729 (1959).

9. R. S Pease, Nuovo Cimento (1960).

10. R. H. Silsbee, "Focusing in Collision Problems in Solids," J. Appl. Phys., 28, 1246 (1957).

11. M. W. Thompson, Phil. Mag., 4, 139, (1959).

12. D. E. Harrison Jr., "Determination of the Maximum Lattice - Chain Energy from Sputtering Yield Curves," J. Appl. Phys., 32, 924 (1961).

13. P. K. Rol, J. M. Fluit, J. Kistemaker, "Sputtering of Copper by Bombardment with Ions of 5-25 Kev," Physica (Neth.), 26, 1000 (1960).

14. P. K. Rol, J. M. Fluit, J. Kistemaker, "Theoretical Aspects of Cathode Sputtering in the Energy Range of 5-25 Kev," Physica (Neth.), 26, 1009 (1960).

15. R. E. Schlier, H. E. Fransworth, Semiconductor Surface Physics, Philadelphia (1957).

16. D. Haneman, Phys. Rev., 119, 563 (1960).

17. H. Paneth, Phys. Rev., 80, 708 (1950).

18. G. K. Wehner, D. Rosenberg, "Angular Distribution of Sputtered Material," J. Appl. Phys., 31, 177 (1960).

19. G. Kuskevics et al., "Ionization, Emission, and Collision Processes in the Cesium Ion Engine," Paper 6364-62, presented at the ARS Electric Propulsion Conference, Berkeley, California, March 14-16, 1962.

20. G. K. Wehner, "Sputtering by Ion Bombardment," Advances in Electronics and Electron Physics, 7, Academic Press, Inc., New York (1955).

21. A. Weiss, L. Heldt, W. J. Moore, "Sputtering of Silver by Neutral Beams of Hydrogen and Helium," J. Chem. Phys., 29, 7 (1958).

22. S. P. Wolsky, E. J. Zdanuk, "Sputtering of Silicon with A^{+2} Ions," Phys. Rev., 121, 374 (1961).

23. T. W. Snouse, M. Bader, "The Sputtering of Copper by N_2^+ as a Function of Pressure and Temperature," paper presented at the Second International Vacuum Congress, October 16-19, 1961.

24. O. Almén, G. Bruce, "Collection and Sputtering Experiments with Noble Gas Ions," Nuclear Instr. and Methods, 11, 257 (1961).

25. R. C. Bradley, "Secondary Positive Ion Emission from Metal Surfaces," J. Appl. Phys., 30, 1 (1959).

26. R. E. Honig, "Sputtering of Surfaces by Positive Ion Beams of Low Energy," J. Appl. Phys., 29, 549 (1958).

27. H. D. Hagstrum, "Reflection of Noble Gas Ions at Solid Surfaces," Phys. Rev., 123, 758 (1961).

28. V. A. Molchanov, V. Telkovskii, "Variation of the Cathode Sputtering Coefficient as a Function of the Angle of Incidence of Ions on a Target," Soviet Physics, Doklady, 6, 136 (1961).

29. R. C.Bradley, E. Ruedl, "Ions Sputtered from Copper," J. Appl. Phys., 33, 880 (1962).

30. H. D. Hagstrum, "Theory of Auger Ejection of Electrons from Metals by Ions," Phys. Rev., 96, 336 (1954).

31. V. A. Arifov, A. KA. Awkhanov, S. V. Starodubtsev, "Ion Scattering Coefficient as a Function of Colliding - Particle Mass Ratio," Soviet Physics JETP, 6, 4 (1958).

32. E. Yoda, B. M. Siegel, J. Appl. Phys., 33, 1419 (1962).

33. G. K. Wehner, "Annual Report on Sputtering Yields," General Mills Report No. 2136, (1960).

34. P. Lukivsky, Z. Physik, 22, 351 (1924).

35. P. A. Ganichev, K. G. Umkin, Soviet Physics, Solid State, 1, 590, (1959).

VI. BIBLIOGRAPHY

A. Sputtering

This bibliography of recent papers on sputtering in the energy range above 1000 electron volts has been prepared to aid both the theoretical studies and comparison of data from this program with that obtained in other investigations. A few papers containing other information pertinent to the sputtering process are included. Part B is a bibliography of recent publications on secondary particle research. We are indebted to Mr. Thomas W. Snouse and Dr. Michel Bader of NASA, Ames Research Center, for supplying many of these references. In addition, much use has been made of bibliographies contained in recently published papers by Harrison and Yonts (1961), and Gale and Nablo (1960).

G. S. Anderson, G. K. Wehner, "Atom Ejection Patterns in Single Crystal Sputtering," J. Appl. Phys., 31, 2505 (1960).

U. A. Arifov, A. Kh Aiukhanov, S. V. Starodubtsev, "Ion Scattering Coefficient as a Function of Colliding-Particle Mass Ratio," Soviet Physics, JETP, 6, No. 4 (1958) or J. Exptl. Theoret. Phys. (USSR), 33, 845 (1957).

M. Bader, F. C. Witteborn, T. W. Snouse, "Sputtering of Metals by Mass-Analyzed N_2^+, N^+", NASA TR R-105, Ames Research Center, Moffett Field, California (1961).

M. Balarin, F. Hilbert, "Effect of Energetic Ions on Metal Surfaces," (German), J. Phys. Chem. Solids (G.B.), 20, 138 (1961).

R. C. Bradley, E. Ruedl, "Ions Sputtered from Copper," J. Appl. Phys., 33, 880 (1962).

R. C. Bradley, "Sputtering of Alkali Atoms by Inert Gas Ions of Low Energy," Phys. Rev., 93, 719 (1954).

J. K. Boggild et al., "Cloud-Chamber Studies of Electronic and Nuclear Stopping of Fission Fragments in Different Gases," Phys. Rev., 71, (1947).

Brown, Leck, Brit. J. Appl. Phys., 6, 161 (1955).

Carmichael, Trendelenberg, "Ion Induced Reemission of Noble Gases from a Nickel Surface," J. Appl. Phys., 29, 1570 (1958).

C. Cassignol, G. Ranc, "On the Non-Linear Character of the Intensity Dependence of Cathodic Sputtering at High Energies and its Variation with Temperature," Acad. Sci. (Paris), 248, 1988 (1959).

J. S. Colligon, "Ion Bombardment of Metal Surfaces," Vacuum (G.B.), 11, (1961).

W. C. Crookes, "On Electrical Evaporation," Proc. Roy. Soc. London, 50, 88 (1891).

R. C. Davis et al., ORNL 2802-67, (1959); ORNL 2926 (1960).

H. M. DeAngelis, I. Feuer, "Positive Ion Bombardment of Metals with Radioactive Krypton - 85", Proceedings of the Second Conference on Nuclear Radiation Effects on Semi-Conductor Devices, Materials and Circuits (1959).

J. A. Dillon, Jr., R. M. Oman, "Ion-Bombardment Etching of Si and Ge", J. Appl. Phys., 31, 26 (1960).

F. Fairbrother, J. S. Foster, "Sputtering of Stainless Steel by Protons in the 30-80 Kev Range," UCRL - 4169, Contr No. W-7405-eng-48, August 11, 1953.

Fisher, Weber, "Cathodic Sputtering for Micro Diffusion Studies," J. Appl. Phys., 23, 181 (1952).

A. J. Gale, S. V. Naglo, Goodrich-High Voltage Astronautics, Inc., Burlington, Mass., "Demonstration of Ion Thrust using the Duoplasmatron Arc-Type Source," Contr No. DA-19-020-ORD-4969, September 15, 1960.

D. A. Ganichev, K. G. Umkin, Soviet Physics, Solid State, 1, 590 (1959).

General Electric Co., Ltd., Phil. Mag., 45, 98 (1923).

Gillam, J. Phys. Chem. Solids, 11, 55 (1959).

D. T. Goldman, D. E. Harrison, R. R. Coveyou, ORNL Report - 2729, (1959).

D. T. Goldman, A. Simon, "Theory of Sputtering by High-Speed Ions," Phys. Rev., 111, 383 (1958).

F. Gronlund, W. J. Moore, "Sputtering of Silver with Light Ions with Energies from 2 to 12 Kev," J. Chem. Phys., 32, 1540 (1960).

A. Guentherschulze, "Cathodic Sputtering, an Analysis of the Physical Process," Vacuum, 3, 360 (1955).

M. I. Guseva, Soviet Physics, Solid State, 1, 1410 (1960).

H. D. Hagstrum, C. Amico, "Production and Demonstration of Atomically Clean Metal Surfaces," J. Appl. Phys., 31, 715 (1960).

D. E. Harrison, Jr., "Determination of the Maximum Lattice - Chain Energy from Sputtering Yield Curves," J. Appl. Phys., 32, 924 (1961).

D. E. Harrison, Jr., "Theory of the Sputtering Process," Phys. Rev., 102, 1473 (1956).

D. E. Harrison, Jr., G. D. Magnuson, "Sputtering Thresholds," Phys. Rev., 122, 1421 (1961).

D. E. Harrison, Jr., O. C. Yonts, "Survey of High Energy Sputtering Experiments," ARS Paper 1752-61, Gatlinburg, Tennessee, May 3-15, 1961.

R. J. Hayes, et al., "The Duo-Plasmatron Ion Rocket," ARS Paper No. 1588-60 (1960).

E. B. Henschke, "New Collision Theory of Cathode Sputtering of Metals at Low Ion Energies," Phys. Rev., 106, No. 4 (1957).

E. B. Henschke, "Collision Theories of Cathode Sputtering of Metals at Low Ion Energies," Phys. Rev., 121, 1286 (1961).

R. L. Hines, R. Arnot, "Radiation Effects of Bombardment of Quartz and Vitreous Silica by 7.5 Kev to 59 Kev Positive Ions," Phys. Rev., 119, 623 (1960).

L. Holland, Sidall, "Reactive Sputtering, and Associated Plant Design," Vacuum, 3, 245 (1953).

D. K. Holmes, Liebfried, "Range of Radiation Induced Primary Knock-ons in the Hard Core Approximation," J. Appl. Phys., 31, 1046 (1960).

R. E. Honig, "Sputtering of Surfaces by Positive Ion Beams of Low Energy," J. Appl. Phys., 29, 549 (1958).

H. B. Huntington, "Mobility of Interstitial Atoms in a Face-Centered Cubic Metal," Phys. Rev., 91, No. 5 (1953).

F. C. Hurlbut, R. P. Stein, "Studies of Sputtering by Beam Techniques," Rand Symposium on Aerodynamics of the Upper Atmosphere, June 1959, R-339-Section 8.

F. C. Hurlbut, R. P. Stein, "Studies of Sputtering by Beam Techniques," Bull. Am. Phys. Soc., Ser II, 127 (1960).

J. M. Hayatt, M. M. Irvine, "Sputtering of Alumina in Argon," Rev. Sci. Inst., 24, 1006 (1953).

W. Janeoff, "Sputtering Chemistry," Z. Phys., 142, 619 (1955).

M. Kaminsky, "Sputtering Experiments in the Rutherford Collision Region," Phys. Rev., 126, No. 4 (1962).

F. Keywell, "A Mechanism for Sputtering in the High Vacuum Based upon the Theory of Neutron Cooling," Phys. Rev., 87, 160 (1952).

F. Keywell, "Measurements and Collision - Radiation Damage Theory of High Vacuum Sputtering," Phys. Rev., 97, 1611 (1955).

K. H. Kingdon, I. Langmuir, Phys. Rev., 22, 148 (1923).

M. Koedam, "Cathode Sputtering by Rare-Gas Ions of Low Energy," Philips Res. Rep. (Neth.), 16, 101 (1961).

M. Koedam, A. Hoogendoorn, "Sputtering of Copper Single Crystals Bombarded with A^+, Kr^+, and Ne^+ Ions with Energies Ranging from 300 - 2000 ev", Physica (Neth.), 26, 351 (1960).

V. E. Krohn, Jr., "Emission of Negative Ions from Metal Surfaces Bombarded by Positive Cesium Ions," J. Appl. Phys., 33, 2523 (1962).

G. Kuskevics et atl., "Ionization, Emission, and Collision Processes in the Cesium Ion Engine," Paper 6364-62, presented at the ARS Electric Propulsion Conference, Berkeley, California, March 14-16, 1962.

M. Laegrid, G. K. Wehner, "Sputtering Yields of Metals and Semiconductors by Ne^+ Ions from 60 to 600 ev", Vacuum Symposium Transactions (1960).

M. Laegrid, G. K. Wehner, Meckel, J. Appl. Phys., 30, 374 (1959).

E. S. Lamar, K. T. Compton, Science, 80, 541 (1934).

E. Langberg, "Analysis of Low-Energy Sputtering," Phys. Rev., 111, No. 1 (1958).

G. Leibfried, "Correlated Collisions in a Displacement Spike," J. Appl. Phys., 30, 1388 (1959).

J. Lindhard, Danske Videnskab Selskab, Mat.-fus. Medd., 28, No. 8 (1954).

J. S. Luce, "Ion Erosion of Accelerating Electrodes in Space Vehicles," ARS Paper No. 1159-60, Los Angeles, California, May 9-12, 1960.

G. D. Magnuson, B. B. Meckel, P. A. Harkins, "Etch Effects from Oblique-Incidence Ion Bombardment," J. Appl. Phys., 32, No. 3 (1961).

P. Lukivsky, Z. Physik, 22, 351 (1924).

D. McKeown, "A New Method for Measuring Sputtering in the Region Near Threshold," 2nd International Symposium on Rarefied Gas Dynamics, August 1960, Rev. Sci. Inst., 32, 133 (1961).

H. S. Massey, E. H. S. Burhop, Electronic and Ionic Impact Phenomena, Clarendon Press, Oxford (1952).

V. A. Molchanov, V. Telkovskii, "Variation of the Cathode Sputtering Coefficient as a Function of the Angle of Incidence of Ions on a Target," Soviet Physics, Doklady, 6, 136 (1961).

V. A. Molchanov, et al., "Anisotropy of Cathodic Sputtering of Single Crystals," Soviet Physics, Doklady, 6, 223 (1961).

W. J. Moore, "The Ionic Bombardment of Solid Surfaces," Amer. Sci., 48, 109 (1960).

W. J. Moore, C. D. O'Brian, A. Lindner, "The Interaction of Ionic Beams with Solid Surfaces," Ann. N. Y. Acad. Sci., 67, 600 (1957).

Morgulis, Tishenko, "The Investigations of Cathode Sputtering in the Near Threshold Region I," Soviet Physics, JETP, 3, 52 (1956).

C. D. O'Brian, A. Lindner, W. J. Moore, "Sputtering of Silver by Hydrogen Ions," J. Chem. Phys., 29, 3 (1958).

M. L. E. Oliphant, "The Action of Metastable Atoms of Helium on a Metal Surface," Proc. Roy. Soc., A124, 1 (1929).

H. R. Panety, "The Mechanism of Self-Diffusion in Alkali Metals," Phys. Rev., 80, No. 4 (1950).

H. Patterson, D. H. Tomlin, "Experiments by Radioactive Tracer Methods on Sputtering by Rare-Gas Ions," Proc. Roy. Sci., A265, 474, (1962).

R. S. Pease, "Sputtering of Solids by Penetrating Ions," (158-65) Physics of Plasma; Experimental and Technical (Fisica de Plasma; Esperimentetechniche), Edited by H. Alfren. Rendiconti della Scuola Internazioale di Fisica Enrico Fermi, Corso XIII. Bologna: Zanchelli (1960).

R. S. Pease, Nuovo Cimento (1960).

B. Dj. Perovic, "Cathode Sputtering of Cu and Pb Single Crystals by High Energy A^+ Ions," Bull. Inst. Nucl. Sci., 11, 37, (1961).

E. T. Pitkin, "Sputtering Due to High Velocity Ion Bombardment," ARS Paper #1377-60, Monterey, California, November 3-4, 1960.

N. V. Pleshivtsev, "Sputtering of Copper by Hydrogen Ions with Energies up to 50 Kev," Soviet Physics, JETP 37, 878, (1960).

J. Plucker, "On the Action of the Magnet on the Electrical Discharge in Dilute Gases," Pogg. Ann., 103, 90 (1858).

M. T. Robinson, "Deduction of Ion Ranges from Collection Experiments," Appl. Phys. Letters, 1, No. 2, 49 (1962).

P. K. Rol, J. M. Fluit, J. Kistemaker, Physica (Neth.) 26, 868 (1960).

P. K. Rol, et al., Proceedings of the International Symposium on Isotope Separation, Amsterdam, p 657 (1957).

P. K. Rol, J. M. Fluit, J. Kistemaker, "Sputtering of Copper by Bombardment with Ions of 5-25 Kev," Physica (Neth.), 26, (1960).

P. K. Rol, J. M. Fluit, J. Kistemaker, "Sputtering of Copper by Ion Bombardment in the Energy Range of 5-25 Kev," ARS Paper No. 1395-60.

P. K. Rol, J. Fluit, J. Kistemaker, "Theoretical Aspects of Cathode Sputtering in the Energy Range of 5-25 Kev," Physica (Neth.), 26, (1960).

Sylvan, Rubin, "Surface Analysis by Charged Particle Spectroscopy," Nuclear Instr and Methods, 5, 177 (1959).

F. Seitz, "On the Disordering of Solids by Action of Fast Massive Particles," Disc. Faraday Soc., 5, 271 (1949).

R. H. Silsbee, "Focusing in Collision Problems in Solids," J. Appl. Phys., 28, 1246 (1957).

J. G. Simmons, L. I. Maissel, "Multiple Cathode Sputtering System," Rev. Sci. Instr., 32, 642 (1961).

T. W. Snouse, M. Bader, "The Sputtering of Copper by N_2^+ as a Function of Pressure and Temperature," Paper for 2nd Inter. Vacuum Congress, October 1961.

A. L. Southern et al.,"Sputtering Experiments with 1- to 5-Kev Ar^+ Ions," J. Appl. Phys., 34, 153 (1963).

G. V. Spivak, A. I. Krokhina, L. V. Lazreva, Doklady, 104, 579 (1955).

R. P. Stein, F. C. Hurlbut, "Angular Distribution of Sputtered Potassium Atoms," Phys. Rev., 123, 790 (1960).

R. P. Stein, F. C. Hurlbut, "Studies of Sputtering of Potassium by Noble Gas Ions," Proceedings of the Atomic Molecular Beams Conference, p. 190, University of Denver, June 20, 1960.

J. F. Strachan, N. L. Harris, "Bombardment of Various Elements by Hg^+ and A^+ Ions," Proc. Phys. Soc., B69, 1148 (1956).

K. Thommen, "The Sputtering of Crystals by Canal Rays," Z. Phys., 151, 144 (1958).

M. W. Thompson, Phil. Mag., 4, 139 (1959).

M. W. Thompson, R. S. Nelson,"The Ejection of Atoms from Gold Crystals during Proton Irradiation," AERE Report No. R3320 (1960).

C. H. Townes, Phys. Rev., 65, 319 (1944).

Trillat, Tertian, Terao, "The Oxidation of Nickel by Ionic Bombardment," (French), Cahiers de Phys., 12, 162 (1958).

M. von Ardenne, Tables of Electron Physics and Electron Microscopy, Deutscher Verlag der Wissenschaften, Berlin, (1956).

G. K. Wehner, "Momentum Transfer in Sputtering by Ion Bombardment," J. Appl. Phys., 25, 270 (1954).

G. K. Wehner, "Sputtering Yields for Normally Incident Hg^+ -Ion Bombardment at Low Ion Energy," Phys. Rev., 108, 35 (1957).

G. K. Wehner, "Controlled Sputtering of Metals by Low Energy Hg Ions," Phys. Rev., 102, 690 (1959).

G. K. Wehner, "Sputtering of Metal Single Crystals by Ion Bombardment," J. Appl. Phys., 25, 1056 (1955).

G. K. Wehner, "Sputtering by Ion Bombardment," Advances in Electronics and Electron Physics 7, Academic Press, Inc., New York (1955).

G. K. Wehner, "Velocities of Sputtered Atoms," Phys. Rev., 114, 1270 (1959).

G. K. Wehner, "Influence of the Angle of Incidence on Sputtering Yield," J. Appl. Phys., 30, 1762 (1959).

G. K. Wehner, "Annual Report on Sputtering Yields," Gen. Mills Mech. Div. Report No.
1902 31 May 1959
1847 30 April 1958
1864 30 May 1958
2136 30 May 1960

G. K. Wehner, "Forces on Ion-Bombarded Electrodes in a Low-Pressure Plasma," J. Appl. Phys., 31, 1392 (1960).

G. K. Wehner, M. Laegrid, Stuart, "Study of Sputtering of Metals," Final Report AFC RL - TR-60-418 - Report No. 2133, Project No. 80087, October 1960.

G. K. Wehner, D. Rosenberg, "Angular Distribution of Sputtered Material," J. Appl. Phys., 31, 177 (1960).

G. K. Wehner, D. Rosenberg, "Mercury Ion Beam Sputtering of Metals at Energies 5-15 Kev," J. Appl. Phys., 32, 887 (1961).

A. Weiss, L. Heldt, W. J. Moore, "Sputtering of Silver by Neutral Beams of Hydrogen and Helium," J. Chem. Phys., 29, 7 (1958).

A. Wilcox, "Experimental Determination of Rate of Energy Loss for Slow H^1, H^2, He^4, Li^6 Nuclei in Au and Al," Phys. Rev., 74, 1743 (1948).

S. P. Wolsky, Phys. Rev., 108, 1131 (1957).

S. P. Wolsky, E. J. Zdanuk, "Investigation of the Sputtering of Silicon," J. Appl. Phys., 32, 782 (1961).

S. P. Wolsky, E. J. Zdanuk, "Sputtering of Silicon with A^{+2} Ions," Phys. Rev., 121, 374 (1961).

E. Yoda, B. M. Siegel, J. Appl. Phys., 33, 1419 (1962).

O. C. Yonts, D. E. Harrison, "Surface Cleaning by Cathode Sputtering," J. Appl. Phys., 31, 1583 (1960).

O. C. Yonts, C. E. Normand, D. E. Harrison, "High-Energy Sputtering," J. Appl. Phys., 31, 447 (1960).

V. E. Yurasova, "Formation of Oriented Figures by Ionic Bombardment of Metals," Kristallografiya 2, 770 (1957).

V. E. Yurasova, "Contemporary Theories of Cathodic Sputtering and the Mirco-Relief of the Eroded Metal Surfaces," Soviet Physics, Tech. Phys., 3, 1806 (1956).

B. Secondary Particle Emission

I. A. Abroyan, "Extraction of Electrons from Germanium by Ions of Cesium, Potassium, Lithium, and Hydrogen," Soviet Physics, Solid State, 3, 431 (1961).

G. M. Batanov, "Secondary Electron Emission from Single Crystals of NaCl and KCl under Bombardment by Lithium and Potassium Ions," Soviet Physics, Solid State, 3, 409 (1961).

D. S. Beers, Bradley, "Reflected Xenon Ions...," Bull. Am. Phys. Soc., 4, 221 (1959).

G. Bimschas, "The Theory of Secondary Electron Emission from Metals I," (German), Z. Phys., 161, 190 (1961).

G. Bimschas, G. V. Schubert, "On the Theories of Secondary Electron Emission of Metals II," (German), Z. Phys., 162, 382 (1961).

R. C. Bradley, "Secondary Positive Ion Emission from Metal Surfaces," J. Appl. Phys., 30, 1 (1959).

R. C. Bradley, E. Ruedl, "Reflection of Inert Gas Ions from Copper," Bull. Am. Phys. Soc., 5, (1960).

R. C. Bradley, E. Ruedl, "Secondary Positive Ion Emission from Cooper," Bull. Am. Phys. Soc., 5, (1960).

R. C. Bradley, "Secondary Positive Ion Emission from Metal Surfaces," J. Appl. Phys., 30, (1959).

I. M. Bronshtein, B. S. Fraiman, "On Certain Regular Features of the Secondary Electron Emission of Thin Layers of Metals and Semiconductors," Soviet Physics, Doklady, 5, No. 6, (1960).

Curt Brunnee, "On Reflection of Ions and Secondary Electron Emission by the Impingment of Alkali Metal Ions on Molybdenum Surfaces," (German), Z. Phys., 147, 161 (1957).

D. Hagstrum, "Auger Ejection of Electrons from Tungsten by Noble Gas Ions," Phys. Rev., 104, 317 (1956).

D. Hagstrum, "Auger Ejection of Electrons from Molybdenum by Nobel Gas Ions," Phys. Rev., 104, 672 (1956).

H. D. Hagstrum, "Electron Ejection from Mo by He^{+}, He^{++}, and He_2^{+}, Phys. Rev., 89, 244 (1953).

D. Greene, "Secondary Electron Emission from Molybdenum produced by Helium, Neon, Argon and Hydrogen," Proc. Phys. Soc., (G.B.) B63, 876 (1950).

H. D. Hagstrum, "Reflection of Noble Gas Ions at Solid Surfaces," Phys. Rev., 123, No. 3 (1961).

D. Hagstrum, "Auger Ejection of Electrons from Tungsten by Noble Gas Ions," Phys. Rev., 96, 325 (1954).

H. D. Hagstrum, "Theory of Auger Ejection of Electrons from Metals by Ions," Phys. Rev., 96, 336 (1954).

H. D.Hagstrum, "Effects of Monolayer Absorption and Bombardment Damage on Auger Electron Ejection from Germanium," J. Appl. Phys., 32, 1015 (1961).

H. D. Hagstrum, "Reflection of Noble Gas Ions at Solid Surfaces," Phys. Rev., 123, 758 (1961).

M. Healea, E. L. Chaffee, "Secondary Electron Emission from a Hot Nickel Target due to Bombardment by Hydrogen Ions," Phys. Rev., 49, 925 (1936).

M. Healea, C. Hauterman, "The Relative Secondary Electron Emission due to He, Ne and A Ions Bombarding a Hot Nickel Target," Phys. Rev., 58, (1940).

V. K. Kopitski, H. E. Stier, "The Mean Kinetic Energy of the Ejected Particle in the Cathode Sputtering of Metals," Z. Naturforsch, 17a, 346 (1962).

V. A. Molchanov, V. Telkovskii, "Variation of the Cathode Sputtering Coefficient as a Function of the Angle of Incidence of Ions on a Target," Soviet Physics, Doklady, 6, 136 (1961).

O. V. Roose, "Theory of the Reflection of Positive Ions on Metal Surfaces," (German), Z. Phys., 147, 184 (1957).

A. Rostagni, "The Reflection of Positive Ions and the Liberation of Secondary Electrons from Metal Surfaces," (Italian) Ricerca Scientifica, 9, 633 (1938).

H. Seiler, "Electron Yield in the Case of Lithium-Ion Bombardment of Image Converter Surfaces," (German) Z. Phys., 163, (1961).

H. E. Stanton, "Yield of Energy Distribution of Secondary Positive Ions from Metal Surfaces," J. Appl. Phys., 13, 678, (1960).

H. E. Stanton, "On the Yield and Energy Distribution of Secondary Positive Ions from Metal Surfaces," J. Appl. Phys., 31, 678 (1960).

R. P. Stein, F. C. Hurlburt, "The Angular Distribution of Sputtered Potassium Atoms," University of Calif. Tech Report He-150-170, January 1961.

A. M. Tyutikov, "The Influence of Mechanical Strain on the Secondary Electron Emission from Beryllium Oxide," Soviet Physics, Doklady, 6, 156 (1961).

V. I. Veksler, "Energy Distribution of Sputtered and Scattered Ions in the Bombardment of Tantalum and Molybdenum by Positive Cesium Ions," Soviet Physics, JETP, 11, 235 (1960).

V. I. Veksler, Ben'iaminovich, "The Production of Secondary Ions from Tantalum and Nickel Bombarded by Positive Cesium Atoms," Soviet Physics, Tech. Phys., 1, 1626 (1957).

VII. APPENDIX A

TABLE OF SPUTTERING RATIO RESULTS

Argon, Copper

Run	Energy Kev	Angle	S. R. atoms/ion	Est. Error atoms/ion	Approx. Current Density 10^{-6} amps/cm^2	Comments
3b	38.5	20°	24.4	0.8	8.7	Not electro-
3a	36.0	30°	16.9	1.0	5.9	polished
1	36.1	90°	7.5	1.6	10.2	
2	36.1	90°	5.5	1.7	9.2	
5	37.1	10°	15.2	1.2	2.7	
6	37.9	10°	14.5	1.0	3.0	
10		45°	10.5	1.6	14.4	
12		90°	6.5	0.8	20	
13		90°	6.1	0.8	20	
14	↓	90°	6.5	0.8	20	↓
Xenon, Copper						Not electro-polished except where noted
19	30.5	20°	59.2	6.9	1.9	
15	30	90°	13	4.3	4.6	
16		90°	16.4	3.0	4.8	
22		90°	15.3	2.5	5.7	
23		90°	18.2	2.9	5.1	
82		90°	16.5	2.5	35	Electro-polished
17		45°	26.5	5.6	3.5	
18		30°	34.3	6.8	2.1	
40	↓	20°	40.8	4.2	1.5	

Xenon, Copper Con'd

Run	Energy Kev	Angle	S. R. atoms/ion	Est. Error atoms/ion	Approx. Current Density 10^{-6} amps/cm^2	Comments
51	0.5	90°	5.22	8.1	2.9	Electro-polished
LN Temperatures and Hot Targets						
97	30	90°	17.0	1.8	22	All electro-polished, 600°C
96		90°	17.6	3.8	10	400°C
80		90°	15.1	2.0	60	LN cooled target
81		90°	11.4	1.3	35	
84		90°	11.7	2.0	14	
87		90°	12.1	1.1	26	
Xenon, Molybdenum						
24	30	90°	3.3	0.8	5.4	Not Electro-polished
25		45°	8.6	0.9	4.0	
26		20°	14.3	1.7	2.1	
27		10°	19.0	2.7	0.7	
34		7°	9.4	1.9	0.3	
37		4°	10.8	1.0	0.4	
33		2°	10.1	2.4	0.05	
58	9.5	90°	1.3	0.4	2.0	
55		20°	2.0	0.3	1.0	
56		15°	2.2	0.9	0.3	
54		10°	4.8	0.5	0.5	
70		4°	1.7	0.5	1.0	

Xenon, Molybdenum Con'd

Run	Energy Kev	Angle	S. R. atoms/ion	Est. Error atoms/ion	Approx. Current Density 10^{-6} amps/cm^2	Comments
57	1.5	90°	0.8	0.2	2.1	Not Electro-polished
59	1.0	90°	0.7	0.2	1.6	"
Xenon, Tungsten						
28	30	90°	4.0	0.4	4.3	Not Electro-polished
30		20°	9.7	1.3	1.5	
29		10°	13.8	1.4	0.7	
35		7°	9.8	0.8	0.4	
31		5°	3.9	1.1	0.4	
41		2°	7.4	1.0	0.07	
74	9.5	90°	3.6	0.6	2.7	
66		20°	7.4-9.9	0.7	1.4	
68		10°	5.7	0.7	0.2	
69		5°	6.5	1.1	0.1	
73	1.5	90°	2.8	0.4	4.0	
75	0.5	90°	0.76	0.2	1.6	
Xenon, Silicon						
79	29.5	90°	24.8	2.6	1.4	Not Electro-polished
Xenon, Tungsten Carbide						
92	30	90°	6.0	0.6	85	LN cup
93	30	90°	8.7	0.8	75	"
Xenon, Titanium						
95	30	90°	13.5	1.3	80	Not Electro-polished, LN cup

VII. APPENDIX B

A. Equipment

1. Noble Gas System

a. Ion Source

The ion source is a Penning electron bombardment (sometimes P.I.G.) type, cf. Figures 1 and 2. Generally, there are two separate problems to be solved with bombardment sources. First, ions must be created by electrons striking the gas atoms, and second, the ions must be extracted from the high pressure region where they are created. Pressures in the ionizing chamber of a Penning source are of the order of 10^{-3} mm Hg; therefore, only a very small exit hole can be tolerated if a high vacuum is to be maintained in the vacuum chamber. On the other hand, the number of ions that can be extracted from the ionization chamber is proportional to the size of the exit hole. A compromise must be made between beam strength, system pressure, and system complexity incurred in differential pumping systems.

With heavy ions, sputtering of the exit hole of the ion source is quite severe; Applied Radiation Corporation, the manufacturer, quoted a lifetime of about 20 hours for this particular part operating with argon. One exit piece with 0.035 inch diameter hole had sputtered away to a 0.100 inch diameter hole in about 40 hours of running with argon. However, the larger hole did not result in an extreme rise in pressure. The running pressure only rose from 4×10^{-6} mm Hg to 5×10^{-6} mm Hg.

A second problem resulting from sputtering inside the ion source is that conducting metal films are formed across the internal insulators of the ion source and must be removed every few weeks by dismantling and chemically cleaning the parts.

b. Analyzing Magnets

During the initial program, one of the analyzing magnets shorted internally. The magnets are water cooled and the water leads were sealed into the side plates of the vacuum chamber with epoxy resin so that the magnets were difficult to remove and repair. The sealing arrangement also immobilized the two side access ports of the vacuum chamber.

After the magnets were removed and the snorted one rewound, they were checked for field strength and reinstalled in the vacuum chamber. In order to leave the access ports free for use, the water connections were made by means of copper tubing and removable fittings through just one of the side ports of the vacuum chamber. The removable AN-type fittings have proved perfectly reliable and very convenient. After some time, another internal short developed, apparently as the result of overheating caused by scale in the cooling lines. A recirculating cooling system utilizing distilled water and rust inhibitor was installed and no further trouble was encountered.

c. Beam Collimation

Considerable time was spent in obtaining a clean, well-focused, and well-collimated ion beam. The importance of proper collimation was emphasized by one run which was expected to remove 2 to 3 milligrams of target material but in fact only caused a change of 0.1 milligrams in target mass. A close examination of the deceleration cup and the sputtering pattern on the target indicated that the beam had just grazed the cup lip, and sputtered off enough material from the cup onto the target to make up for the material sputtered from the target.

To insure proper beam alignment a pair of collimating electrodes were then installed in the box a few inches from the target chamber. The uses of these electrodes are threefold. They are used primarily to align the beam. The second electrode, cf. Figure 2, is shielded by the first if the beam is centered on the hole, therefore when the current to the second electrode is minimized the beam is properly aligned. Second, they act as a collimator, not of the main beam, but to keep any secondary beams or neutral particles out of the target section. Since it is not intended to collimate the main beam, the hole can be kept relatively large to eliminate any chance of being grazed by the beam. Third, the electrodes provide a potential barrier to keep stray electrons out of the target section where they would introduce errors in measuring beam strength. A series of four electrodes were installed just before the target section, Figure 14, and a well-focused beam can be produced at the target, at least for higher ion energies.

d. Vacuum System

In the light of the pressure dependent effects discussed in the theoretical section, II-A, it was felt that no fully reliable data could be obtained until the background pressure of the system was reduced to at least 10^{-6} mm Hg. The changes listed below lowered the background pressure from $5 - 10 \times 10^{-6}$ mm Hg to $2 - 4 \times 10^{-7}$ mm Hg and the running pressures from 4×10^{-5} to 4×10^{-6} mm Hg.

Several major modifications were made in the interest of improving the vacuum. First, a cryogenic pump in the form of a stainless steel can, occupying a little under one quarter of the volume of the vacuum box, was installed (cf. Figure 15). When filled with liquid nitrogen, this cold pump reduced the ultimate and running pressure of the system by a factor of ten. The pump-down time was also greatly reduced.

The second major modification involved simplification of the pump inlet. As the system was used originally in the first part of this test series, the diffusion pump (a six inch pump with a freon cooled baffle) was connected to the vacuum box through a six-inch valve and a four-inch diameter flange fitted to a four-inch hole in the box. The valve and flange were removed, and the hole in the box was enlarged to six inches. The pump and baffle were connected directly to the box thereby reducing the distance from the pump to the vacuum box by nearly a foot.

A six-inch valve was placed between the target section and the rest of the apparatus, so that the vacuum could be maintained in most of the system while targets were changed. A second ionization gauge was also added near the target to obtain a more reliable indication of pressure there. As described above, a liquid nitrogen cooled cup was installed surrounding the target; this installation

rapidly reduced the pressure in the target section to the low 10^{-7} mm range after the section was opened and, it is believed, reduced the effective pressure at the target considerably below this level. Figure 1 is a drawing of the final apparatus and Figure 13 is a photograph of it.

It is believed that the following experience gained with O-ring seals may be of use to others working with high vacuum. The large access ports of the vacuum box were designed to employ tin O-rings made up of butt-welded 1/8 inch wire. No tin wire was in stock so 1/8 inch solid solder was tried temporarily and proved quite satisfactory. In contrast with the usual practice of employing knife edges to insure a good seal with metal O-rings, no special devices were found necessary. The O-ring simply fits snugly around a projection on the flange and the projection slides into the hole in the vacuum box, leaving the O-ring to be compressed between the flat surfaces of the flange lip and the vacuum box. Reasonable precautions were taken to avoid any large scratches on the sealing surfaces in contact with the O-rings but nothing beyond elimination of clearly visible scratches leading across the O-ring was attempted. Solder O-rings have been found convenient for many applications where the proper size n-butyl O-ring was not on hand.

Teflon, silicon, and n-butyl O-rings have been tried and tight seals have been obtained easily with all of them up to the accuracy of a helium mass spectrometer leak detector. In general, n-butyl is used for seals that are opened often, since these O-rings are almost always reusable and make good seal over a wide range of clamping pressures.

2. Cesium Ion Sputtering Equipment

A contact ionizer type source was built, cf. Figure 48, to provide a beam of cesium ions. Cesium vapor is delivered to the rear of a porous tungsten ionizer, cf. Figure 2, diffuses through the tungsten and is ionized on the front face of the ionizer. The ions are extracted, accelerated and focused by the extraction electrode. The ionizer, field shaping electrode and accelerating electrode were made to a Rocketdyne design. It was found that the focusing of an unneutralized beam was greatly improved if an electrode at ground (ionizer) potential was inserted between the heat shield (cf. Figure 2) and the electron surpressing electrode. The target was biased positive relative to the last electrode (or cup) in order to prevent the escape of secondary electrons. This system ultimately produced a beam density of approximately 175 microamps/cm^2 with currents between 150 and 200 microamps.

The target holder had space for several targets and could be rotated or translated without interrupting a run. Targets could therefore be sputtered at different energies and angles by merely adjusting the target holder and acceleration voltage during a run.

The pumping equipment consisted of a six-inch diffusion pump with a water cooled baffle, and a cold pump suspended above the diffusion pump. The connection to the remainder of the system was between these two pumps. The system remained in the 10^{-6} mm Hg range under almost all conditions. The vacuum envelope consisted of pyrex pipe which bolted together with "O" ring seals. The target section of the other test stand is of the same construction, therefore target holders may be exchanged readily.

CESIUM TEST STAND

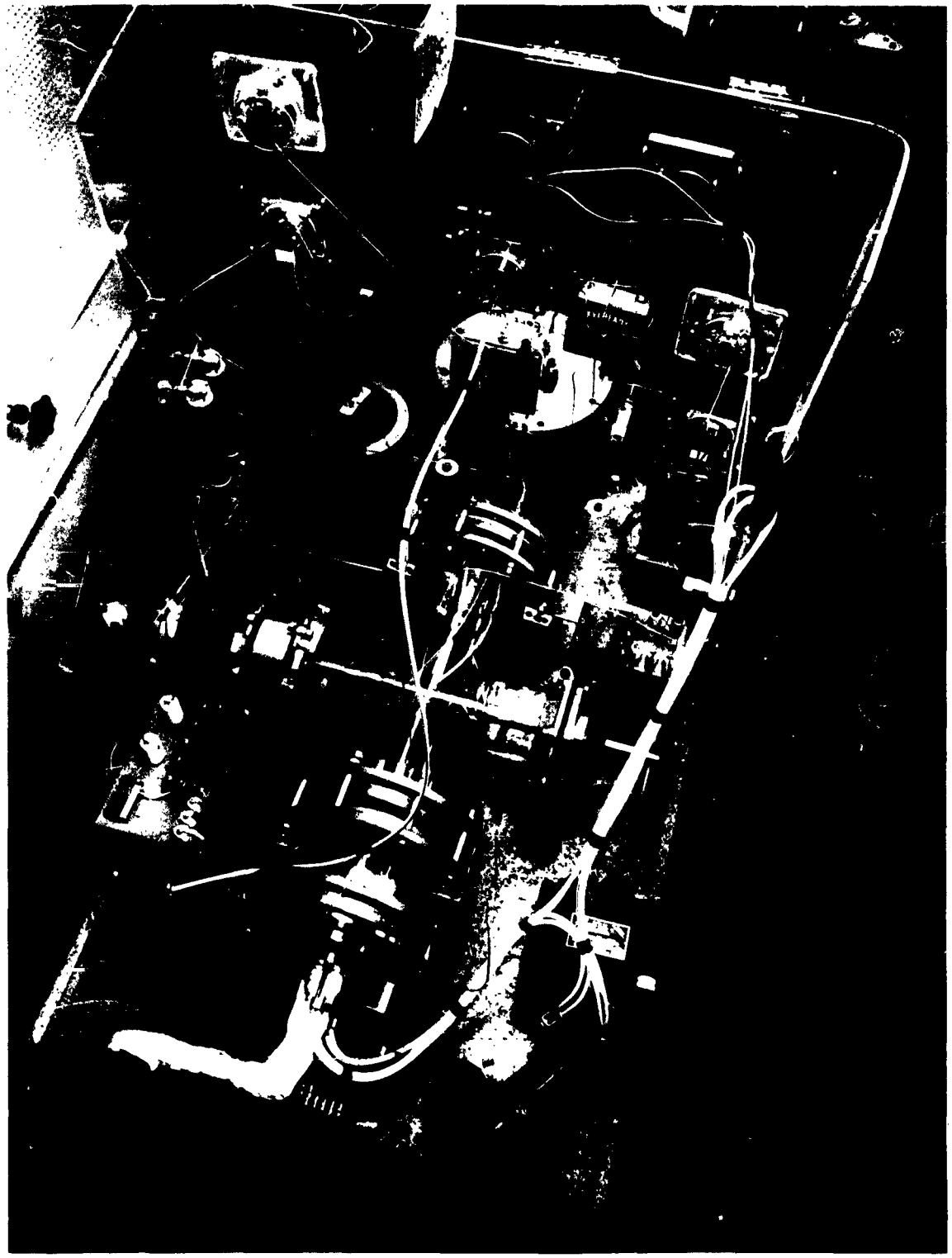

FIGURE 48

Aerospace Research Laboratories, Wright-Patterson Air Force Base, Ohio. RESEARCH ON EXPERIMENTAL EVALUATION OF SPUTTERING YIELD RATES by K. B. Cheney, E. E. Rogers, E. T. Pitkin, ASTRO, an Office of The Marquardt Corporation, Van Nuys, California. July 1963 [illegible] p. incl. illus. (Project 7116; Task 7 11603) (Contract AF 33(616)-8120 (ARL 63-125).

Unclassified Report

Phenomena associated with the impact of high energy ions upon solid surfaces under conditions relevant to ion rocket operation have been investigated. The sputtering ratio has been determined for xenon and argon ions incident upon copper, tungsten, molybdenum, silicon and titanium with energies from 1500 to 32,000 e.v. and at incidence angles from 2° to 90°. The effect of target temperatures on the sputtering ratio has also been investigated. The number of secondary particles produced per incident ion, along with their energy and angular distribution, has been determined as functions of ion energy and incidence angle. Analysis of theoretical concepts of sputtering and existing empirical data have led to recommendations of likely materials for ion rocket use. A bibliography of relevant papers has also been compiled.

(over)

UNCLASSIFIED

Aerospace Research Laboratories, Wright-Patterson Air Force Base, Ohio. RESEARCH ON EXPERIMENTAL EVALUATION OF SPUTTERING YIELD RATES by K. B. Cheney, E. E. Rogers, E. T. Pitkin, ASTRO, an Office of The Marquardt Corporation, Van Nuys, California. July 1963 [illegible] p. incl. illus. (Project 7116; Task 7 11603) (Contract AF 33(616)-8120 (ARL 63-125).

Unclassified Report

Phenomena associated with the impact of high energy ions upon solid surfaces under conditions relevant to ion rocket operation have been investigated. The sputtering ratio has been determined for xenon and argon ions incident upon copper, tungsten, molybdenum, silicon and titanium with energies from 1500 to 32,000 e.v. and at incidence angles from 2° to 90°. The effect of target temperatures on the sputtering ratio has also been investigated. The number of secondary particles produced per incident ion, along with their energy and angular distribution, has been determined as functions of ion energy and incidence angle. Analysis of theoretical concepts of sputtering and existing empirical data have led to recommendations of likely materials for ion rocket use. A bibliography of relevant papers has also been compiled.

(over)

UNCLASSIFIED